Department of Civil Engineering

The University of Michigan

STRENGTHENING AND MODELING OF REINFORCED CONCRETE FRAMES FOR SEISMIC FORCES

by
Gary L. Krause
and
James K. Wight

August, 1990 Report No. UMCE 90-23

A Report on Research Sponsored by
National Science Foundation
Grant No. 8610963

ABSTRACT

STRENGTHENING AND MODELING REINFORCED CONCRETE FRAMES FOR SEISMIC FORCES

The research described herein is part of a research project which studied repair and strengthening procedures for buildings damaged by the Mexico City Earthquake of 1985. A typical two-story reinforced concrete frame school building was selected as the prototype building for this study. A two-thirds scale model of this reinforced concrete frame was constructed in the structures laboratory at the University of Michigan. This frame was then subjected to three tests of reversed cyclic deformations to obtain insights into the behavior of the frame. The objective of this research was to test and model a typical strengthening scheme for this type of building to gain a better understanding of how the strengthened frame would respond during an earthquake.

The testing program indicated that the original and infilled frames experienced distress during testing due to the weak nature of the columns and the beam to column joints. The strengthened frame test showed that when a reinforced concrete jacketing technique was used to strengthen the columns and beam to column joints, the strengthened frame responded much better to reversed cyclic deformations.

The nonlinear computer models of the original frame and the strengthened frame were benchmarked against the laboratory test results, and then subjected to actual earthquake acceleration records. The results showed improved behavior of the strenghtened frame versus the original frame for each record.

The conclusions from this research were that the strenghtening technique effectively improved the performance of the frame both in the laboratory and in the computer modeling. The response of the original frame was improved by the strengthening, but care must be taken when applying the reinforced concrete jacket so that the beam reinforcing bars are properly anchored in the beam to column joint areas.

ACKNOWLEDGMENTS

This report was submitted by Gary L. Krause to The Horace H. Rackham School of Graduate Studies in partial fulfillment of the requirements for the degree of Doctor of Philosophy (Civil Engineering) in The University of Michigan. I would like to thank my advisor Dr. James K. Wight for his assistance, support, perseverance, and guidance throughout the course of my work here. I would also like to thank the members of my committee, Dr. Goel, Dr. Naaman, Dr. Nowak, and Dr. Scott for their helpful suggestions and comments on this report.

I would also like to thank Kevin Schmidt, Jim Wancek, Rick Burch, Bob Spence, Carlos Lopez, and Juan Villareal for all of their help in preparing the laboratory specimens and performing the tests.

The National Science Foundation provided the monetary support for this research, and I thank them for their foresight in sponsoring basic research at this level.

Very special thanks go to my family and friends for their support and encouragement during my years as a graduate student.

Finally, I wish to thank my wife, Amy Kragnes, for her undying support and encouragement during these very trying years in graduate school. It would not have been possible to fulfill my goal of attaining a doctorate without her love, patience, understanding, and trust.

TABLE OF CONTENTS

LIST OF TABLES

LIST OF FIGURES

CHAPTER 1
INTRODUCTION

1.1 General

The research project described herein arose from the experiences of the 1985 Mexico City Earthquakes. The first earthquake shock was recorded on September 19, at 7:18 a.m., and it measured 8.1 on the Richter scale. A modified Mercalli scale intensity of IX was registered in Lazano Cardenas, 30 km from the epicenter. Intensity IX was also recorded at locations in Mexico City, some 400 km from the epicenter. The effects of the original shock were compounded by an aftershock the next day that registered 7.5 on the Richter scale.

In Mexico City, accelerations of 0.04g were recorded on solid ground. In the central parts of the city, which are built on lake bed fill soil of volcanic origin, the accelerations were magnified by that soil to approximately 0.2g. This value is almost 50% higher than the 0.14g value used in the 1977 Mexico City building code. The earthquake records showed that the strong ground shaking lasted for almost 60 seconds and motion was perceptible for almost 3 minutes. During the 60 seconds of strong motion the cycles were very regular at a period of 2 seconds. This caused the lake bed fill soil to be in resonance with the base rock motion because the natural period of the soil was also 2 seconds. This resonance

caused considerable magnification of the ground motions (Corley, Kluver, Ghosh, Fratessa, Moreno, and Hogan 1986, and Esteva 1988).

Buildings with natural periods of 2 seconds (approx. 20 stories) also vibrated in resonance with the ground motions until their natural periods elongated due to structural damage. Buildings 5-15 stories high were not initially vibrating in resonance with the ground motions, but once structural damage occurred and their periods lengthened to about 2 seconds they went into resonance with the ground. Because the ground motion lasted so long and was so consistent in its 2 second period, the buildings whose periods were lengthened by structural damage over time were still subjected to many cycles of the strong motion. This caused many buildings, that might have survived an event of shorter duration, to collapse. Approximately 265 buildings collapsed or were demolished immediately after the earthquake due to severe damage. The majority of these buildings were 5-15 stories high and approximately 228 of the 265 were of concrete construction. An estimated 10,000 people lost their lives and 250,000 people were left homeless (Rosenblueth 1986 and Fintel 1986).

1.2 Mexico City Research Program

A coordinated international research program was initiated to study the Mexico City Earthquakes. Several universities in the United States and Mexico received research grants from the National Science Foundation and Departamento del Distrito Federal and Consejo Nacional de Ciencia Tecnologia of Mexico to study all aspects of the earthquakes. Major research areas included: (1) strong ground motion, (2) geotechnical and foundation aspects, (3) response and performance of structures, (4) materials, repair and retrofitting, (5) lifelines, disaster response and

mitigation, (6) architectural considerations, and (7) cladding and non-structural components. A summary of this effort can be found in EERI (1989).

At the University of Michigan a study was undertaken to analyze the performance of reinforced concrete frame structures during the earthquake. Specifically, a typical school building design was evaluated and ideas were developed for strengthening and retrofitting of the building. The investigation centered on the behavior of a typical two-story reinforced concrete frame building during reversed cyclic deformations similar to those which might occur during an earthquake. A two-thirds scale model of the frame was constructed in the structures laboratory at the University of Michigan. The model had structural details that were typical of many school buildings in Mexico. The testing phase for this portion of the research consisted of three separate tests of this model. The analytical phase of the research consisted of the development of nonlinear computer models of the test frames, and the subjection of those computer models to several earthquake records.

1.3 Objectives and Scope

The objectives of this research program were: (1) build and test a two-thirds scale model of a typical reinforced concrete frame, (2) use the results of the laboratory testing program to create a nonlinear computer model of the frame specimen and the strengthened frame specimen, and (3) use the computer models to check the effectiveness of the repair/strengthening scheme during earthquakes.

The knowledge obtained by accomplishing these objectives provides a better understanding of the benefits and limitations of this

repair/strengthening scheme. This increased understanding can help engineers repair and strengthen reinforced concrete frame buildings to withstand future earthquakes. This will lead to fewer collapsed buildings and, most important, to fewer lives lost.

CHAPTER 2
REVIEW OF PREVIOUS RESEARCH

2.1 General

Reinforced concrete frames and subassemblages and their behavior when subjected to reversed cyclic deformations have been the subject of numerous research projects. This chapter presents an overview of research involving reinforced concrete frames, subassemblages, infilled frames, strengthening methods, and analytical modeling.

2.2 Testing of Reinforced Concrete Frames and Subassemblages

Bertero and Popov (1977) showed that reinforced concrete members subjected to reversed cyclic flexure and shear produced load versus displacement curves that were pinched in shape. The pinching in these hysteresis curves was attributed to shear effects and to cracking of the concrete. As the shear to moment ratio increased, the pinching of the curves became more pronounced. Their research showed that the negative effect of the shear can be controlled by proper detailing of the reinforcement, and that the properly detailed members exhibited the strength and ductility necessary for earthquake resistant design.

Gergely (1977) provided an extensive report on reinforced concrete frame research. The studies showed that the hysteresis curves, whether they are force versus displacement, moment versus curvature, or shear

versus slip, are of considerable importance in understanding the energy dissipation mechanisms and capacities of reinforced concrete frames. The research also showed that reversed cyclic loading greatly changed the behavior of reinforced concrete as compared to monotonic loading. This made it difficult to use test results from monotonic testing to predict the hysteretic behavior of a reinforced concrete frame. Many of the studies also detailed the pinching of the hysteresis curves due to shear effects. Most of the research into preventing shear failures recommended the use of closely spaced transverse ties. The close spacing of the ties was found to enhance the energy dissipation capacity of the section.

Scribner and Wight (1977) proposed the use of supplemental longitudinal reinforcing bars at the beam to column joints in order to delay the shear strength decay in those regions. Their tests indicated that the supplemental reinforcing was effective in delaying shear strength decay in regions of high shear stress.

Jirsa (1977) presented an overview of numerous testing programs on reinforced concrete subassemblages and frames. The studies indicated that the loading history used in testing affected the response characteristics of the test specimen. Jirsa noted that complete uniformity in the loading histories used in testing was not necessary, but care should be exercised when comparing the results from testing programs with different loading histories. The research programs also showed that shear failure of flexural hinging zones was a typical failure mode for reinforced concrete structures, and that with proper detailing it can be controlled. Jirsa called for testing of large scale structures to eliminate the effect of scale found in many testing programs.

2.3 Testing of Infilled Frames

Early work in the area of lateral load resistance of masonry walls was performed by Benjamin and Williams (1958). They tested scale model and full size unreinforced masonry walls with and without bounding frames. Monotonic loading was used and cyclic behavior was not addressed. The authors found the lateral load resistance of the walls without bounding frames to be very poor. However, when the walls were used to infill a frame there was a significant increase in the lateral strength of the system due to the wall. The same result was noted for both concrete and steel bounding frames. The authors also found no significant errors resulting from scale effects of the models.

Stafford Smith and Carter (1969) summarized the behavior of infill frames observed in their research. The frames were subjected to monotonic lateral loading to the point of failure. When the load was first applied, the wall and frame separated over a large part of the length of each side, and contact remained only at the ends of the compression diagonals. In effect, the infills behaved as diagonal struts. As the racking load was increased, failure occurred. The usual modes of failure resulted from tension in the windward column, or from shearing of the columns or beams. If the frame strength was sufficient to prevent collapse by one of these modes, the increasing load eventually produced failure of the infill. If the infill was constructed of unreinforced brick masonry, successive failures by cracking along the compression diagonal and then by crushing near one end of the loaded corners led to collapse. It was also possible for a shearing failure to occur along the mortar planes of the wall. From this observed behavior the authors derived a model for the infilled frame using the equivalent

compression strut concept. This model was used by many other researchers to describe the behavior of infilled frames.

In Mexico, Esteva (1966) conducted experimental and analytical research into the behavior of unreinforced masonry infill walls. He employed cyclic loading conditions to observe the behavior of the walls during a seismic event. Three distinct phases of behavior were noted. At initial loading the frame and wall acted as a monolithic unit. In the second phase, cracking occurred along the joint between the wall and frame causing separation between them. At that point the load was still fairly low and the behavior was nearly linear. The infill wall behaved like a compression strut and the contact between the wall and frame was limited to the corner areas at the ends of the compression strut. The third stage was the diagonal cracking of the infill wall. When the bounding frame was not strong enough, this diagonal cracking led immediately to a cracking of the frame members near the compression joint. This cracking of the frame severely reduced the resistance of the structure to further cycles of loading. This was marked by a sudden drop in the load during testing. If the frame did not fail, the capacity of the infill wall was maintained or even slightly increased. That capacity was maintained if the infill material did not fall away from the frame after diagonal cracking occurred. The author concluded that the frame should be designed to resist the maximum infill wall capacity without failing in order to obtain good cyclic performance of the infilled frame system.

Fiorato, Sozen, and Gamble (1970) studied masonry infilled frames at the University of Illinois. They found that the failure mechanism for an infilled frame involved plastic hinges that formed at locations along the length of the columns, as well as at the column ends. An analytical model

that they used to predict the ultimate strength of infilled frames assumed hinges would form at the midheight of the columns, as well as at the top of one column and at the bottom of the other. This model gave results that were consistent with their experimental results.

Klingner and Bertero (1976) conducted experimental and analytical work on a one-third scale multistory infill wall frame building. The analytical work was based on the equivalent strut concept, as well as on the observed behavior of the test specimens.

The experimental testing was performed on a one-third scale model representing the lower three stories of an eleven-story infilled frame building. Reinforced masonry infill walls were used, with the reinforcing thoroughly tied into the bounding concrete frame members. The frame members were carefully designed and detailed to prevent their failure during loading. The lateral loading was applied in a reversed cyclic pattern and vertical loading was applied to the columns to simulate the effects of the upper stories of the building. The observed behavior of the infill walls and frames upheld the theories put forth by Stafford Smith and by Esteva for the phases of behavior and failure modes. The lateral load versus displacement hysteresis curves clearly showed that the infilled frame dissipated much more energy than the original bare frame when the infilled frame members were properly designed and detailed to avoid shear failure. The curves for all of the specimens showed that there was some shear degradation in the system as evidenced by the pinching in the curves. It was noted that the curves remained stable through many cycles, and the resisted load was always greater than that predicted for the bare frame. It was also noted that the major portion of the damage to the structure occurred in the first story.

At the University of Michigan, Kahn and Hanson (1976) investigated the cyclic behavior of four different types of single-story infilled frames. Testing was performed on one-half scale models of a reinforced concrete monolithic wall and frame, and a post-cast reinforced concrete infill wall with reinforcement tied into the bounding frame members. Two other walls tested were a single precast reinforced concrete panel and a system of multiple precast panels. These two precast systems were connected to the beam and base only, with gaps left between the walls and the columns. The post-cast wall and the monolithic wall were found to behave in the same manner when subjected to cyclic lateral load. These walls increased the load capacity and stiffness of the frame, but they did not show good energy dissipation or good ductility during cyclic loading. The final failure of both specimens was a shear failure of one of the bounding columns, which could be disastrous in an actual seismic event. The single precast wall provided three-fourths of the strength of the monolithic wall and twice the ductility. The multiple precast unit wall provided one-half the strength of the monolithic wall and twice the ductility. The multiple panel system was the only one that did not exhibit significant degradation of maximum load with repeated deflections greater than the yield deflection.

An important consideration for these precast systems was the use of a gap between the wall and the frame columns to keep any interaction of these members to a minimum. The authors said that this was important because it helped to keep the vertical load resisting system of the building intact.

Other tests that indicated the effectiveness of a gap between the infill wall and the frame columns were the ones conducted by Parducci and Mezzi (1980). In their testing program they used hollow bricks, semi-solid blocks,

and semi-solid blocks with a gap between the wall and the columns as infill wall materials. They ran a series of tests on one-half scale, one-story, cyclically loaded, reinforced concrete infilled frames. From their results the authors recommended against the use of hollow bricks because of the large loss of material after cracking of the wall. The semi-solid blocks performed better than the hollow bricks, but still showed significant strength degradation in the cycles following cracking of the wall. The semi-solid block walls with gaps between the wall and the columns provided only slightly lower strength than the specimen without gaps, and showed much improved ductility and energy dissipation in the cycles following cracking.

Priestly (1980) discussed the fact that total isolation of an infill wall is very difficult to accomplish; therefore, accounting for the added stiffness and strength of an infill wall is a better approach to designing such systems. It was also his opinion that even though high ductilities can be obtained from the shear failure mode when the frame and infill wall were extensively reinforced and connected together, the more common construction practice is to use little or no reinforcing in the wall. Since this practice leads to rapid strength degradation and shear failure of columns, he recommended that these infilled frames be designed to respond elastically to seismic events.

Bertero and Brokken (1983) continued the study of infill walls that began with Klingner and Bertero (1976). Similar one-third scale, three-story models were subjected to reversed cyclic loading with different types of materials used for the infill walls. The experimental program showed that all of the types of infill materials were able to respond to the cyclic loading with relatively good ductility and energy dissipation after cracking. The unreinforced infill did not perform as well as the reinforced, but it did perform adequately. The system found to perform the best was a solid brick

masonry wall with welded wire fabric reinforcement grouted to the external faces of the masonry. The welded wire fabric was also attached to the bounding beams and columns. The external coating helped provide good ductility and energy dissipation while also confining the masonry so that debris was not a problem. It was also noted in these tests that the damage to the walls was confined mostly to the first story. This was seen as beneficial for repairing and retrofitting after a seismic event.

Computer models of the specimens were analyzed and a maximum allowable acceleration value was found for each. An analysis was also performed for the possibility of infill walls in only some of the lateral load resisting frames. The results showed slightly lower allowable acceleration values for each specimen, but the externally coated wall was still adequate for any seismic zone in the United States.

Research by Kahn (1984), Hutchinson et al. (1984), and Prawel et al. (1986) showed the effectiveness of various coatings externally applied to masonry walls. These tests further indicate the usefulness of these coatings for improving the performance of masonry infill walls under reversed cyclic loading.

2.4 Methods of Strengthening Reinforced Concrete Frames

Various methods for strengthening reinforced concrete frames have been tested. The three most prevalent methods for strengthening are (1) adding shear walls to the frame, (2) adding steel bracing to the frame, and (3) jacketing the columns and/or beams with reinforced concrete. The addition of shear walls to a frame creates an infilled frame system. This type of system was discussed in section 2.3.

Bush, Roach, Jones, and Jirsa (1987) and Lee and Goel (1990) achieved good results by adding steel bracing members to reinforced concrete frames. The results from their tests indicated that the behavior of the braced frames was controlled by the buckling of the braces. Weld quality and connection detailing were also important to the overall behavior of the braced frame system. Miranda and Bertero (1990) tested the effectiveness of using pretensioned strands as diagonal bracing in a reinforced concrete frame building. The results of their tests indicated that the strands increased the strength and stiffness of the existing frame, and produced very good results when subjected to reversed cyclic deformations. They concluded that this system was a very economical solution to strengthening this type of frame building.

Su and Hanson (1990) conducted experiments using Added Damping and Stiffness (ADAS) devices. The ADAS devices were connected to steel braces that had been inserted into a two-story reinforced concrete frame. The results of the test indicated that these devices substantially increased the strength, stiffness, and ductility of the reinforced concrete frame.

Reinforced concrete jacketing has been used extensively for strengthening reinforced concrete beams and columns (Iglesias 1986). The jackets are usually made with deformed steel reinforcing bars encased in concrete or welded wire fabric wrapped around the element and encased in concrete. The welded wire fabric jacket is usually used to increase the confinement of the existing element and the steel is not utilized as structurally active longitudinal steel. When longitudinal deformed steel bars are used they are usually anchored so as to fully develop their strength. They are then considered to be structurally active and contributing to an increase in the flexural strength of the element. The

lateral steel spacing is usually close so that the shear strength and confinement of the new section will meet the standard requirements to prevent brittle shear failures. By applying this type of jacket to a column, the strength of the column can be increased, shear failures can be prevented, and plastic hinging can be forced to occur in the beams which leads to more stable behavior of the frame.

Tests were conducted at the University of Texas at Austin on columns that were strengthened with unanchored longitudinal reinforcing bars and closely spaced stirrups (Bett, Klingner, and Jirsa 1985). The results showed that the ductility of the frame and the stability of the lateral displacement hysteresis curves were greatly improved by the additional confinement and the increase in shear strength provided by this strengthening method. The results also showed that the behavior of a column that was damaged and then strengthened was very close to that of a column that was strengthened, but not initially damaged. Sugano and Endo (1987) report that the use of a welded wire wrap for improved confinement of damaged columns improved the ductility of the frame during cyclic loading.

Stoppenhagen and Jirsa (1987) tested a two-third scale model of a two-story two-bay reinforced concrete exterior moment frame. Tests of the original frame showed that the columns had insufficient ductility during cyclic motion. Longitudinal reinforcing bars with closely spaced stirrups encased in concrete were used to strengthen the frame. The longitudinal bars were anchored at the foundation and continuous through the floor slabs. The results of the strengthening were that the stiffness of the strengthened frame was about the same as that of the original frame while the strength was substantially increased. The plastic hinges were moved from the columns to the ends of the beams which increased the ductility of

the frame. The repair materials were found to have acted nearly monolithically with the existing concrete.

Alcocer and Jirsa (1990) performed bidirectional reversed cyclic deformation testing of repaired beam to column joint specimens. The results of their tests indicated that a reinforced concrete jacket can be used to improve the hysteretic behavior of seismically weak designs. The jacketing of the column alone provided significant increases in the strength and stiffness of the specimens, and improved the ductility and energy dissipation capacities.

2.5 Analytical Modeling of Reinforced Concrete

Analytical modeling of reinforced concrete frames and members has been the subject of much research. Many different models have been proposed to simulate the observed hysteretic behavior of reinforced concrete. Most of these have met with some success. Advances in digital computers have made the modeling of inelastic behavior and dynamic response of frames more practical.

Clough (1966) developed a bi-linear hysteresis model based on actual tests of a reinforced concrete frame. This model accounted for stiffness degradation in the concrete. The model was used to predict the response of a single degree of freedom system and the results showed good agreement between the model and the actual test.

Takeda, Sozen, and Nielsen (1970) developed a tri-linear hysteresis model which included a cracking point, yield point, and post-yield stiffness in the primary curve. Bond slip was incorporated in the definition of the yield displacement. A set of rules was developed to govern any cycles after the primary curve. Stiffness degradation was accounted for by defining a

relationship between unloading stiffness and yield stiffness using the maximum deflection in the loading cycle and the yield deflection. This model was based on test results of a single degree of freedom system. Comparisons of the model with the tests indicate good agreement.

Saiidi and Sozen (1979) developed the Sina model, which was derived from the Takeda model. This model used fewer rules for the cycles after the tri-linear primary curve. The model also included the pinching effect that is observed in actual reinforced concrete hysteretic behavior by defining crack closing points at which the stiffness changes from a small cracked value to a larger "closed crack" value. They also developed the Q-Hyst model. This was a modification of the bi-linear model. The model simulated the stiffness degradation of reinforced concrete while still remaining fairly simple. Comparisons showed that this simple model simulated the measured shaking table displacement response of small scale frames fairly well.

Otani (1974) developed a two-component beam element for use in nonlinear analysis of reinforced concrete frames. The element had an inelastic line element and an elastic line element connected to nonlinear springs at their ends. The springs represented plastic hinges at the beam ends and were given a modified Takeda bi-linear hysteresis curve. Rules were developed to govern further cycling after the primary curve. The model incorporated a movable point of countraflexure, stiffness degradation, and bond slip. Comparisons to actual tests showed good agreement for large amplitude motions.

Al-Haddad and Wight (1988) developed a one-component beam element with movable plastic hinge locations and rigid ends to simulate end connections. The nonlinear plastic hinge zones were governed by a modified Clough hysteresis model based on test results from beam to column joints.

been strengthened with reinforced concrete jackets. The results of the analyses indicated that designing the strengthened portions of the structure to resist the entire code specified base shear does not guarantee the adequacy of the design. The unstrengthened members may still be forced into their inelastic ranges. The stiffness and strength of the strengthened members needed to be several times that required by current codes in order to prevent inelastic action in the unstrengthened members.

CHAPTER 3
ORIGINAL FRAME TEST AND INFILLED FRAME TEST

3.1 General

A two-thirds scale model of a two-story reinforced concrete frame was assembled in the structures laboratory at the University of Michigan. Two tests of reversed cyclic deformations were performed on that model. The first test (Test #1) was a test of the original bare frame specimen. The second test (Test #2) was a test of the frame with unreinforced brick masonry infill walls added. A complete summary of these tests and results can be found in reference (Krause, Lopez, and Wight 1988).

3.2 Construction and Test Setup

The original frame specimen was sized to represent a typical two-story school building in Mexico (Figs. 3.1 and 3.2). The reinforced concrete foundation blocks were cast first and then anchored to the laboratory strong floor. The next step was to assemble the reinforcement cages for the beams and columns and to erect them in place on top of the foundation blocks (Figs. 3.3-3.5). Once the reinforcement cages were in place, the formwork for the first floor was assembled around the reinforcing steel. The formwork was then aligned to its correct position on the foundation blocks and braced in place (Figs. 3.6-3.8). Additional bracing was added to ensure a stable and stationary working platform for the concrete casting. Ready-mix

concrete was delivered to the laboratory and placed into a concrete bucket. The overhead crane was used to lift and maneuver the bucket into position. Internal vibration was used to consolidate the concrete in the forms. After the first-story concrete hardened, the reinforcement for the second-story beam was attached and the formwork for the second story was assembled. The formwork was braced and shored to provide stability, and the concrete was placed in the same manner as for the first story (Figs. 3.9 and 3.10).

Cross section dimensions and reinforcement details for the frame columns and beams are shown in Fig. 3.11. All beam and column bars were continuous. The only bar splices were at the column bases.

Before testing could begin, hydraulic actuators needed to be attached to the laboratory reaction wall and to the frame specimen. A loading apparatus was designed to apply the forces at the center of the beam at each story level (Fig. 3.12). Additional steel members were designed to attach the actuators to the reaction wall at the correct heights (Fig. 3.13). Once the steel members had been fabricated and attached to the wall and the specimen, the actuators were raised into position and attached to the wall steel. The final attachment to the specimen was not made until the day of the test.

For the infilled frame test, brick infill walls were added to the test frame (Fig. 3.14). The work was performed by two masons using a regular mortar mix and soft silica bricks. This type of brick was used to simulate the soft bricks found in construction in Mexico City. The work was performed to typical construction standards, and no other repairs or changes were made to the frame.

3.3 Materials and Member Strengths

Segments of the reinforcing bars used in the frame specimen were tested in direct tension to obtain their yield stress. The bars tested included sizes No. 2, 5, 6, and 7. The average values of yield stress from four tests for each bar are given in Table 3.1. The results show that all of the bars had higher yield stresses than their specified minimum values.

Table 3.1. Values of Yield Stress For Reinforcing Bars

Bar No.	Spec. Min. Yield Stress (ksi)	Measured Yield Stress (ksi)
2	60	81.0
5	60	69.6
6	60	66.1
7	60	72.4

Average of four tests.

The concrete used in this project was ready-mix concrete delivered to the laboratory in standard trucks. The frame specimen was cast in two separate lifts. Therefore, two different concrete batches were used. Table 3.2 gives the strength values, the average of at least two tests of standard 6 in. by 12 in. cylinders, for both batches. The results show that both batches of concrete had an average 28 day compressive strength near 5000 psi. The average compressive strength for both batches on both test days was at or above 5000 psi.

The brick masonry units used in the infill walls were specified as silica bricks in order to simulate the soft bricks used in construction in Mexico City. The mortar mix used in the walls was not specified. The results of the compression tests of six masonry prisms showed that the prisms had an average compressive strength of 710 psi, and a value of 2,400,000 psi for the modulus of elasticity.

Table 3.2. Values For Concrete Compressive Strength

Time	Compressive Strength (psi)	
	Batch 1	Batch 2
28 Day	4781	5105
Test 1	4952	6145
Test 2	5641	5712

Average of at least two tests of 6"x 12" cylinders.

Using the measured values for the yield strength of the reinforcing bars and the compressive strength of the concrete, the "actual" strengths of the beam and column members were calculated. The "design" values were also calculated using the specified minimum strengths. The results of these calculations are given in Table 3.3.

Table 3.3 Member Flexural Strengths

Member	Nominal Moment Capacity (in.-kips)	
	Design	Actual
Second-Story Beam	580	650
First-Story Beam	1210	1460
Column*	690	800

*Flexural strength with no axial load.

These calculated moment values show that this frame was theoretically a strong column and weak beam system; that is, at each joint the sum of the column moment resisting capacities was greater than the sum of the beam moment resisting capacities. The ratio of the sum of the "actual" column moment capacities, at zero axial load, to the "actual" beam moment capacity was 1.3 for the second-story joints and 1.1 for the first-story joints.

The ratio of the sum of the "design" column moment capacities to the "design" beam moment capacity was 1.2 for the second-story joints and 1.1 for the first-story joints.

3.4 Equipment and Test Procedures

The actuators used for the tests were 110 kip capacity MTS hydraulic actuators with a maximum stroke of 12 in. They were mounted on the wall and attached to the frame loading apparatus in order to provide a $\pm$ 6 in. range of motion during testing.

The controllers were MTS model 458.10 Micrconsoles. Two separate controllers were used. One was used in displacement control mode to control the top actuator, while the other was used in load control mode to control the bottom actuator.

All of the strain gages and actuators were connected to a junction box, which in turn was connected to a Hewlett Packard model 3497A Data Aquisition/Control Unit. This system was used to record the data from these sources at all of the selected data points in the loading cycles.

The loading procedures were the same for both tests. The lateral load was applied by controlling the displacement of the top actuator. The force from the top actuator was then scaled to 80% and used as an input signal for the bottom actuator in force control mode. This scaling was meant to simulate a first mode vibration of the frame. Positive displacement of the frame represented an eastward movement of the frame and negative displacement represented a westward movement (Fig. 3.1). The loading procedure was to displace the frame to a given level for two cycles and then to increase that level for the next two cycles (Fig. 3.15). This procedure was continued until the test was completed. Cracking patterns in the test frame

were recorded at the peak points of each cycle to a new displacement level. Strain gage and potentiometer data were recorded at the peak points and several other points during each cycle.

3.5 Results of Original Frame Test and Infilled Frame Test

The original frame specimen was tested in reversed cyclic deformations up to a level of 2% average story drift. Data were recorded from potentiometers, actuators, strain gages, and observations. Hysteresis curves of the lateral force versus the lateral displacement were plotted using data from the actuator load cell and displacement transducer (Fig. 3.16). The first cycle (0.5% drift) is fairly rounded in shape while the rest of the curves show some pinching due to cracking of the concrete and yielding of the reinforcing bars. The curves also show that although the stiffness of the frame was degrading, the peak load at each new displacement level was higher than the previous one. At the seventh cycle (2% drift) the resistance level of the frame was still increasing which indicated that the frame had good ductility and energy dissipation capacity.

The failure mechanism for Test #1 is shown in Fig. 3.17. This mechanism was determined by strain gage data and observations of the cracking patterns (Fig. 3.18). A plastic mechanism analysis showed that the maximum roof level force for this failure mechanism was 28.3 kips. The maximum roof level force recorded from the actuator was 28.8 kips. The close agreement of these two values indicates that the assumption that the plastic hinges occurred in the columns at the beam to column joint areas was correct. The damage to the columns in the beam to column joint areas was significant by the end of the test. Although the member strengths indicated that this was a strong column and weak beam system, insufficient

detailing of the joints caused the frame to behave as a strong beam and weak column system. The detailing of the joint was checked according to the recommendations of ACI-ASCE Committee 352 (1985). The results showed that three of the four criteria (i.e., moment ratio, joint confinement, and beam bar development length) were not satisfied.

After completion of the first test, brick infill walls were added to the frame. This infilled frame specimen was tested in reverse cyclic deformation up to 1.5% average story drift. Hysteresis curves of the lateral force versus lateral displacement were plotted using the actuator data (Fig. 3.19). The hysteresis curves showed an increase in the initial stiffness and lateral load capacity of the frame. The curves also showed significantly more pinching than in the original frame test and a nonsymmetrical pattern between the positive and negative displacement zones. The force value leveled off during the final cycles in the positive direction, while the force values increased through the last cycle in the negative direction. The different behavior in the two directions was due to the nonsymmetrical cracking patterns of the infill walls. The first-story infill wall was cracked in the positive direction by the fifth cycle, but it did not crack in the negative direction until the ninth (final) cycle (Fig. 3.20).

This nonsymmetrical behavior led to different failure mechanisms in the two directions, which are shown in Fig. 3.21. A plastic mechanism analysis for the positive direction showed a maximum roof level force of 33 kips. The maximum force recorded from the actuator in the positive direction was 31.9 kips. A plastic mechanism analysis for the negative direction showed a maximum roof level force of 44 kips. The maximum value recorded from the actuator in the negative direction was 42.5 kips. In each direction, three plastic hinges were located at the ends of the columns

and the fourth hinge was located near midheight of the column in tension. The midheight hinges were located adjacent to cracks in the infill wall. These plastic hinges created "short column" effects in both columns. The corresponding high shear forces caused severe cracking at the beam to column joints and led to poor hysteretic behavior of the infilled frame. The testing was stopped at 1.5% drift due to the extensive damage to the first-story beam to column joints (Fig. 3.22).

The ductility of the infilled frame specimen was lower than for the original frame specimen. The infilled frame specimen also sustained more damage at a lower drift level than the original frame. This damage was concentrated at the first-story beam to column joints and was attributed to the high shear forces caused by the "short column" effects.

3.6 Conclusions

The introduction of infill walls into a two-story reinforced concrete frame had both positive and negative effects on its behavior during cyclic loading. Although the infill walls increased the ultimate load, initial stiffness, and total energy dissipation of the frame, the ductility was reduced and the amount of damage to the frame was greater at a lower drift level. The lower ductility and increased damage to the columns led to poor behavior of the infilled frame specimen. The fact that the damage was located in the columns indicated that the vertical load resisting system of the frame was threatened with collapse. The use of infill walls in reinforced concrete frames should be considered carefully, and great care must be taken to eliminate the detrimental effects cited here and to obtain a more ductile behavior for the infilled frame system.

The next step in the research project was to investigate methods of strengthening the damaged frame in order to improve its behavior during future possible earthquakes. The method selected for this strengthening was a column jacketing technique. The construction, testing, and evaluation of this strengthening method are covered in the following chapters of this report.

CHAPTER 4
TEST OF STRENGTHENED FRAME

4.1 General

Test #3 consisted of using a reinforced concrete jacketing technique to strengthen the columns which were damaged during Test #1 and Test #2, and then testing the repaired frame by subjecting it to reversed cyclic deformations similar to the first two tests. The goals of this strengthening method were to: (1) increase column moment strength and ductility, (2) improve the ductility of the beam to column joints, and (3) improve the hysteretic behavior of the frame by changing the failure mechanism.

4.2 Damage from Previous Tests

The previous testing of the frame specimen caused significant damage to the frame (Krause, Lopez, and Wight 1988, Lee and Goel 1990, and Su and Hanson 1990). While cracking was apparent in all beams and columns, damage was concentrated specifically at the base of the columns and at the first-story beam to column joints. Further inspection revealed that the concrete cross section at the base of the columns had been reduced considerably. Very little sound concrete remained after loose and cracked concrete was removed, particularly in the core area of the column (Fig. 4.1). At the first-story beam to column joint areas the cover concrete, as well as

some of the core concrete, had cracked and spalled away exposing the reinforcing bars of the column (Fig. 3.22).

4.3 Column Jacketing Procedure

The loose and damaged concrete at the column bases and at the first-story beam to column joints was removed by using a small pneumatic hammer to chip away all of the unsound concrete. These areas were brushed with a wire brush and sprayed with compressed air to remove dust and loose particles.

The strengthening of the columns was accomplished by applying a reinforced concrete jacket along the entire height of the columns. The jacket consisted of both longitudinal and transverse reinforcement and two inches of concrete on all sides of the existing columns (Fig. 4.2). The longitudinal reinforcement consisted of one No. 8 bar placed at each corner of the existing column section. These bars were continuous through the floor slabs, and extended along the full height of the columns. The bars were also attached to coupling devices which were previously embedded in the concrete foundation blocks (Fig. 4.3). These coupling devices were used to simplify construction of the jacket and were designed to attain full development of the longitudinal bars. In an actual strengthening scheme the longitudinal bars would probably be developed by epoxy grouting into drilled holes in the foundation (Warner 1982 and Luke, Chon, and Jirsa 1985). This jacketing was different from other techniques that utilized the reinforcement only for additional confinement of the column section. Because the longitudinal reinforcement in this scheme was embedded in the foundation, the moment capacity of the column was increased significantly.

The transverse reinforcement consisted of No. 3 U-shaped stirrups placed in an overlapping pattern to create complete hoops (Fig. 4.4). The stirrups were spaced at four in. center to center. At the beam to column joint areas, holes were drilled horizontally through the beams to allow stirrups to be placed in the joint areas (Fig. 4.5). After the stirrups were placed in the holes, pressure grouting of the holes was used to obtain bond between the stirrups and the new concrete.

The formwork used to cast the additional concrete was cut from plywood and assembled so that it could be easily aligned for each separate lift of concrete placement. For each column six separate lifts of concrete were used to complete the two-story jacket (Fig. 4.6). The forms were reused for each of the separate lifts. A different set of forms was used at the beam to column joint areas.

4.4 Materials

Test pieces of the reinforcing bars used in the jacket were tested in direct tension to obtain their yield stress. All bars had a specified minimum yield stress of 60 ksi. The measured yield stress for each bar size is given in Table 4.1. The results showed that all of the bars had a higher yield stress than the specified minimum value.

Table 4.1. Values of Yield Stress For Reinforcing Bars

Bar No.	Spec. Min. Yield Stress (ksi)	Measured Yield Stress (ksi)
3	60	72.1
8	60	74.3

Average of four tests.

The concrete was batched in the laboratory and was specified to have a 28-day compressive strength of 5000 psi in order to match the strength of the existing concrete. The mix was proportioned using 3/8 in. maximum size aggregate and a high slump in order to facilitate proper placement and consolidation of the concrete. Placement was accomplished by hand and bucket, and consolidation was accomplished with an internal vibrator and by manual vibration of the outside of the formwork. The 28-day strength of 6 in. by 12 in. cylinder specimens is given in Table 4.2. The results show that the average 28-day strength was very close to 5000 psi.

Table 4.2 Values For Concrete Compressive Strength

Batch #	Number of Cylinders	28-Day Compressive Strength (psi)
1	3	5100
2	2	5100
3	2	4200
4	2	5200
5	3	5300

Average of at least two tests of 6"x 12" cylinders.

4.5 Strain Gages and Potentiometers

In all 16 strain gages were attached to the longitudinal reinf in the column jackets (Fig. 4.7). In accordance with standard procedures, the gages were epoxied to smoothed areas on the bars and covered with a protective coating to keep out moisture.

Two potentiometers were attached to each end of the first-story beam as shown in Fig. 4.7. These were used to measure the rotations of the beam ends during testing. The recorded rotation values were compared to

theoretical yield rotation values of the beam to help determine the location of yield hinges in the frame.

4.6 Member Strengths

Using the measured values for the yield strength of the reinforcing bars and the compressive strength of the concrete, the "actual" strengths of the beam and column members of the frame specimen were calculated. The "design" values were also calculated using the specified material strengths. The results of these calculations are given in Table 4.3.

Table 4.3 Member Flexural Strengths

Member	Nominal Moment Capacity (in.-kips)	
	Design	Actual
Second-Story Beam	580	650
First-Story Beam	1210	1460
Strengthened Column*	2200	2650

*Flexural strength with no axial load.

The nominal moment capacities of the two beams were calculated for positive (tension on the bottom of the section) and negative bending. The positive and negative moment values were approximately equal.

An axial force versus moment interaction diagram was plotted to calculate the nominal moment capacity of the strengthened column section for various axial load levels. For calculation purposes the new concrete jacket was considered to be monolithic with the original column section and all of the reinforcement from the original column was considered to be effective in the strengthened section. The interaction curve is shown in Fig. 4.8. The maximum axial load was 1262 kips, the balance point was at 293 kips axial force and 3413 in.-kips moment, and the nominal moment

capacity at zero axial load was 2600 in.-kips. The interaction diagram shows that there is a variation of $\pm$ 100 in.-kips in the nominal moment value for axial load between positive 20 kips and negative 20 kips. The axial loads that the columns support during the test and at failure are approximately 20 kips in compression and tension. This indicates that the axial loads during the test changed the moment capacity of the columns only slightly. This slight increase in moment capacity had very little if any effect on the test results.

The nominal moment values of the columns and beams show that the strengthened frame was theoretically a strong column and weak beam system; that is, at each joint the sum of the column moment capacities at zero axial load was greater than the beam moment capacity. The ratio of the sum of the "actual" column moment capacities to the "actual" beam moment capacity was 4.0 for the second-story joints and 3.6 for the first-story joints. The ratio of the sum of the design column moment capacities to the design beam capacity was 3.8 for the second-story joints and 3.6 for the first-story joints.

CHAPTER 5
RESULTS OF STRENGTHENED FRAME TEST

5.1 General

After the reinforced concrete jacket was constructed and all of the testing and recording devices were connected, the strengthened frame test was performed in a similar manner to the first two tests which are outlined in Chapter 3. The test ended after the fifteenth cycle (maximum drift of 3%). Data were recorded from the potentiometers, actuators, strain gages, and observations.

5.2 Lateral Force vs. Displacement Relationships

Figs. 5.1 to 5.3 show the lateral force versus displacement curves that were plotted using data recorded from the actuators. Fig. 5.1 shows the relationship between total base shear and roof displacement. The first eight cycles show nearly elastic behavior of the frame up to an average drift of 1% (1.5 in.). Up to 2% drift (3.0 in.) the strength increased at each new displacement level, the pinching of the curves was slight, and the stiffness of the frame decreased slowly. At 2.5% drift (3.75 in.) the stiffness decreased more quickly and at 3% drift (4.5 in.) the strength dropped to approximately 80% of the maximum.

At an average story drift of 3% (4.5 in.)the hysteresis curves were fairly stable although pinching of the curves was more pronounced. While

the reduction in strength and stiffness was significant, the hysteresis curves indicated good energy dissipation and ductility in the frame. It can be seen that the repeat cycle at each displacement level usually reached a slightly lower peak load than measured in the first cycle at that displacement level. This was expected because the stiffness of the frame was reduced by the opening of new cracks and additional reinforcement bar yielding during the first full cycle at every displacement level.

Hysteresis curves of the story shear versus story displacement for the first and second stories are shown in Figs. 5.2 and 5.3, respectively. These curves are also stable and show increasing loads at each new displacement level. There is a slight drop in the strength and stiffness in the last three cycles, but the shape of the curves indicate good behavior by each story. Fig. 5.2 indicates that pinching was more significant in the first story than in the second story. Fig. 5.3 shows that the displacement in the second story was much larger than that in the first story, indicating that the second story was more involved in the inelastic behavior of the frame than the first story.

Fig. 5.4 shows that the second story contributed approximately 60% of the total displacement of the frame during the test. This percentage was the same for both the positive and negative directions. This result agrees with the hysteresis curves which indicated that there was substantially increased participation by the second story in the inelastic behavior of the frame. The increased participation of the second story was a direct result of the strengthening of the columns. The stronger columns forced the plastic hinges to occur in the beams. This changed the failure mechanism to one where the plastic hinges had to occur in the ends of both the first- and

second-story beams, thus forcing the second story to more fully participate in the inelastic behavior of the frame.

5.3 Strain Gage Measurements

Values of strain recorded from the strain gages attached to the new column longitudinal reinforcing bars were plotted versus total base shear and versus roof displacement. Plots for gages 1 and 15 are shown in Figs. 5.5 and 5.6, respectively. The location of the gages is shown in Fig. 4.7. Each figure shows the strain versus roof displacement in part a and the strain versus total base shear in part b. Positive values for strain represent tension and negative strain values represent compression. It should be noted that due to a power drop during the test, the strain gage initialization data were lost during cycle 11 (2% drift). Therefore, there were no accurate strain gage readings after cycle 11.

Fig. 5.5 shows the strain from gage 1 which was located at the base of the west column. Yielding of the bar occurred in cycle 11 when the strain suddenly increased with little increase in load. The change in the rate of straining between tension and compression was attributed to the closing of flexural cracks which were opened in the previous half cycle of loading.

The curves in Fig. 5.6 show the strain from gage 15 which was located at the top of the east column. This gage shows no apparent yielding of the bar. That was the expected result at that location in the frame. These curves also show the changes in the rate of straining between tension and compression.

Other strain gage values are shown in Figs. 5.7-5.13. These data were used to post predict the location of yield hinges in the frame specimen.

The location of the yield hinges established the failure mechanism for the frame.

5.4 Potentiometer Measurements

Potentiometers were positioned as shown in Fig. 4.7 to record the rotations of the first-story beam ends. The results are plotted in Figs. 5.14 and 5.15. The curves in these figures show that the beam ends experienced rotations well beyond their yield rotations during the test. The yield rotations were first exceeded during the ninth cycle (1.5% drift). At the end of the test (3% drift) the rotation demand was approximately two times the yield value.

5.5 Observed Behavior

The cracking patterns for the columns and beams were recorded at the peak loads of the first cycle to each new maximum displacement level. The cracking patterns are shown in Figs. 5.16-5.31. Cracks formed at the areas of flexural tension in the members as well as in areas of high shear. The cracks overlapped in many areas due to the reversed cyclic loading.

The pattern of cracking indicates that the highest stress concentrations were at the base of the columns and at the ends of the beams. In the early cycles the cracks occurred in the areas of flexural tension in the beams and columns. As the test continued cracks concentrated at the column bases and beam ends. During cycle 11 (2% drift) very wide cracks were observed in the beam ends at the face of the columns in both stories. After these wide cracks occurred at the beam ends damage began to concentrate more at the column bases. These observations suggest that yield hinges were formed at these locations in the beams and

columns, thus creating a potential collapse mechanism. The locations of these yield hinges corresponded to the data obtained from the strain gages.

The first story beam ends suffered significant damage during the test. This damage was a direct result of the rotation ductility demand placed on the beam ends. The damage was primarily limited to one very wide crack at the column face. The fact that there was only one large crack instead of several smaller cracks indicated that there was some slippage of the longitudinal beam bars. Cracking in the beam to column joint areas was limited and the cracks were not very wide. These observations indicate that the column jacketing was successful in eliminating the joint deficiencies found in Tests #1 and #2. However, the anchorage of the beam bars was not improved. These beam bars had been worked by many cycles of loading, and the column strengthening did not reestablish adequate anchorage for them.

The ends of the second-story beam also had a very wide crack at the face of the columns. This corresponded to the conclusion from the story shear vs. story displacement hysteresis curves that the second story contributed significantly to the inelastic behavior of the frame during the test.

5.6 Stiffness Degradation

The plots in Fig. 5.32 show the change in story stiffness versus the average story drift for the frame. The value of the stiffness was calculated as the slope of a line connecting the positive and negative peaks in a cycle, as suggested by Mayes, Omote, and Clough (1976). The curves show an expected decrease in stiffness at each new maximum displacement level.

The curves also show that each story had a similar percentage loss of stiffness during the test.

5.7 Adequacy of the Beam to Column Connections

An investigation into the detailing of the strengthened first-story beam to column joints was performed using the guidelines given by ACI-ASCE Committee 352 (1985). The joints of the original frame specimen were also investigated (Krause, Lopez, and Wight 1988). There are four major criteria for this type of joint: (1) confinement of column longitudinal bars and concrete core by stirrups, (2) anchorage of beam and column bars in the joint, (3) shear strength of the joint, and (4) moment strength ratio at the joint.

The confinement is checked by calculating the required areas of transverse steel using Eq. 5.1 shown below. The actual amount of confinement steel must be greater than or equal to the area required.

$$A_{sh} = 0.3 \frac{s_h h'' f_c'}{f_{yh}} (A_g/A_c - 1) \quad \text{or} \quad A_{sh} = 0.09 \frac{s_h h'' f_c'}{f_{yh}} \qquad (5.1)$$

The required area of steel was 0.33 sq.in. and the actual area of steel provided was 0.22 sq.in. Therefore, this requirement was not met. However, the original column stirrups were not accounted for in this check. It seems clear that these original stirrups would work to help confine the concrete core of the strengthened column section, but there are no provisions to account for this type of "inner" stirrups. Because axial loads were very low in this test, the confinement of the column section was not severely tested and it was difficult to determine if the confinement of the column in the joint areas was adequate for high axial loads.

The anchorage of the beam bars was checked using Eq. 5.2 to calculate the development length for the hooked bars.

$$\ell_{dh} = \frac{\alpha f_y \text{ (psi) } d_b}{75 \sqrt{f'_c} \text{ (psi)}} \tag{5.2}$$

The required development length was 11.6 in. The length provided by the column jacket was 12. Therefore, the beams had sufficient development length according to the guidelines. However, observations during the test indicated that the bar anchorage was not sufficient primarily due to prior testing.

Using the new column longitudinal bars, the ratio of total beam depth to column bar diameter was 18, which was less than the recommended value of 20. It was thought that this was probably acceptable because the column bars were not expected to yield.

The shear strength was checked using Eq. 5.3.

$$\phi V_n \geq V_u \qquad \text{and} \qquad V_n = \gamma \sqrt{f'_c} \text{ (psi) } b_j h \tag{5.3}$$

The calculated ultimate horizontal shear force transferred to the joint was 67 kips, while the joint capacity from Eq. 5.3 was 131 kips. Therefore, the shear strength of the joint was more than adequate.

The ratio of the sum of the column moment capacities to the beam moment capacity was 3.6, which was greater than the required minimum value of 1.4. This indicates that the column strengthening scheme made the frame a strong column and weak beam system.

Because three of the four criteria were met, and the fourth was close to being met, it was thought that the column strengthening scheme had

adequately strengthened the joint areas to prevent significant cracking and damage to these areas during the test. The test showed that while the shear strength of the joint was improved, the anchorage of the beam bars was not adequate to keep them from slipping during testing. The test also showed that at low axial load levels the confinement of the column core was adequate. Despite the bar slippage, the strengthening led to a shifting of the yield hinges from the column areas to the beam ends, which was one of the goals of the column strengthening.

CHAPTER 6
ANALYSIS AND COMPARISON OF RESULTS

6.1 General

The data from Test #3 showed that the strengthened frame had increased lateral load resistance, increased stiffness, and better hysteretic behavior than the original frame (Test #1). The strain gage data and the beam end rotation data showed that the yield hinges occurred at the column bases and at the ends of the first-story beam. The beam to column joints were not severely damaged and both story levels contributed to the inelastic behavior of the frame.

6.2 Analysis of the Collapse Mechanism for Test #3

The failure mechanism that was derived from the reinforcement strains, beam end rotations, and observed cracking patterns is shown in Fig. 6.1. The sidesway mechanism was caused by the formation of yield hinges at the base of the columns and at the ends of both the first- and second-story beams. A plastic mechanism analysis was performed using the nominal moment capacities of the frame members. The result of that analysis was a value of 50.0 kips for the force at roof level. The maximum recorded value for the force at roof level was 56.9 kips. The difference in these two values was thought to be due to the strain in the beam bars reaching the strain hardening level during the test. This was primarily due

to the large rotations at the beam ends. The extensive testing that the beam bars had been subjected to prior to this test was also a contributing factor to the bars reaching strain hardening.

6.3 Comparison of Test Results and Effectiveness of Strengthening

The results of Test #3 show that the strengthening scheme produced the desired improvements in the behavior of the frame during reversed cyclic loading. The lateral load resistance was increased from 49 kips to 100 kips by the column strengthening. Fig. 6.2 shows a comparison of stiffness values from Test #1, Test #2, and Test #3. The plots show that the initial stiffness was much larger for the strengthened frame in Test #3.

The hysteresis curves for both tests showed good ductility and energy dissipation. "Energy Index" values were calculated for each test and are shown in Table 6.1. The "Energy Index" values are values of energy dissipation for each cycle normalized by a value of energy dissipated at yield. The energy dissipated at yield was calculated as follows (Fig. 6.3). First, the maximum load (P_{max}) was defined as the lateral load measured at an average story drift of 1.5%. Second, a secant line was drawn from the origin through a point corresponding to 75% of P_{max} (point A) on the measured lateral force versus displacement curve. An artificial yield point was taken as the point where the secant line intersects P_{max} (point B). The energy dissipated at yield was then defined as the area of the shaded triangle OBC. The energy dissipated at yield in both the positive and negative directions was calculated and averaged to determine an average value for each test. The values of energy dissipation for each cycle were then divided by this yield point energy value to obtain the "Energy Index" values shown in Table 6.1. The energy dissipation values for Test #3 were

normalized by the yield point energy from Test #1 as well as Test #3. This made comparisons between the two tests possible. From the values in the table, it is clear that the strengthened frame of Test #3 had higher energy dissipation than the original frame of Test #1 at each drift level.

Table 6.1 Energy Index Values For Test #1 and Test #3

	Test #1		Test #3		
Drift %	Energy (E_1) (in.-kips)	$E_1/EI1$	Energy (E_3) (in.-kips)	$E_3/EI3$	$E_3/EI1$
0.25			2.99	0.030	0.093
0.25			1.28	0.014	0.043
0.5	13.67	0.424	10.41	0.104	0.323
0.5	4.48	0.139	4.22	0.042	0.130
0.75			20.13	0.201	0.623
0.75			12.59	0.126	0.391
1.0	30.39	0.943	34.45	0.345	1.070
1.0	13.83	0.429	22.65	0.227	0.704
1.5	61.57	1.900	103.33	1.033	3.203
1.5	42.48	1.318	58.24	0.582	1.805
2.0	100.22	3.108	192.5	1.925	5.970
2.0			141.15	1.411	4.376
2.5			272.41	2.724	8.449
2.5			176.57	1.766	5.477
3.0			272.78	2.728	8.461

EI1 = 33.2 in.-kips EI3 = 100.0 in.-kips

The failure mechanism of Test #3 was an improvement over that of Test #1 because the yield hinges occurred in the beam members and not in the joint areas. Beam hinging is usually a more ductile failure mode and clearly a safer mode with respect to structural stability than plastic hinging in the beam to column joints. By forcing the plastic hinges to occur in the

beams, the second story had to participate more in the inelastic behavior of the frame. In the original frame test the first story became a "soft" story and the second story did not fully participate. Shifting the yield hinges to the beam members also decreased the damage to the columns in the joint areas. By minimizing the damage to the joint areas, the strengthening scheme of Test #3 helped to keep the vertical load resisting system intact.

Although the beam hinging is a more ductile failure mode than hinging in the joint areas, in Test #3 the cracking in the beam member was primarily confined to one flexural crack at the face of the column. This indicated that the plastic hinging zone was spread over a very small area of the beam. It was thought that this small hinging zone was due to the beam reinforcing bars pulling loose in the joint areas which were damaged in previous tests. It was also thought that this bar slippage could have contributed to the reduction in stiffness during the last three cycles of the test. It is not known if epoxy injection or other repair methods would have prevented this slippage of the beam bars.

6.4 Summary

The results of Test #3 showed that the reinforced concrete column jacketing scheme was successful in shifting the yield hinge away from the beam to column joints to the beam member. However, the cracking in the beam member at the yield hinge location was primarily confined to one flexural crack at the face of the column. By shifting the yield hinges to the beam members, the failure mechanism for the frame was changed as compared to Test #1. This changing of the failure mechanism and increased strength of the columns resulted in decreased joint damage, increased stiffness, increased lateral load resistance, better ductility, and better

energy dissipation for the frame. Therefore, the strengthening scheme accomplished the main goals of its application, but questions remain about the concentration of damage at the beam ends and the inability of current repair techniques to restore the original bond strength of anchored bars.

CHAPTER 7
ANALYTICAL MODELING AND EARTHQUAKE ANALYSIS

7.1 General

The information obtained from the laboratory tests was used to create an analytical model of each test specimen using the DRAIN-2DM computer program. This program is a version of DRAIN-2D (Kanaan and Powell 1973) that was modified at the University of Michigan (Tang and Goel 1988). The models were benchmarked against the results from the laboratory tests, and then subjected to ground acceleration records from three different earthquakes. The results of this analysis provided insight into the behavior of the frame when subjected to an earthquake record, and the effectiveness of the strengthening scheme that was tested in the laboratory.

7.2 Analytical Model of the Original Frame

It was decided that the DRAIN-2DM program should be used to model the laboratory specimens so that the nonlinear properties of the frames could be included in the analysis. Element 5 was selected to model the members of the frame. This element employs a bi-linear moment curvature model (Fig. 7.1). The element was used to represent both columns and beams in the frame model (Fig. 7.2). The columns were represented by a beam element because the axial load effects in this frame

were very small. Thus, the columns could be modeled quite accurately without including axial load effects.

Using the measured values for the material properties of the concrete and the reinforcing steel, a moment versus curvature diagram was plotted for both the beams and the column sections (Figs. 7.3-7.5). From these curves the values of M_y and EI were obtained for use as input for each element of the computer model (Fig. 7.6). The value for the modulus of elasticity (E) was determined by the standard methods given by ACI Committee 318 (1989). The strain hardening modulus (K_2) was assumed to be 4% of the elastic modulus value (K_1) (Fig. 7.1).

To verify the model parameters, the model was loaded with a monotonically increasing static load using the static load option of DRAIN-2DM. A comparison of that analysis versus the laboratory test results of the original frame specimen is shown in Fig. 7.7. The correlation between the computer model curve and the laboratory test lateral hysteresis curves was good. The results from the computer analysis also showed that the failure mechanism of the model was the same as the observed failure mechanism of the test frame, that is, plastic hinges occurred at the top and bottom of both first-story columns. It was thought that this model was a good representation of the laboratory test frame.

7.3 Analytical Model of the Strengthened Frame

For the strengthened frame model the same beam elements were used to represent the beams and columns. The column elements had new properties because of the jacket that was used to reinforce the existing columns. The moment versus curvature diagram for the strengthened column section is shown in Fig. 7.8. Because the beams had not been

repaired or strengthened, the moment values (M_y) and the modulus of elasticity (E) described above remained the same. The moment of inertia values (I) were changed due to the presence of cracks in the beam members. In order to determine the reduced value of the moment of inertia for the beams, a parametric study was performed using different moment of inertia values for the beams and for the strengthened columns. The values of I for both the beams and the columns were varied and then the frame was analyzed under monotonic lateral load. The results were plotted and compared to the laboratory test lateral hysteresis curves for the strengthened frame specimen (Figs. 7.9 and 7.10). The results indicated that a 5% reduction in column stiffness coupled with a 50% reduction in beam stiffness provided a good correlation between the computer model and the laboratory specimen (Fig. 7.11). Studies performed at the University of Texas at Austin (Stoppenhagen and Jirsa 1987 and Bett, Klingner and Jirsa 1985) showed that these values for reduced moment of inertia for the beams and the columns were reasonable and very close to values used in those studies. The results of the analysis also showed that the failure mechanism of the computer model was the same as the observed failure mechanism for the strengthened frame specimen; that is, plastic hinges formed at the base of the first-story columns and at the ends of both the first-story and second-story beams. It was thought that this model was a good representation of the strengthened frame specimen.

7.4 Earthquake Analysis

For the purpose of dynamic analysis, the frame model was assumed to be an interior frame with the spacing between adjacent bents equal to the centerline dimension between the columns of the frame (Fig. 7.12). The

tributary mass for each frame was calculated assuming 200 psf (1000 kg/sq.m) for the first story and 100 psf (500 kg/sq.m) for the second story. The damping values for the frames were calculated as shown by Al-Haddad and Wight (1988).

Three earthquake acceleration records were used as input for the computer analysis of the frame models: (1) the 1985 Mexico City SCT record, (2) the 1986 San Salvador CIG record, and (3) the 1940 El Centro record. The Mexico City SCT record had a maximum acceleration of 0.16g and was used because the research program was based on that event, and because of the long duration and high energy release of the earthquake (Esteva 1988). The 1986 San Salvador CIG record had a maximum acceleration of 0.7g and was used because of its high content of short period motions, a characteristic that made this earthquake very destructive to low rise buildings similar to the prototype building for this project (Anderson 1987, Sauter 1987, and Lara 1987). The 1940 El Centro record had a maximum acceleration of 0.33g and was used due to its extensive use in seismic research as a benchmark event. The El Centro record had a significant energy release over a broad range of periods.

The fundamental period for each model was calculated by exciting the model with a pulse type ground acceleration load of 0.1g and then plotting the results. The results are shown in Figs. 7.13 and 7.14. The original frame model had a fundamental period of 0.36 seconds, and the strengthened frame model had a fundamental period of 0.28 seconds.

7.5 Response of Models to Earthquake Records

Both of the models were subjected to the north-south acceleration record of the 1940 El Centro earthquake. The results are shown in Fig.

7.15. It can be seen that the original frame model was displaced to a maximum value corresponding to approximately 0.9% average story drift at about 2 seconds into the record. After that point the original frame model continued to respond to the ground acceleration and sustained some residual displacement by the end of the record. The strengthened frame model was displaced to a maximum value corresponding to approximately 0.5% average story drift at 2.5 seconds into the record. The model responded elastically throughout the input of ground accelerations and sustained no residual displacement by the end of the record.

The data from the analyses indicated that the original frame model formed a mechanism at approximately 2 seconds into the record. The mechanism consisted of plastic hinges at the top and bottom of each first-story column. This resulted in inelastic response of the frame, and led to residual displacement of the model. The rotation ductility demand on the columns of the original frame model was 2.6, and is shown in Table 7.1.

Hysteresis curves plotting base shear versus lateral roof displacement for both models are shown in Figs. 7.16 and 7.17. Both plots show some energy dissipation, but the plot of the original frame model showed a residual displacement of approximately 0.3 in. in the later cycles of the record. The plot for the strengthened frame model showed no residual displacement as the curves remain near the zero point during the later cycles.

The next earthquake record used to test the models was the 1986 San Salvador CIG earthquake record. The results of the analyses are shown in Fig. 7.18. The original frame model was displaced to a maximum value corresponding to approximately 1.2% average story drift at about 1.3 seconds into the record. The later cycles showed some residual

Table 7.1 Rotation Ductility Factors

	Original Frame Model	Strengthened Frame Model		Double Mass Model	
	Column	Column	Beam	Column	Beam
θ_y (rad.)	0.00618	0.00484	0.0119	0.00484	0.0119
El Centro					
θ (rad.)	0.00989	N.A.	N.A.	0.00019	0.00036
Ductility*	2.6	N.A.	N.A.	1.04	1.03
San Salvador					
θ (rad.)	0.02492	0.00152	0.00172	0.0055	0.00596
Ductility*	5.0	1.3	1.14	2.14	1.5

*Ductility is calculated as $(\theta + \theta_y)/\theta_y$

displacement in the model. The strengthened frame model was displaced to a maximum value corresponding to approximately 1.2% average story drift at about 1.6 seconds into the record. The strengthened frame model also showed some residual displacement in the later cycles. The residual displacement of the strengthened frame model was less than that of the original frame model.

The data from the analyses indicated that the original frame model had formed a sway mechanism at approximately 1.5 seconds into the record. The mechanism was formed when plastic hinges occurred at the top and bottom of each of the first-story columns.

The strengthened frame model formed a partial mechanism at approximately 1.5 seconds into the record. Plastic hinges formed at the base of each of the first-story columns and at the ends of the first-story beam. A complete mechanism would have included plastic hinges at the ends of the second-story beam. Because these hinges did not form and a full mechanism did not develop, the strengthened frame model had lower displacement levels and less residual displacement than the original frame model. If a full mechanism had developed in the strengthened frame model, it would have been more stable and ductile than the single story column mechanism developed in the original frame mechanism.

The rotation ductility demand on the columns was 5.0 for the original frame model and 1.3 for the strengthened frame model. The rotation ductility demand on the first-story beams of the strengthened frame model was 1.14. These values are shown in Table 7.1. The time history data and these rotation ductility demand values indicated that the first-story beam hinges formed before the column hinges in the strengthened frame model.

The beam was also subjected to more total inelastic deformation than the columns.

Hysteresis curves plotting base shear versus roof displacement for both models are shown in Figs. 7.19 and 7.20. The curves showed energy dissipation and some residual displacement for both models. The permanent deformation for the strengthened frame is approximately 0.2 in. versus 0.4 in. for the original frame model. The curves for the original frame model are less stable and more irregular than the curves for the strengthened frame model.

For the final analytical test the models were subjected to the 1985 Mexico City SCT acceleration record. The results are shown in Fig. 7.21. Only the last 30 seconds of response were plotted to give an indication of the response of each model. The magnitude of the displacements in the first 30 seconds was even smaller than that of the second 30 seconds for both models. Both models responded elastically to the record. The original frame model was displaced to a maximum value corresponding to approximately 0.25% average story drift at around 60 seconds into the record, and the strengthened frame model was displaced to a maximum value corresponding to approximately 0.2% average story drift at nearly the same time. The two response records were nearly identical in shape. The magnitudes of roof drift were only slightly smaller for the strengthened frame model.

Hysteresis curves plotting base shear versus roof displacement for both models are shown in Figs. 7.22 and 7.23. These curves indicated some energy dissipation and no permanent deformation for each model.

A third set of analyses was performed using the strengthened frame with increased mass values to simulate a building where only every other frame bent was strengthened by this jacketing technique. The mass for this

new model was double the amount used for the first two models. The fundamental period for this model was calculated as described before (Fig. 7.24). The result was a fundamental period of 0.41 seconds. The results of the earthquake analyses of the double mass model are shown in Figs. 7.25-7.27. Fig. 7.25 showed that the double mass model was displaced to a maximum value corresponding to approximately 1.1% average story drift at about 2.2 seconds into the El Centro record. The model formed a partial mechanism with plastic hinges at the ends of the first-story beam and at the column bases. This resulted in only slightly higher displacement levels than those of the original frame model. There also was no residual displacement in the double mass model.

Fig. 7.26 showed the response of the double mass model to the San Salvador CIG record. The results showed that the model was displaced to a maximum value corresponding to approximately 1.3% average story drift at around 1.3 seconds into the record. Again, a partial mechanism was formed with plastic hinges forming at the ends of the first-story beam and at the column bases. The results of that partial mechanism were a maximum displacement that is the same as that for the other two models, and no residual displacement of the model.

Fig. 7.27 showed the response of the double mass model to the Mexico City SCT record. The results showed that the model responded elastically to the record and was displaced to a maximum value corresponding to approximately 0.34% average story drift at around 59 seconds into the record. No residual displacement was apparent in the plot.

The rotation ductility demands for the beam and columns during the El Centro and San Salvador CIG records are shown in Table 7.1. For the El Centro record the rotation ductility demand was 1.04 on the columns and

1.03 on the first-story beam. The rotation ductility demand was 2.14 for the columns and 1.5 for the first-story beam for the San Salvador record. The plastic hinge rotation values indicated that the beam hinges formed first, and were subjected to more total inelastic deformation than the column hinges for both earthquake records.

Hysteresis curves plotting base shear versus roof displacement for the El Centro, San Salvador CIG, and Mexico City SCT records are shown in Figs. 7.28-7.30, respectively. The curves for the El Centro record are regular in shape and fairly stable. The curves for the San Salvador CIG record are more irregular in shape than those for El Centro. The curves for the Mexico City SCT record are fairly regular and stable. All of the plots showed some energy dissipation for the model, but no permanent deformation.

7.6 Evaluation and Comparison of Analytical Results

Response spectra for the three earthquake records are shown in Figs. 7.31 and 7.32. The fundamental periods of the three models were plotted on the figures to show the relationships to the peak acceleration and energy input from each of the records.

The strengthened frame model showed improved behavior over the original frame model in all three earthquake analyses. Fig. 7.31 showed that the fundamental periods of all three frames were near the area of maximum acceleration and high energy input for the El Centro record. With the acceleration values nearly the same for each model, it seemed reasonable that the strengthened frame would have better response than the other two models because the strengthened frame had the same amount of mass as the original frame model and higher strength, and less mass and

the same strength as the double mass model. During the El Centro record the strengthened frame model responded elastically while the original frame formed a failure mechanism and sustained permanent deformation during its inelastic response. The strengthened frame model was only displaced to a maximum value corresponding to approximately 0.5% average story drift versus 0.9% average story drift for the original frame model. The double mass model responded inelastically to the record and was displaced to a maximum value corresponding to approximately 1.1% average story drift. This was a slightly higher displacement than the original frame model, but the double mass model did not sustain any residual displacement. The column plastic hinge rotation value for the double mass model was lower than the demand for the original frame model, but higher than the values for the strengthened frame model.

Fig. 7.32 shows that for the San Salvador CIG record the fundamental periods for all three models were in the period range of the maximum acceleration value and the maximum energy input. Because the maximum acceleration of the record was very high (0.7g) it was reasonable to expect that the strengthened frame model as well as the other two models would respond inelastically to the record. The strengthened frame model responded inelastically to the San Salvador CIG record, and formed a partial failure mechanism. Because a complete failure mechanism was not formed, the strengthened frame model sustained 50% less residual displacement than the original frame model, and more stable hysteresis curves than the original frame model. The plastic hinge rotation values for the columns were also lower for the strengthened frame model than for the original frame model. The double mass model responded inelastically to this record. The maximum displacement was only slightly higher than the

maximum displacement of the other two models. The double mass model showed no residual displacement, and the plastic hinge rotation values were smaller than those for the original frame model, and larger than those for the strengthened frame model.

It was thought that the low level of response by all three models to the Mexico City SCT record was because the majority of the large energy input of the record is near the 2 second period range (Fig. 7.31). All three models had fundamental periods near 0.3 seconds. Thus, the models were not vulnerable to the high energy input of the Mexico City SCT record, and the energy input at the shorter periods was substantially lower than that from the other two records. During the Mexico City SCT record the strengthened frame and the original frame responded nearly identically. Both models stayed elastic and the maximum displacement values were practically the same as well. The double mass model also responded elastically to this record and the maximum displacement was only slightly larger than that of the other two models.

CHAPTER 8
RESULTS AND CONCLUSIONS

8.1 Results and Conclusions from the Strengthened Frame Test

The damaged frame was strengthened by applying a reinforced concrete jacket to the columns. The goals of the strengthening scheme were to (1) increase the strength and ductility of the columns, (2) improve the ductility of the beam to column joints, and (3) improve the hysteretic behavior of the frame by changing the failure mechanism.

The increase in the strength of the jacketed columns was evident and led to an increase in lateral strength and stiffness of the frame. The improvement in ductility for the beam to column joints was accomplished by placing more stirrups in the joint areas to control the shear cracking and confine the column core. These joints sustained much less damage in the strengthened frame test than in the original frame test. Finally, test data from the strengthened frame test indicated that the plastic hinges had been shifted away from the beam to column joints and into the beam ends at both story levels. These hinges combined with plastic hinges at the base of the columns to form a failure mechanism that was more ductile and dissipated more energy than the original frame. The second story of the strengthened frame was forced to participate more in the inelastic behavior of the frame than in the original frame test.

The one area where the strengthening scheme was not completely successful was in restoring the anchorage of the beam bars in the beam to column joint areas. These beam bars appeared to loosen and slip during testing. This behavior is undesirable and should be addressed when applying this type of strengthening technique to actual building frames.

8.2 Results and Conclusions for the Analytical Modeling

The goals of the analytical modeling were to (1) develop a computer model of the original frame and the strengthened frame, (2) check the accuracy of these models by using static lateral loading to compare the behavior of the models with that of the laboratory test specimens, and (3) subject the models to earthquake acceleration records to study their behavior during earthquake loading.

The results showed that the original frame model very accurately simulated the results of the original frame test. All of the members were modeled using the measured material properties and calculated nominal strengths and stiffnesses. The strengthened frame model required some modification of the beam and column stiffnesses in order to accurately simulate the results of the strengthened frame test. When the stiffness of the beams was reduced by 50% and the stiffness of the columns was reduced by 5%, the model behavior was reasonably close to that of the laboratory specimen.

Three models were subjected to earthquake acceleration records: the original frame model, the strengthened frame model, and the double mass model. The double mass model was used to simulate a building where every other frame was strengthened with the column jacketing scheme. The double mass model was simply the strengthened frame model with the mass

doubled to account for the tributary mass of adjacent unstrengthened frames.

All of the models were subjected to the 1940 El Centro earthquake record. The results showed that the original frame model responded inelastically to the record and formed a failure mechanism. The strengthened frame model responded elastically and did not form a mechanism. The double mass model had some inelastic behavior, but did not form a complete failure mechanism. Both the strengthened frame model and the double mass model had no residual displacements and had better overall behavior than the original frame model.

The models were next subjected to the 1986 San Salvador CIG record. The results showed that the original frame model responded inelastically and formed a failure mechanism during the record. The strengthened frame model responded inelastically as well, but had less permanent deformation and more stable hysteresis curves than the original frame model. The strengthened frame did not form a complete failure mechanism during its inelastic response. The double mass model responded inelastically without forming a complete failure mechanism, and without sustaining any residual displacements. Both the strengthened frame model and the double mass model had better overall behavior than the original frame model.

The 1985 Mexico City SCT record was the last record used in the analytical tests. All of the models responded elastically to the record with very low values for base shear and roof displacement. The cause of this limited response to the record was the fact that the fundamental periods of the models were so much shorter than the dominant period of the earthquake energy input that the ground accelerations were unable to excite

the models. In the other two records the earthquake energy input period was very near the fundamental periods of the models.

8.3 Conclusions on the Effectiveness of the Strengthening Scheme

In the laboratory test, the column strengthening scheme (jacketing) was quite successful. The strengthening improved the strength and ductility of the columns, the ductility of the beam to column joints, and the hysteretic behavior of the frame. The strengthening of the frame helped to dissipate more energy, increase the lateral stiffness and strength of the frame, and change the failure mechanism from an unstable weak column and strong beam mechanism to a more ductile strong column and weak beam mechanism.

In the analytical modeling, the strengthened frame model had better behavior during the El Centro and San Salvador records than the original frame model. The double mass model also performed well during these two records. The behavior of the double mass model showed that strengthening only every other frame in a building would lead to some inelastic behavior, but a complete failure mechanism would not form. The response of the double mass model was not very different from that of the strengthened frame for the San Salvador record. The response of the two models was quite different for the El Centro record. This indicated that the decision to strengthen only every other frame in a building should take into account the site specific earthquake for that particular building when possible. All three models responded elastically to the Mexico City record, and little difference was noted between the original frame model and the strengthened frame model. The double mass model had higher drift values, but remained well in the elastic range.

8.4 Conclusions and Recommendations

The objectives of the research, (1) to construct and test laboratory models of the original frame, infilled frame, and strengthened frame, (2) to use the laboratory test results to create accurate computer models of the original and strengthened frames, and (3) to use the computer models to evaluate the effectiveness of the strengthening scheme during earthquakes, were accomplished. The strengthening scheme was successful in the laboratory and in the computer model at improving the response of the original frame to reversed cyclic deformations. The computer models provided some guidance for the modeling of this type of strengthening scheme in actual buildings.

Overall the column jacketing proved to be a good way to strengthen the columns and to improve seismic resistance of this type of reinforced concrete frame structure.

The testing and modeling of this widely used strengthening system supplied some much needed data and analytical models which can be used to better understand the behavior and effectiveness of the system. This will lead to more consistent and accurate use of this type of strengthening system.

8.5 Future Research

Future research in this area should address the problems encountered with the slipping of the beam bars in the strengthened beam to column joint areas. The use of epoxy injection or other repair techniques to restore a significant percentage of the original bond strength of the bars is important for the successful implementation of this type of strengthening scheme. Another area that could be addressed is that of recommendations for the

evaluation of the beam to column joint areas for jacketed structures. The original column stirrups supply some measure of confinement to the strengthened column section, but at the present time there is no method to account for their effect.

FIGURES

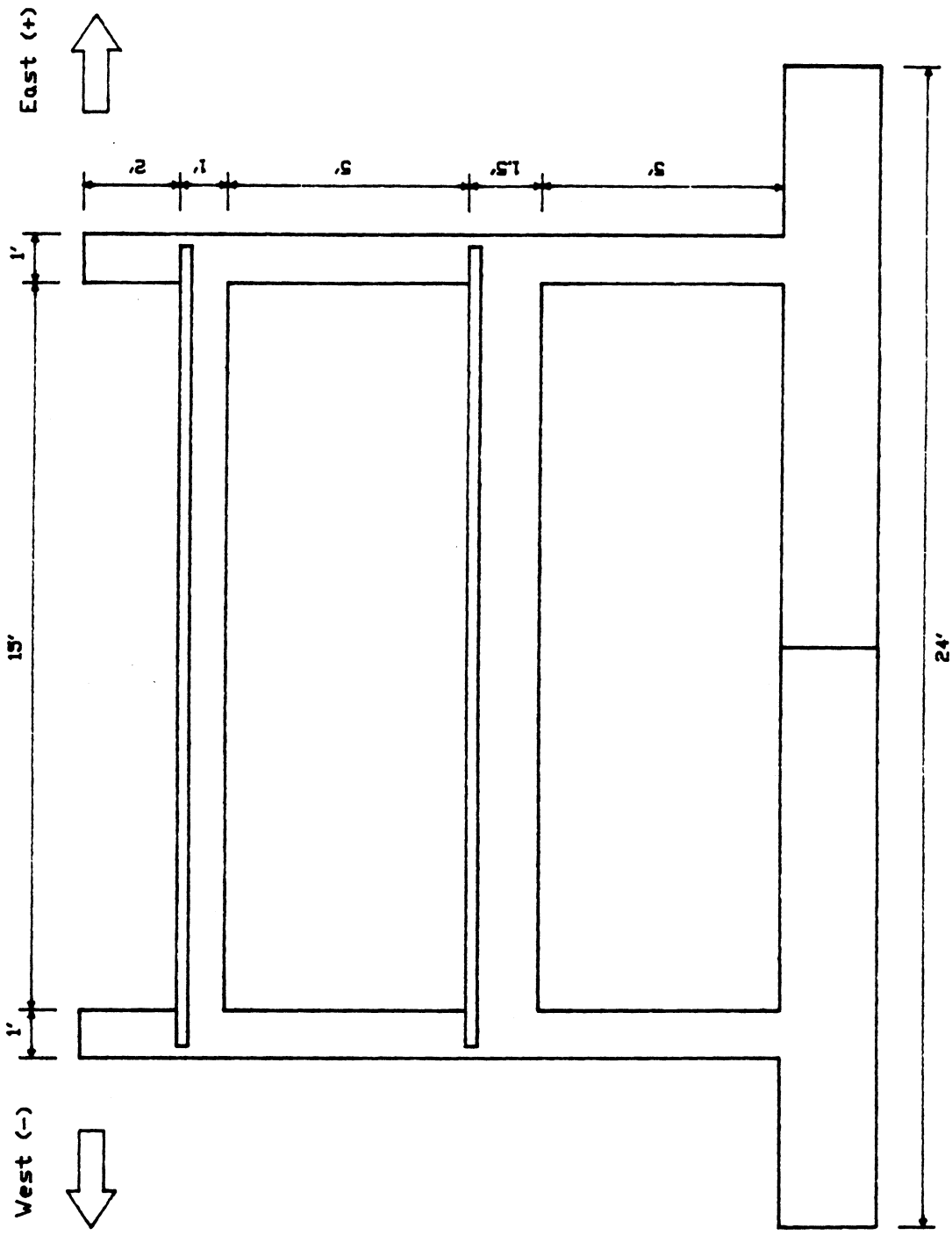

Fig. 3.1 Dimensions of The Original Frame Test Specimen

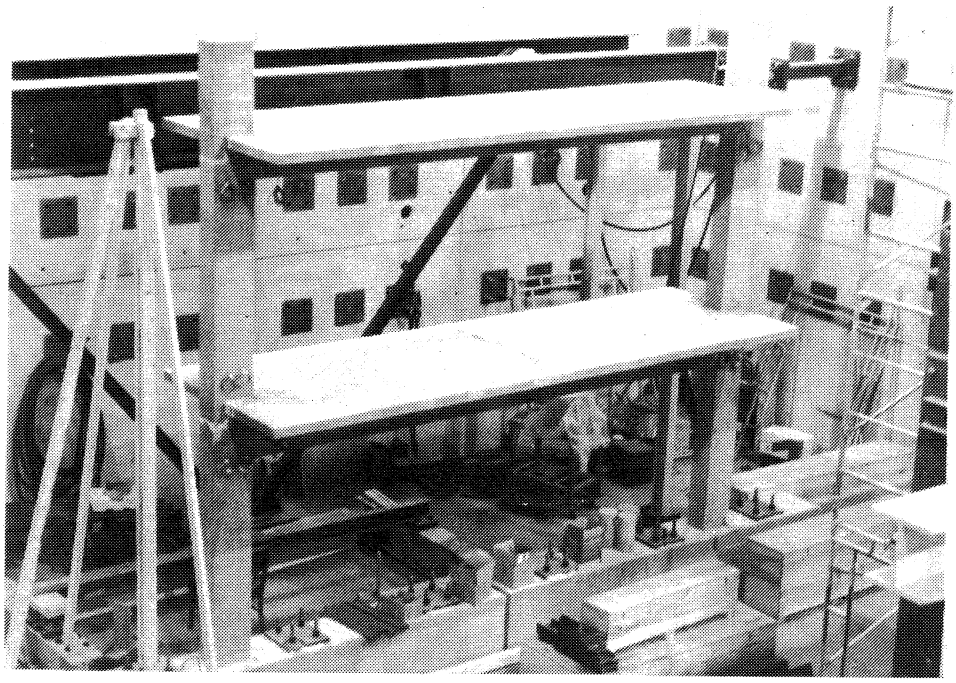

Fig. 3.2 Original Frame Specimen in The Structures Lab

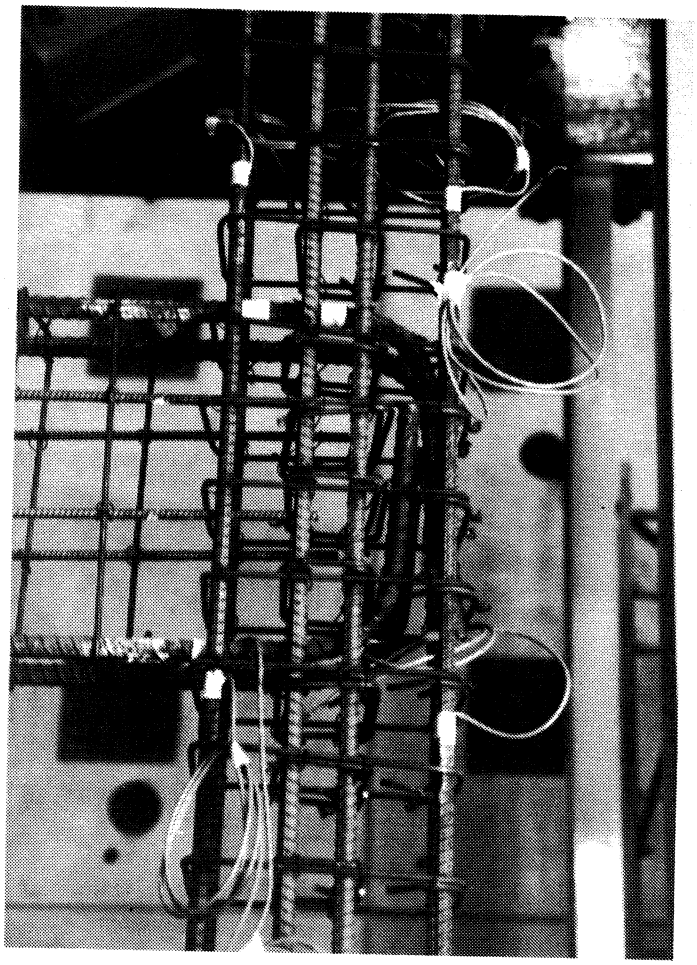

Fig. 3.3 Stirrups in The Beam/Column Joint

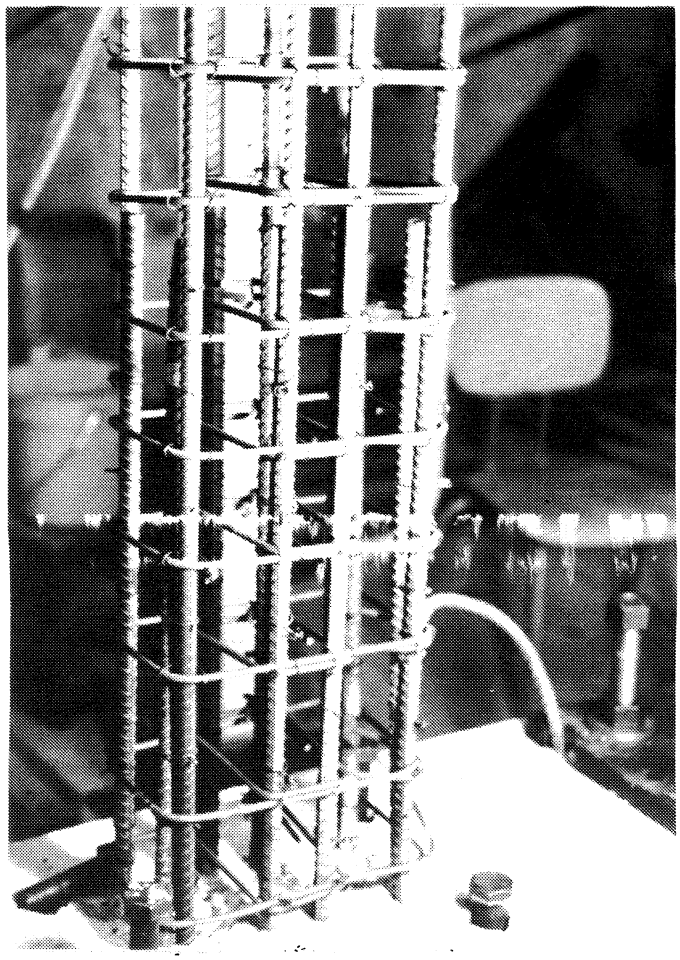

Fig. 3.4 Lap Splice of The Column Bars at The Foundation

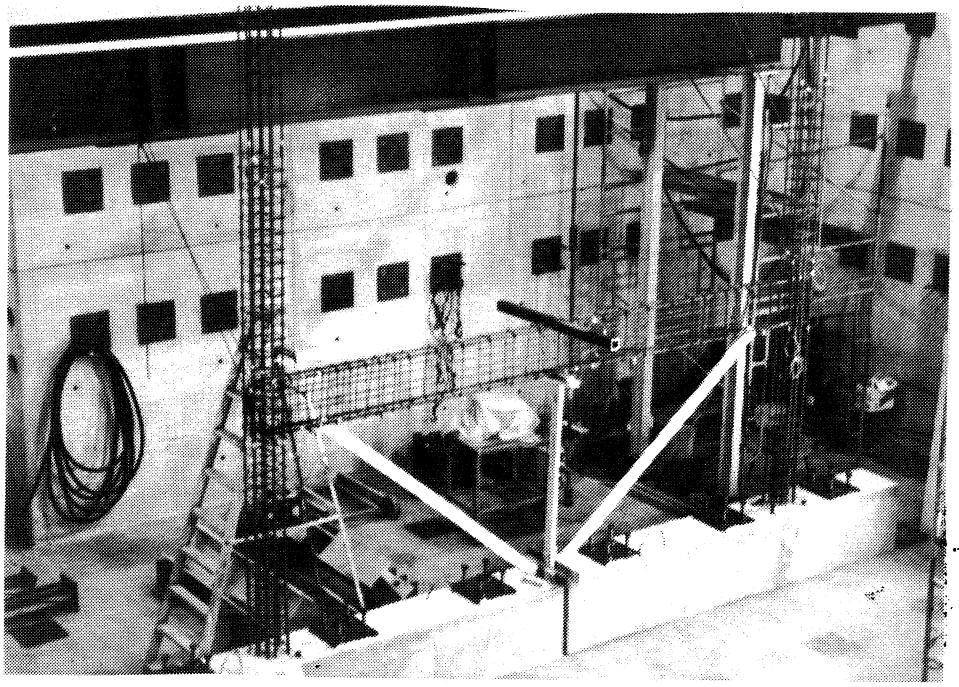

Fig. 3.5 Placement of The Reinforcing Cages on The Foundation

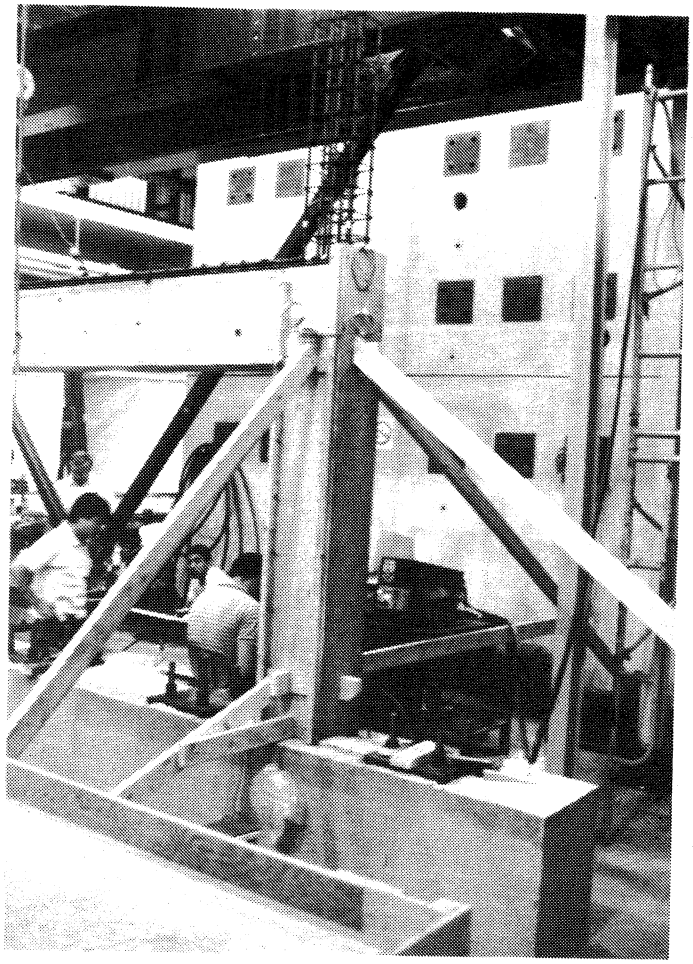

Fig. 3.6 First–Story Column Formwork Bracing

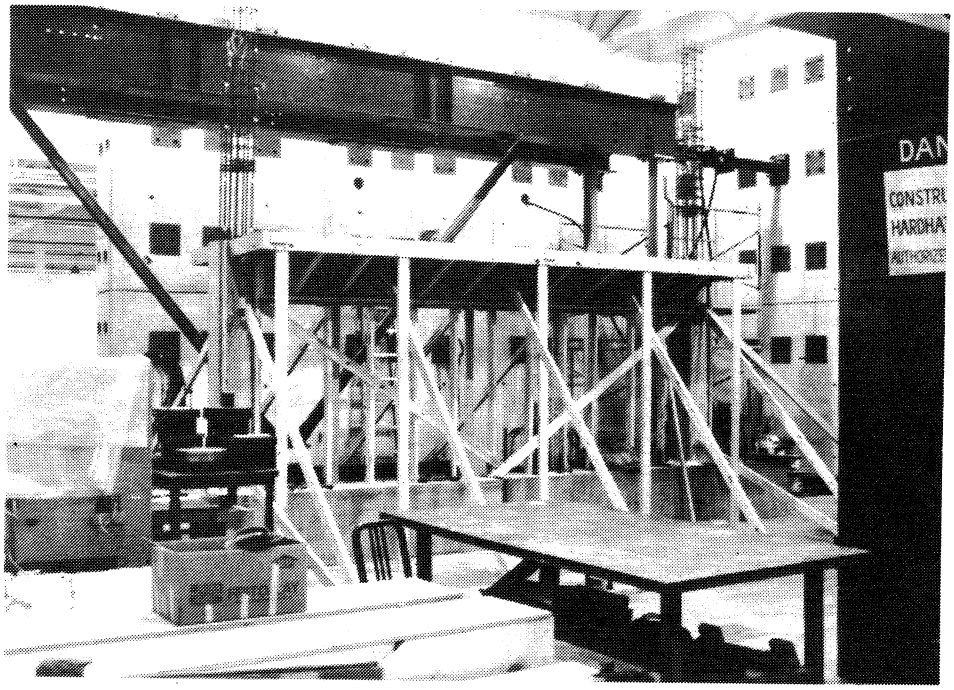

Fig. 3.7 First–Story Beam and Slab Formwork Shoring

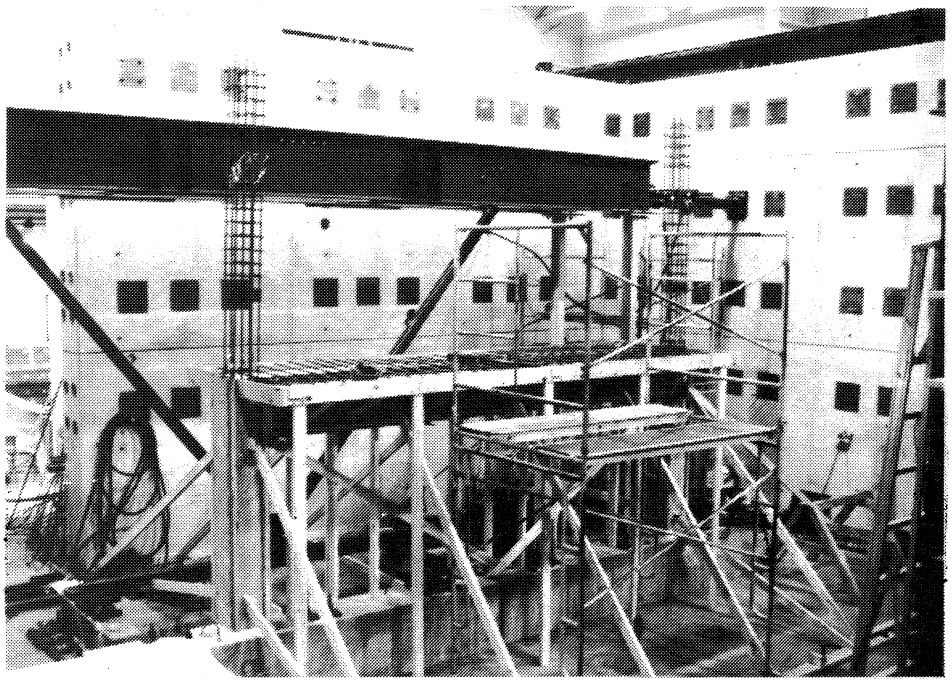

Fig. 3.8 Formwork Shoring and Working Platform

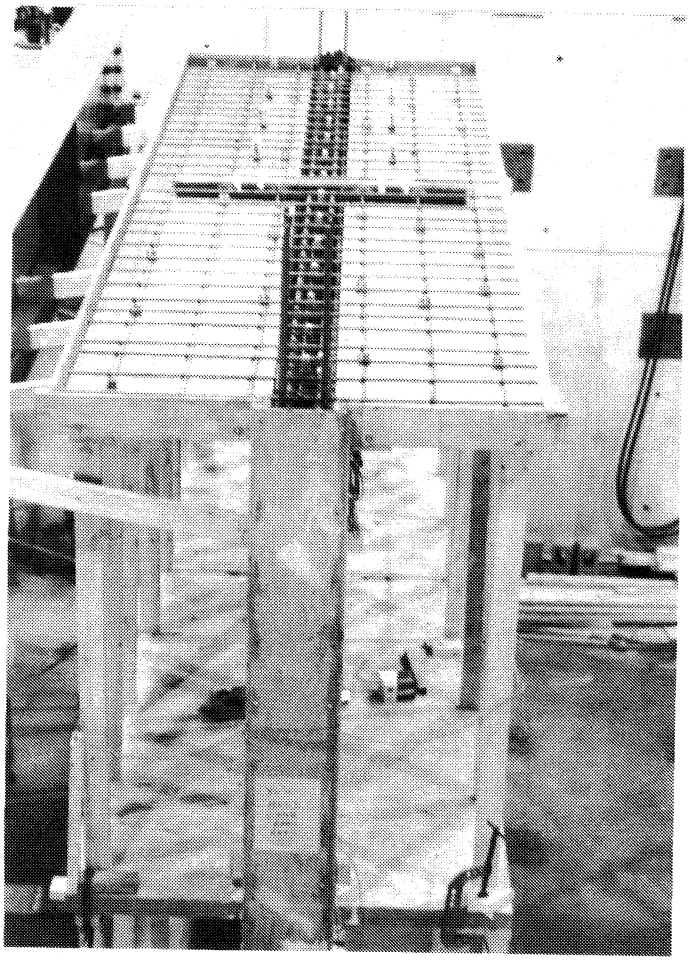

Fig. 3.9 Second–Story Column and Beam Lateral Bracing

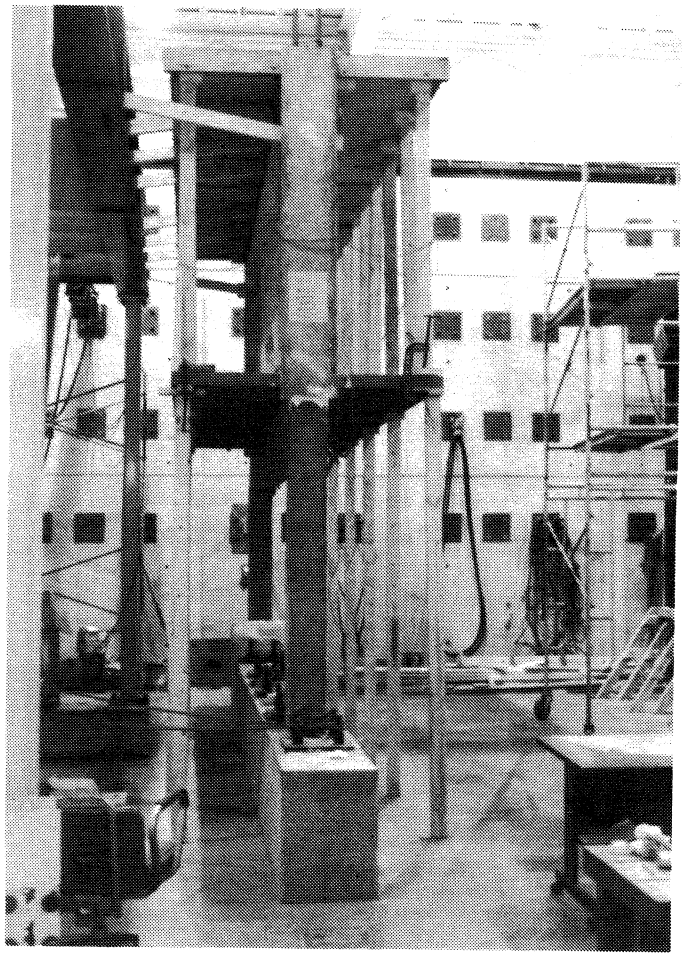

Fig. 3.10 Second–Story Shoring and First–Story Reshoring

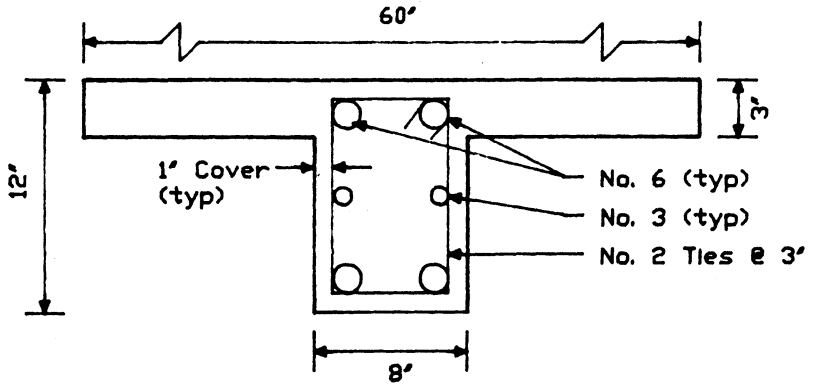

Second Story Beam Section

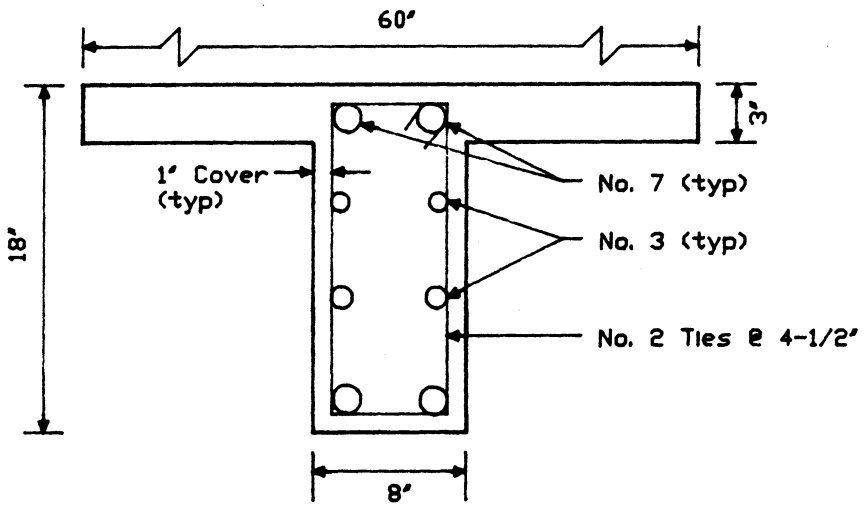

First Story Beam Section

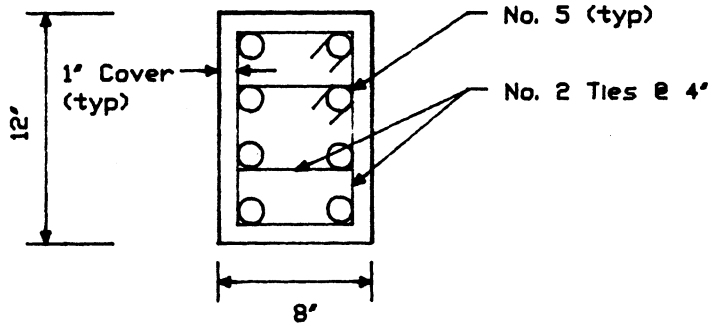

Column Section

Fig. 3.11 Frame Member Cross Sections

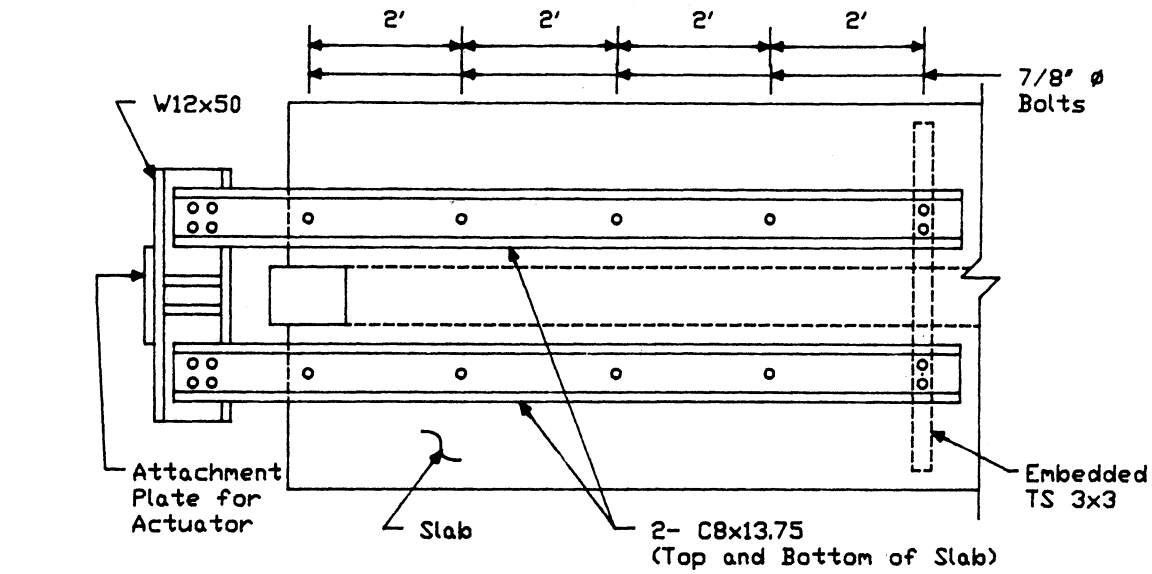

Plan

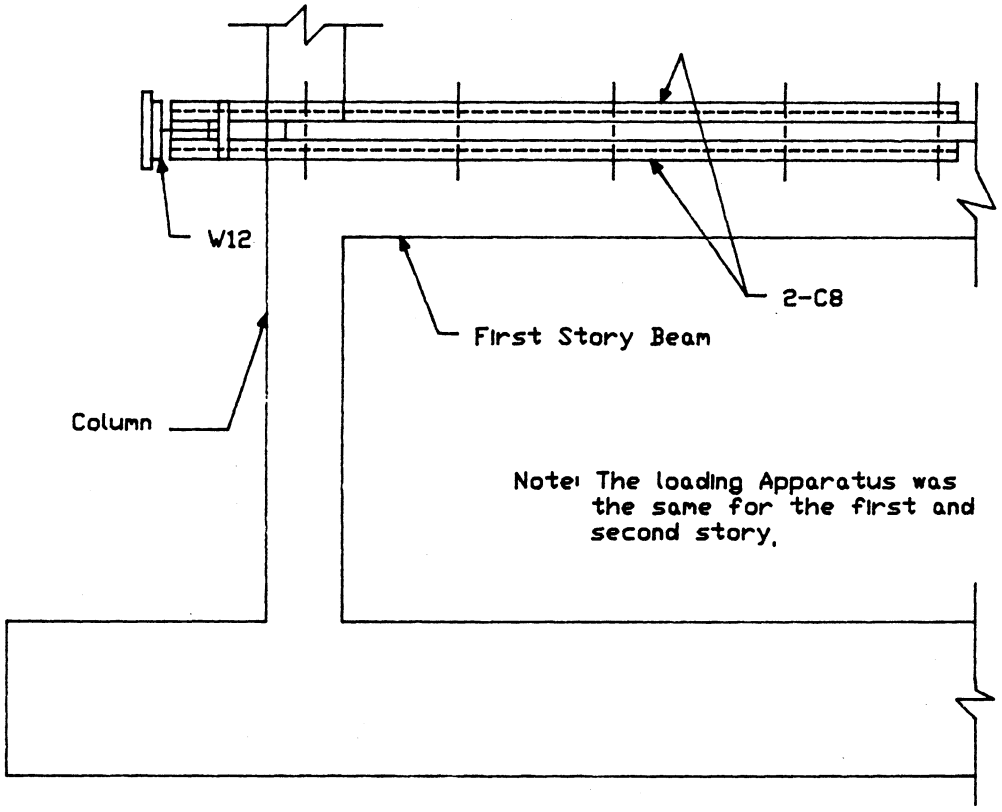

Elevation

Fig. 3.12 Loading Apparatus

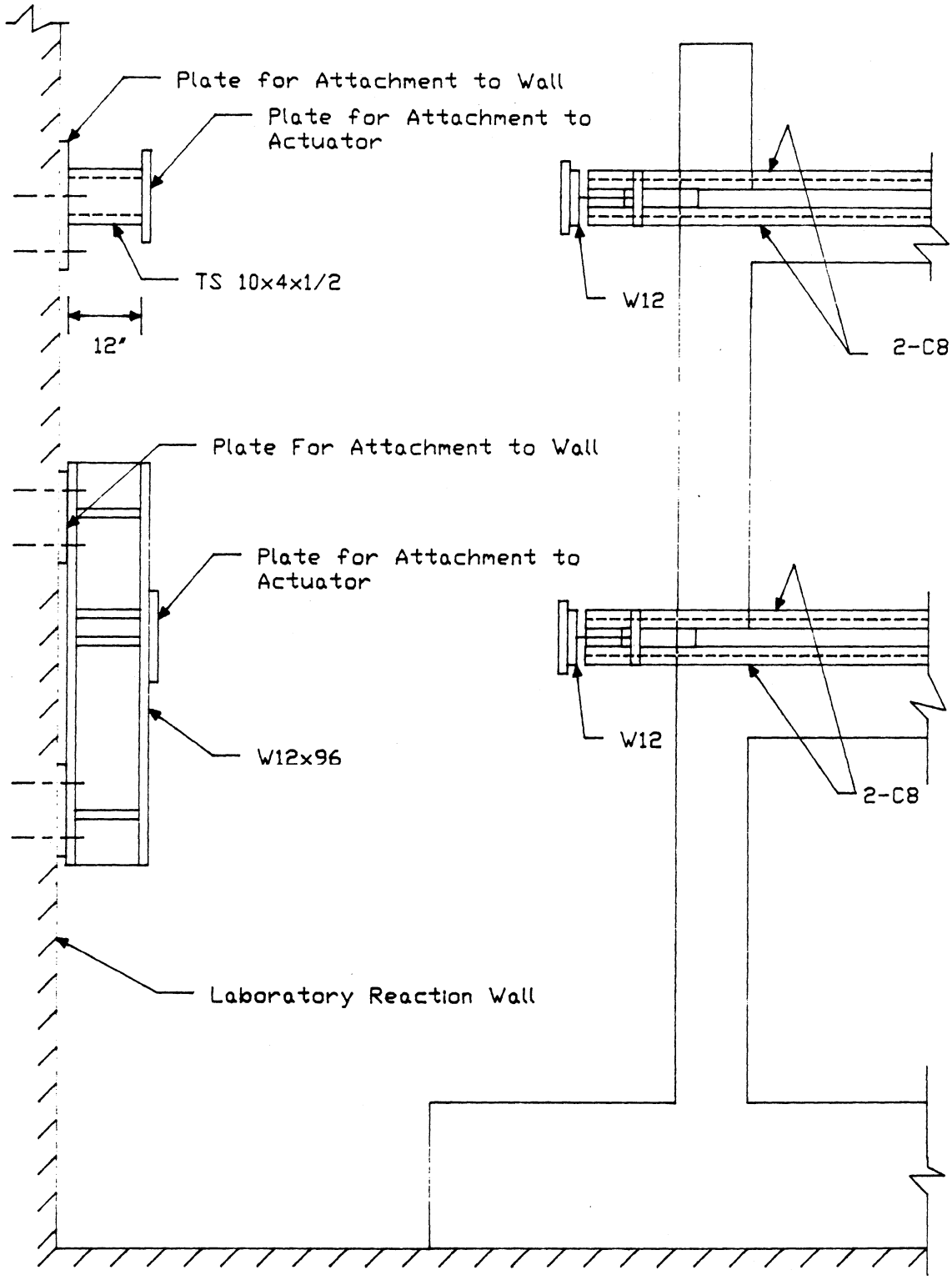

Elevation

Fig. 3.13 Auxiliary Steel Used to Attach Actuators to the Laboratory Reaction Wall

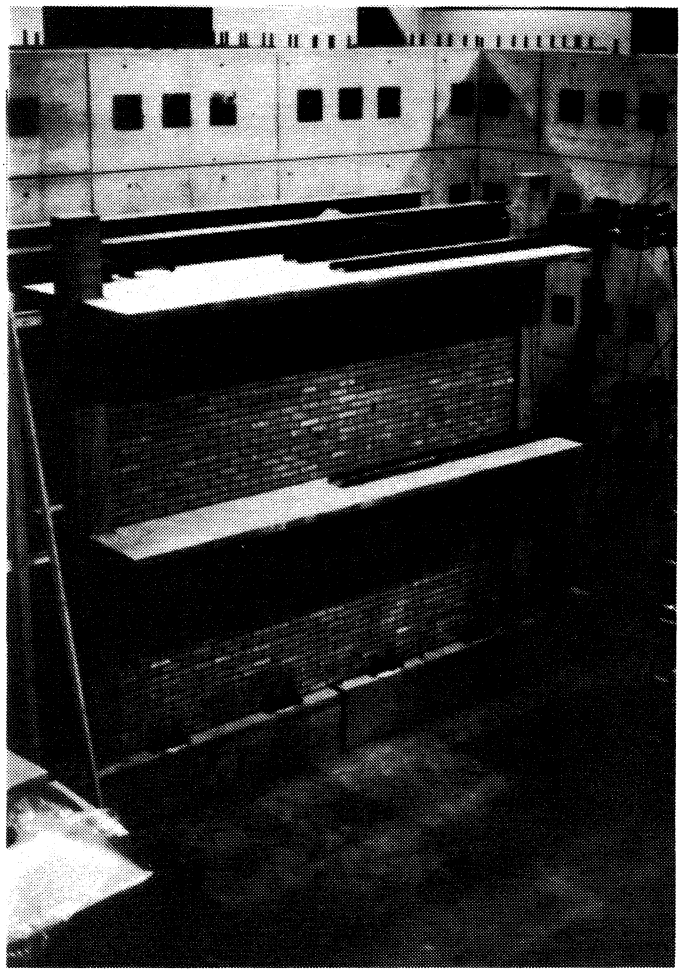

Fig. 3.14 Infilled Frame Specimen in The Structures Lab

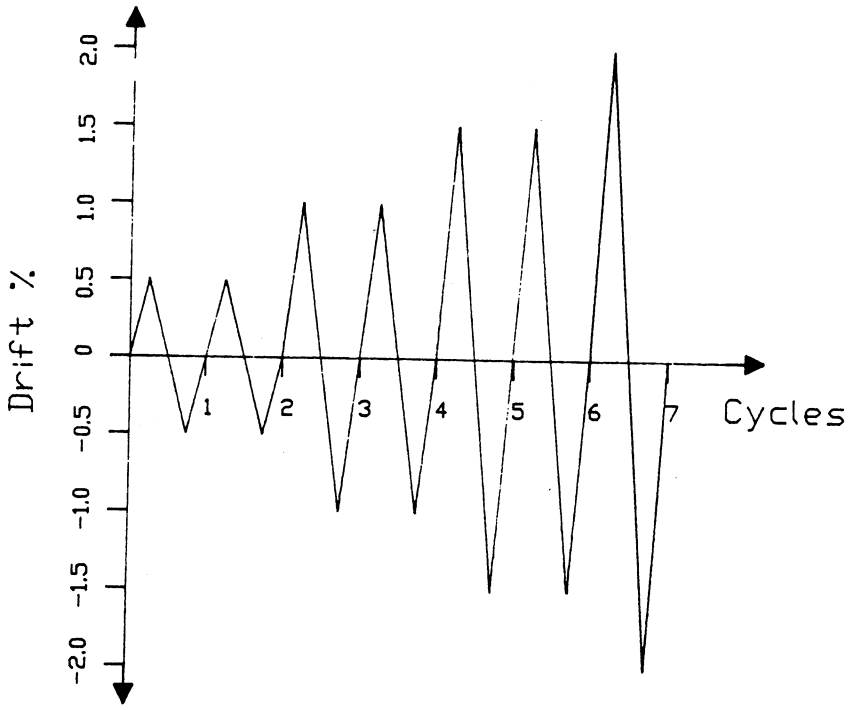

A) Test #1

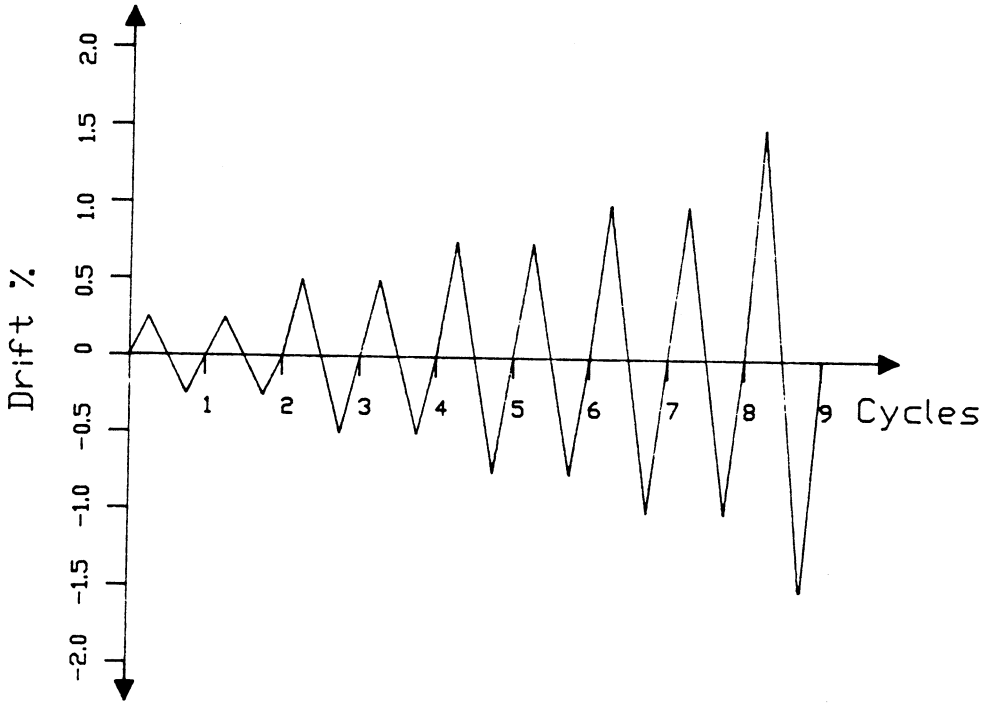

B) Test #2

Fig. 3.15 Reversed Cyclic Loading Patterns

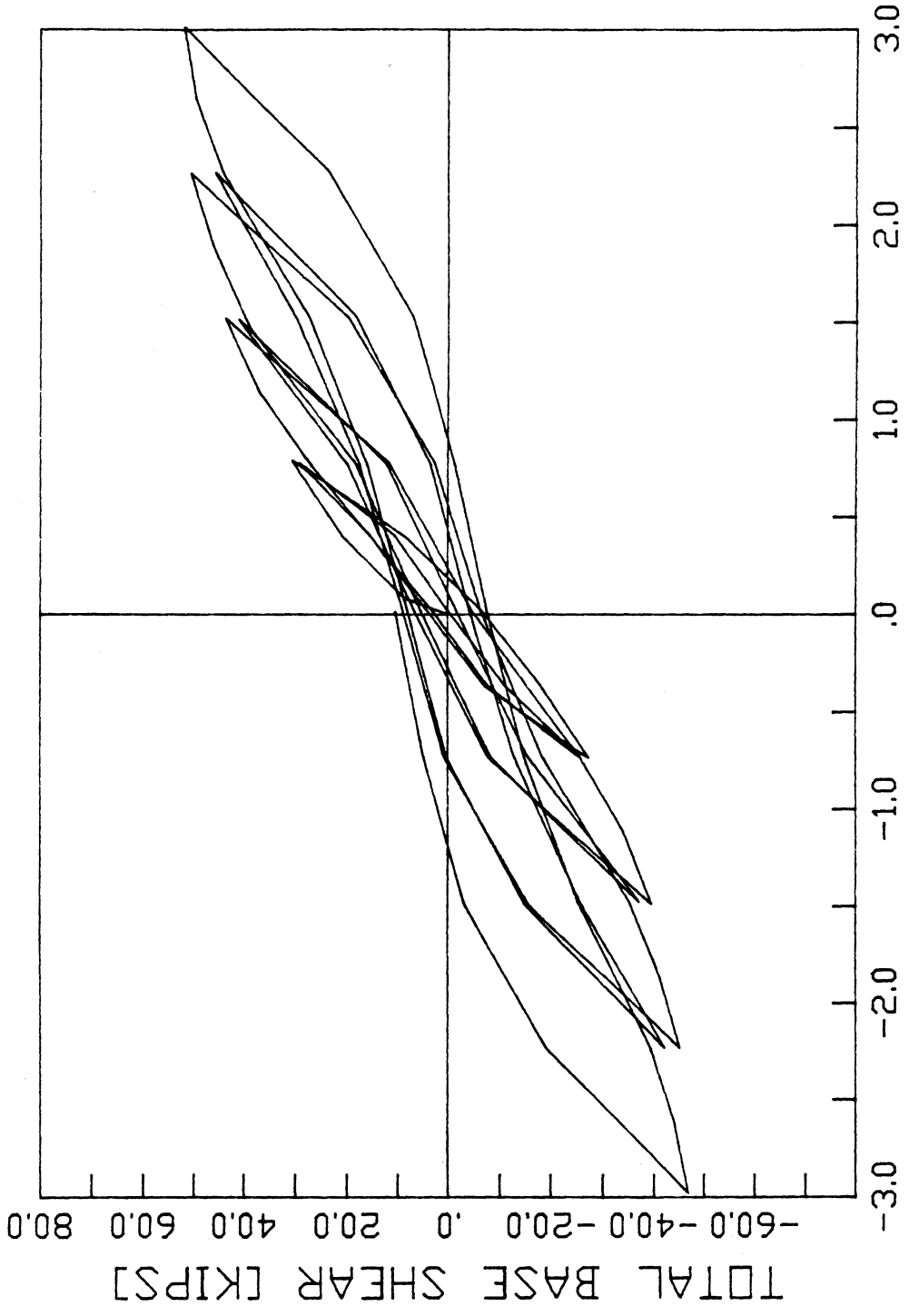

Fig. 3.16 Hysteresis Curves for The Original Frame Test

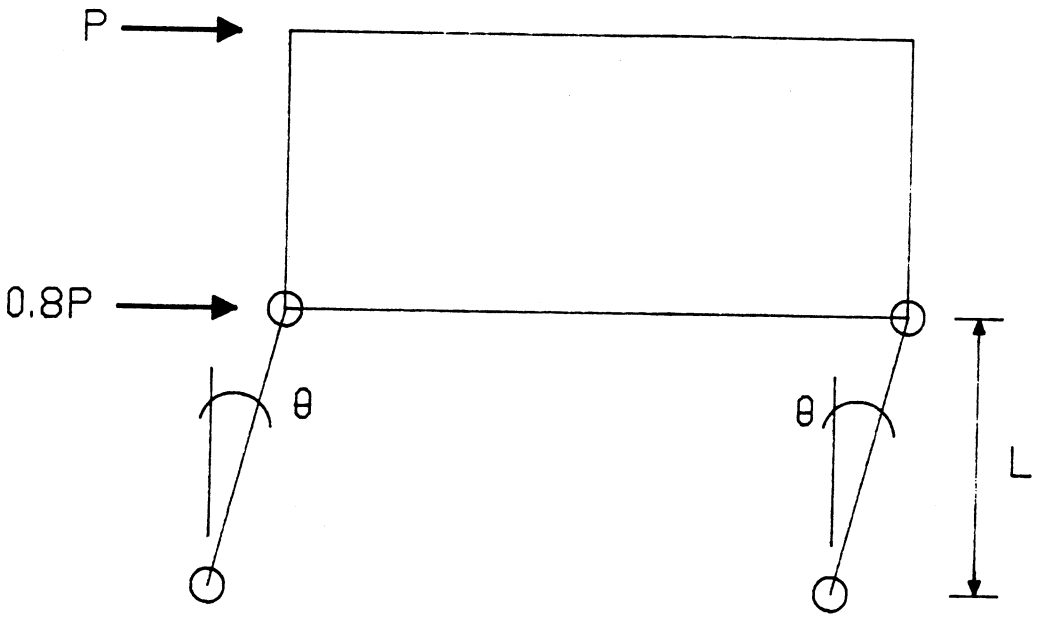

$$L = 69''$$

$$I.W. = 2\theta (M_{col.})_c + 2\theta (M_{col.})_t$$

$$E.W. = P\theta L + 0.8P\theta L$$

$$P = 28.3 \text{ kips}$$

Fig. 3.17 Failure Mechanism Test #1

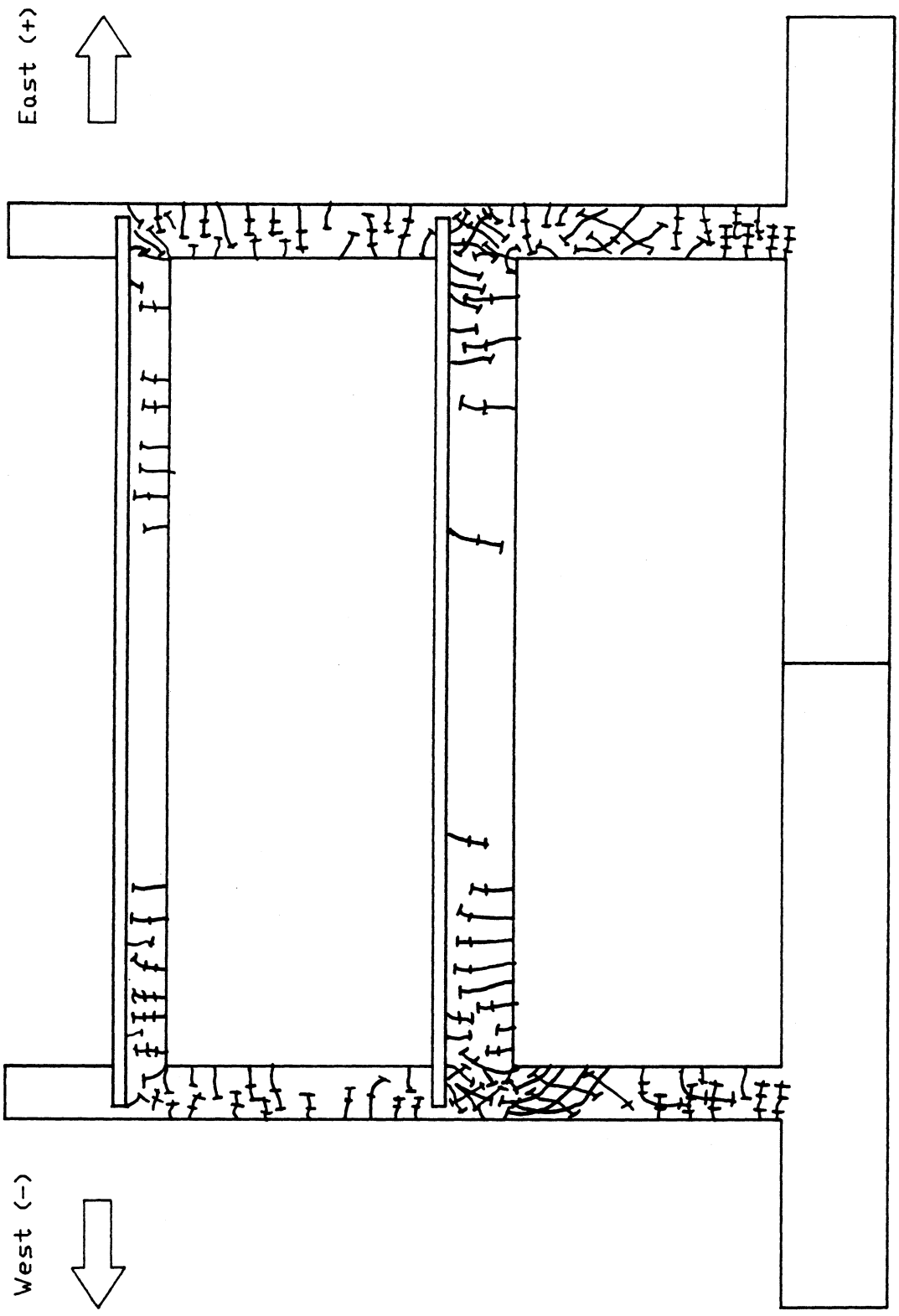

Fig. 3.18 Cracking Patterns Cycle 7, Test #1

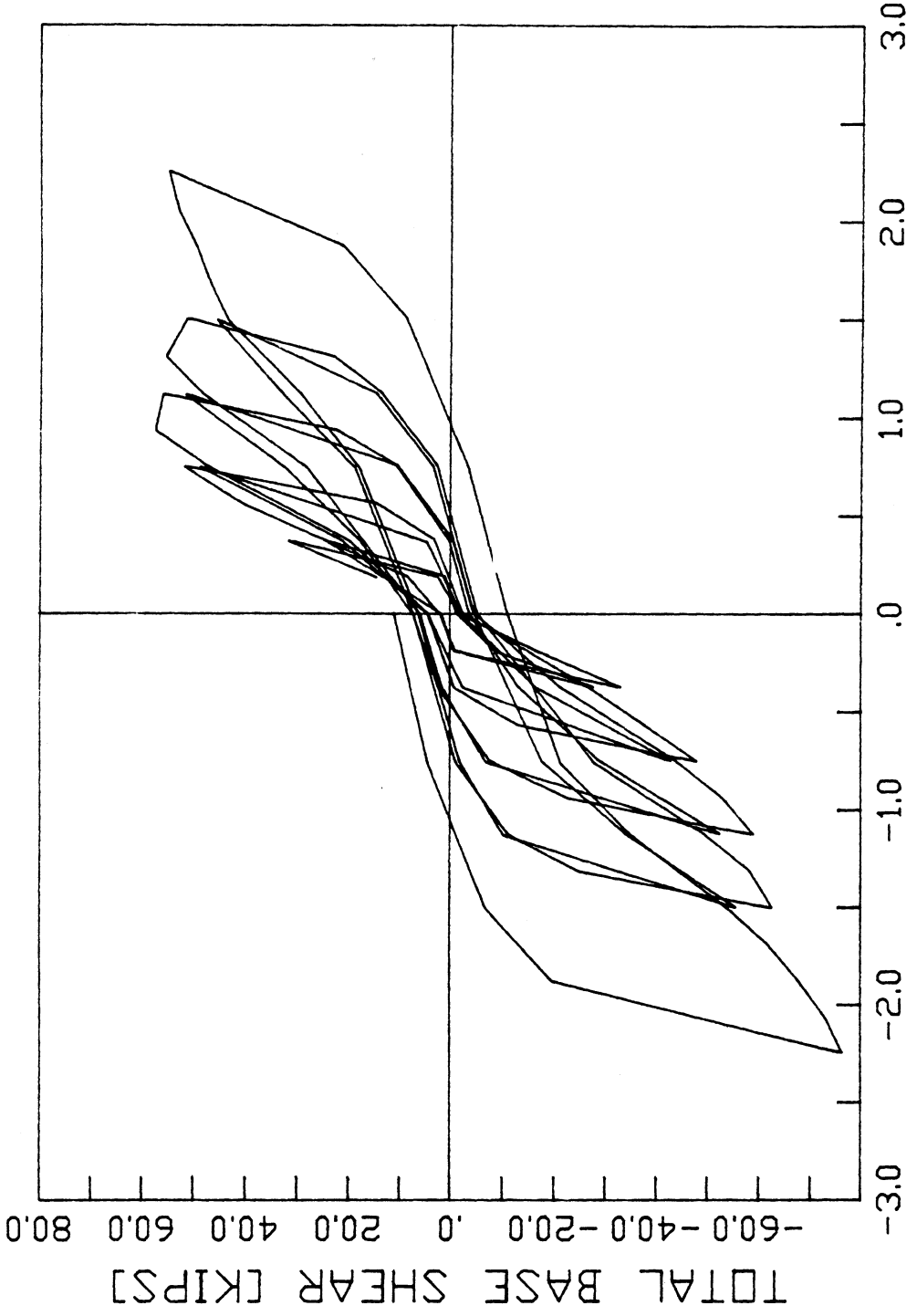

Fig. 3.19 Hysteresis Curves for The Infilled Frame Test

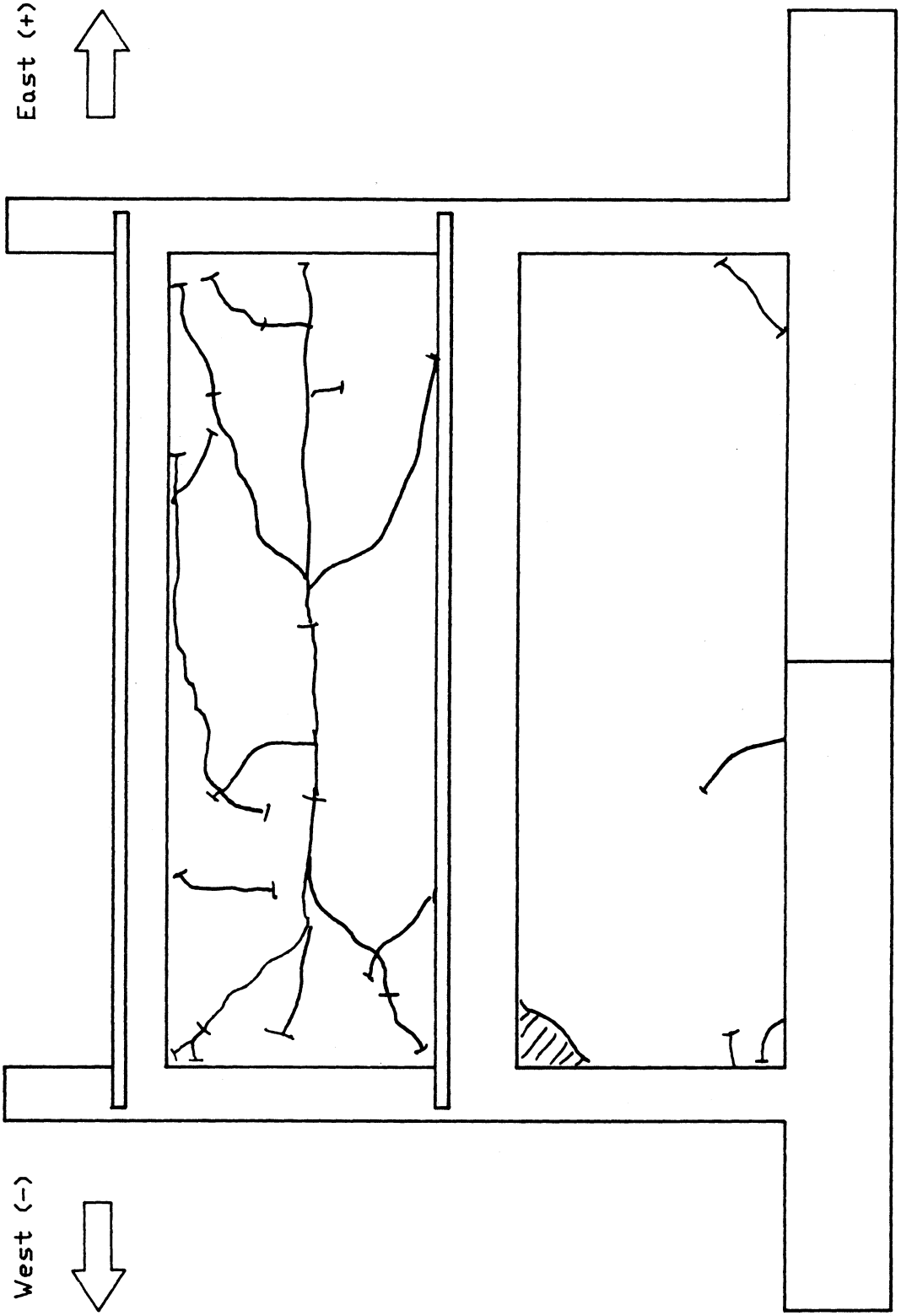

Fig. 3.20 a) Cracking Patterns Cycle 5, Test #2

Fig. 3.20 b) Cracking Patterns Cycle 9, Test #2

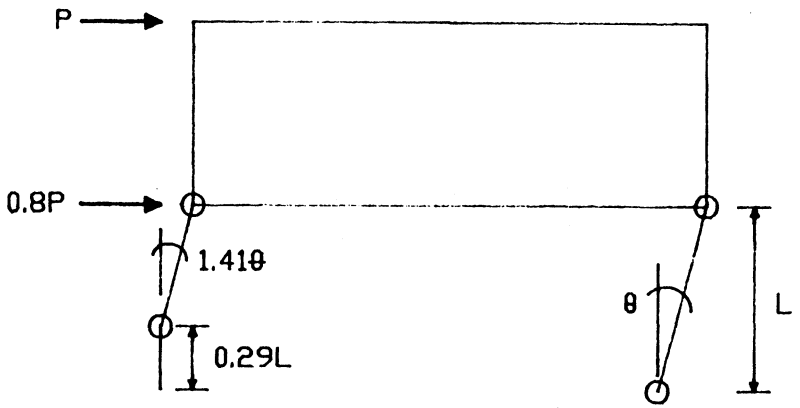

L= 69"

I.W.= $2\theta(M_{col})_c + 2(1.41\theta)(M_{col})_t$

E.W.= $P\theta L + 0.8P\theta L$

P= 33 kips

A) Positive Direction

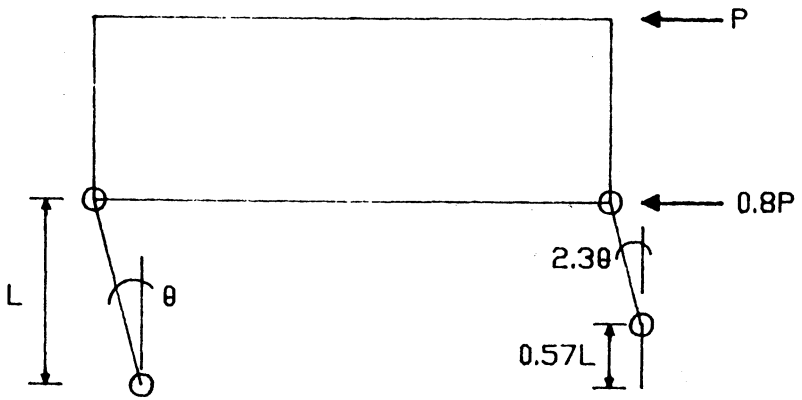

L= 69"

I.W.= $2\theta(M_{col})_c + 2(2.3\theta)(M_{col})_t$

E.W.= $P\theta L + 0.8P\theta L$

P= 44 kips

B) Negative Direction

Fig. 3.21 Failure Mechanisms Test #2

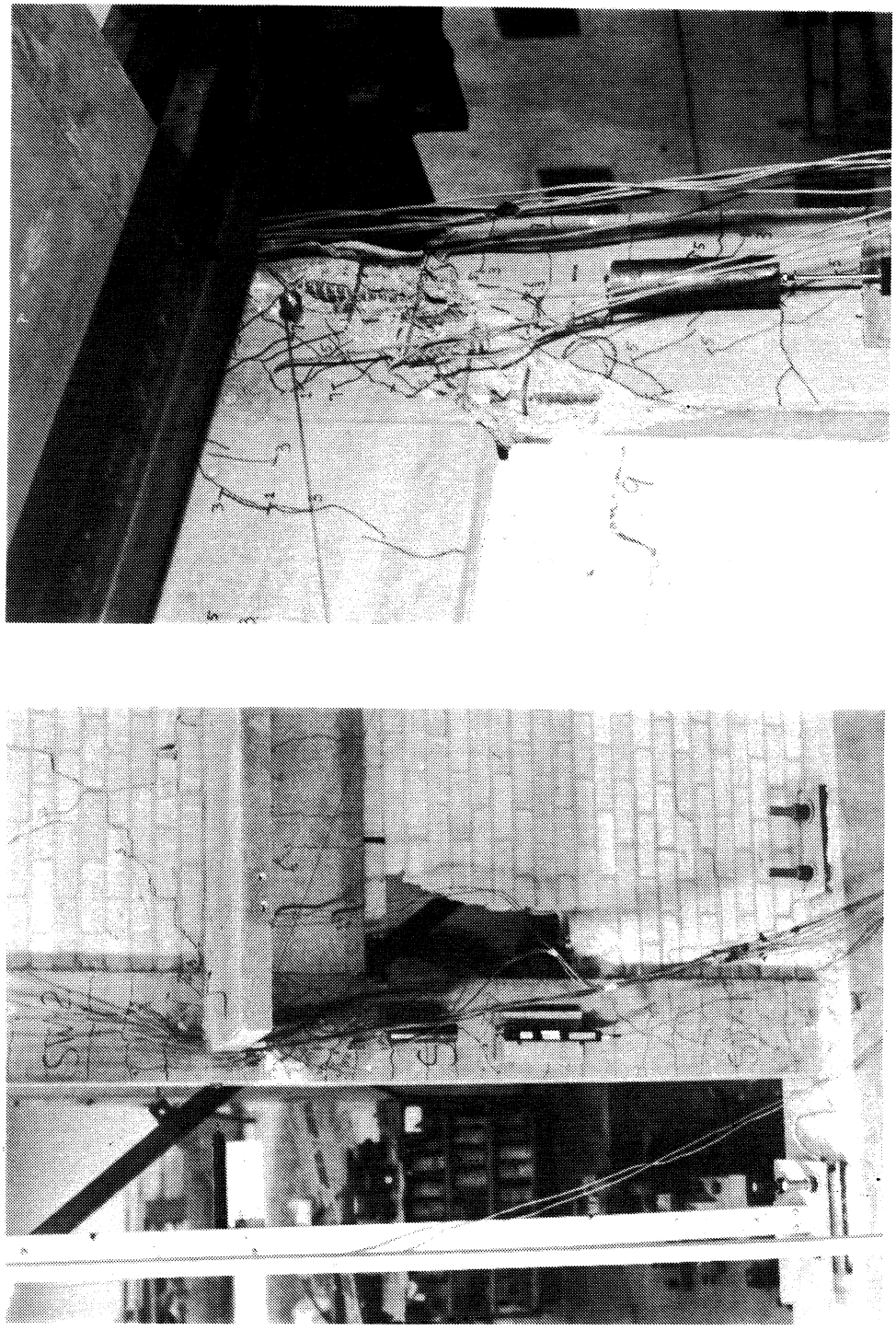

Fig. 3.22 Damage at First-Story Beam/Column Joints

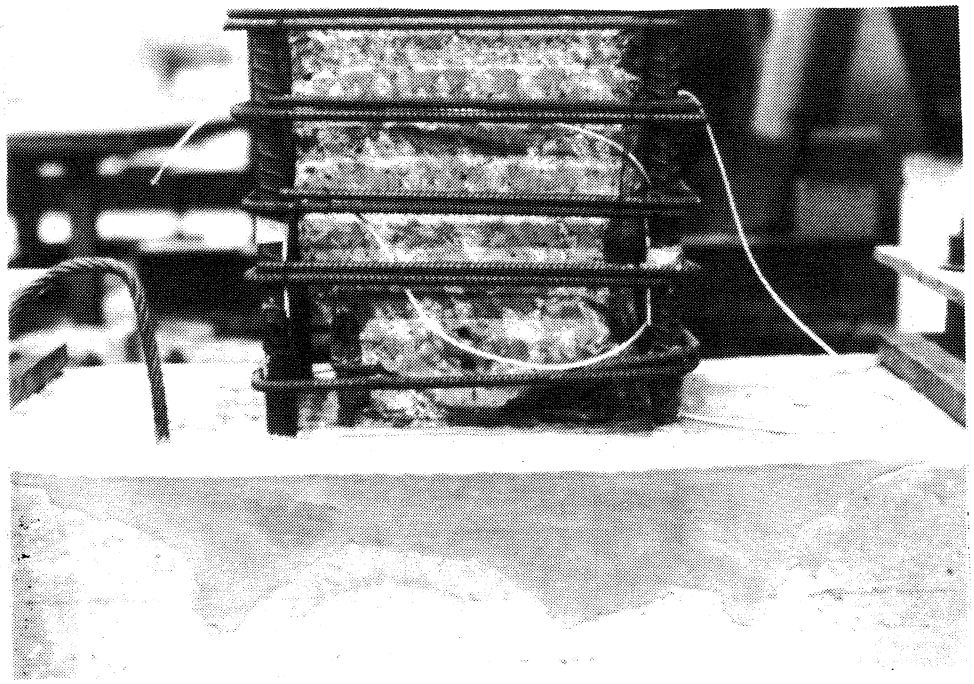

Fig. 4.1 Reduced Column Section at The Foundation

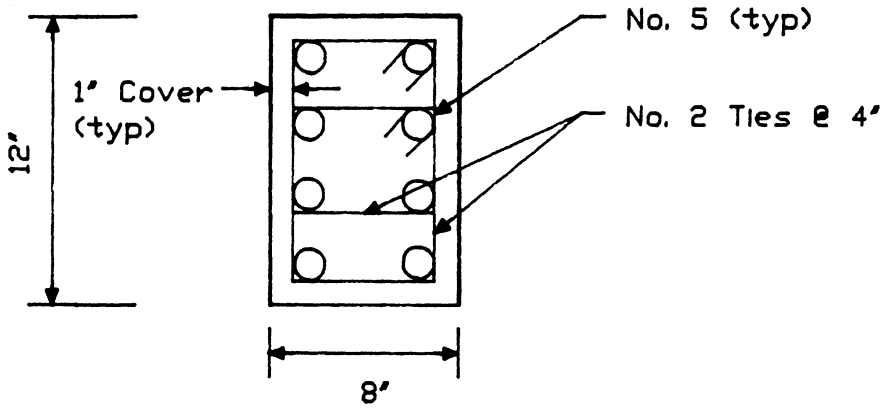

Column Section

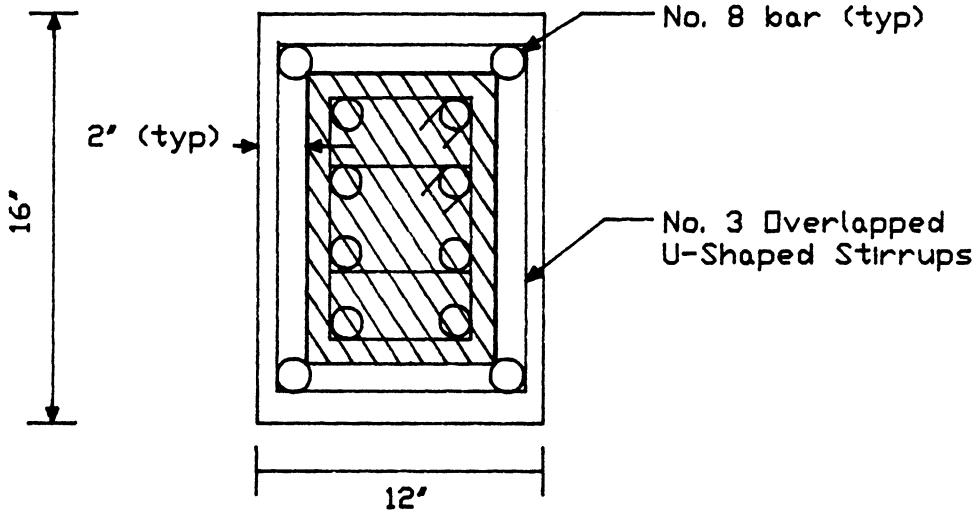

Column Jacket Section

Fig. 4.2 Original and Jacketed Column Sections

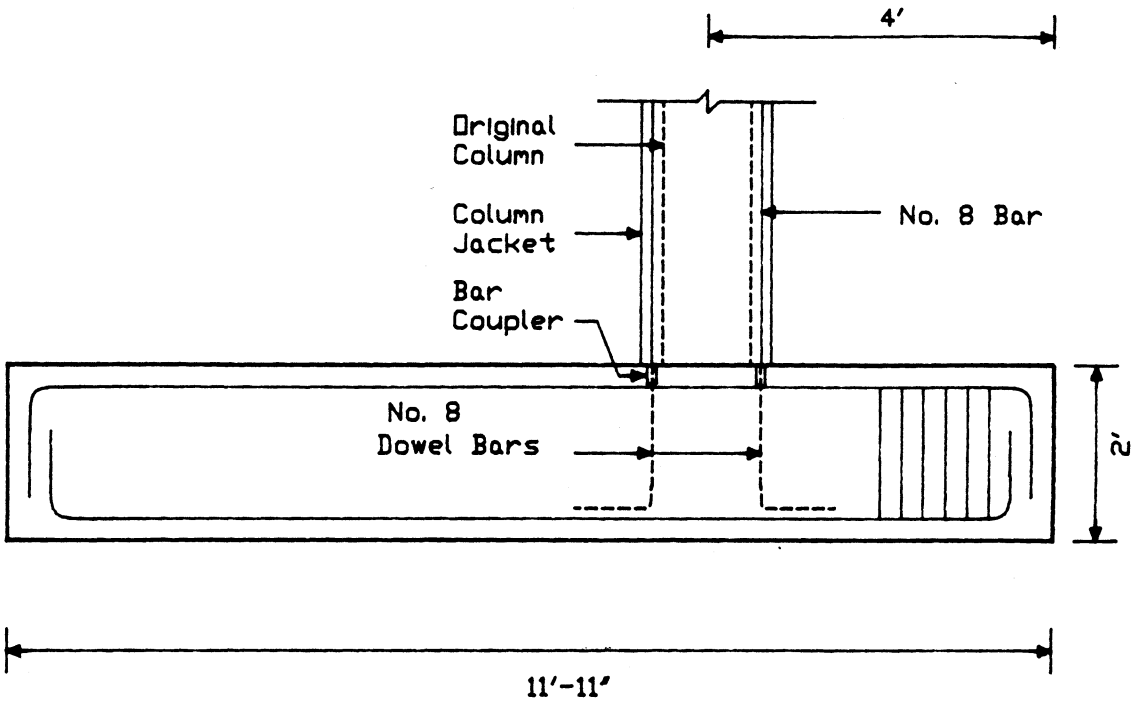

Elevation

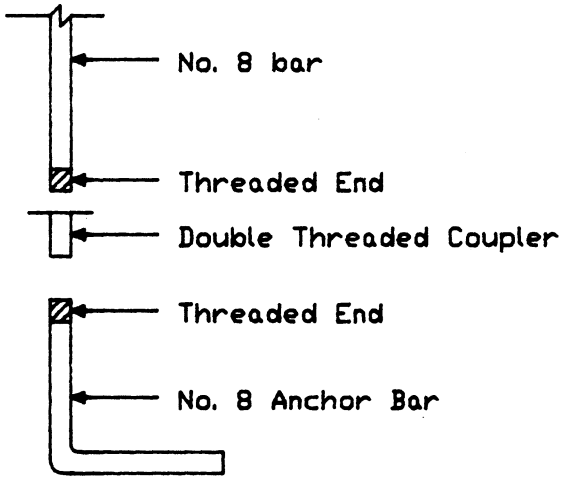

Detail

Fig. 4.3 Bar Coupling Configuration at The Foundation

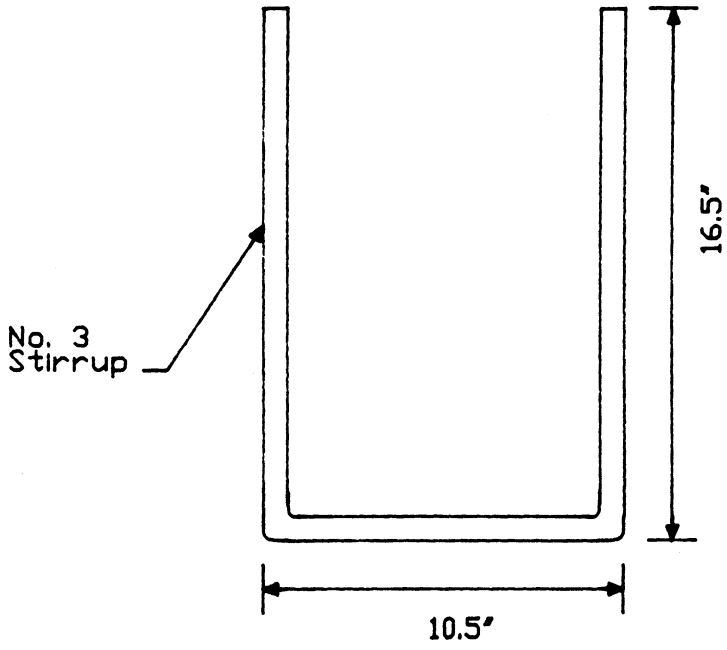

U-Shaped Stirrup

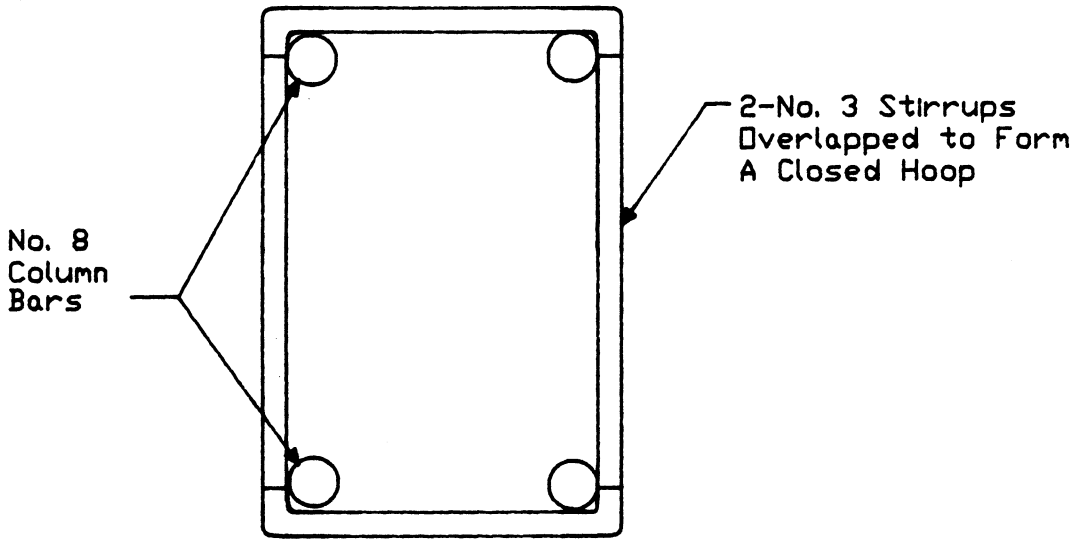

Overlapped Stirrups

Fig. 4.4 Stirrups Used in The Column Jackets

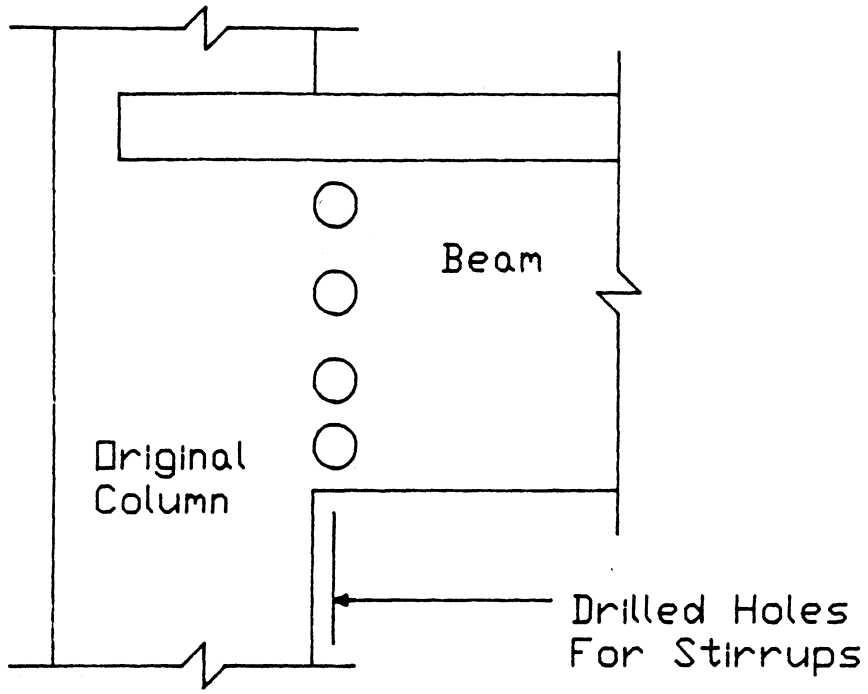

Elevation Of Beam/Column Joint

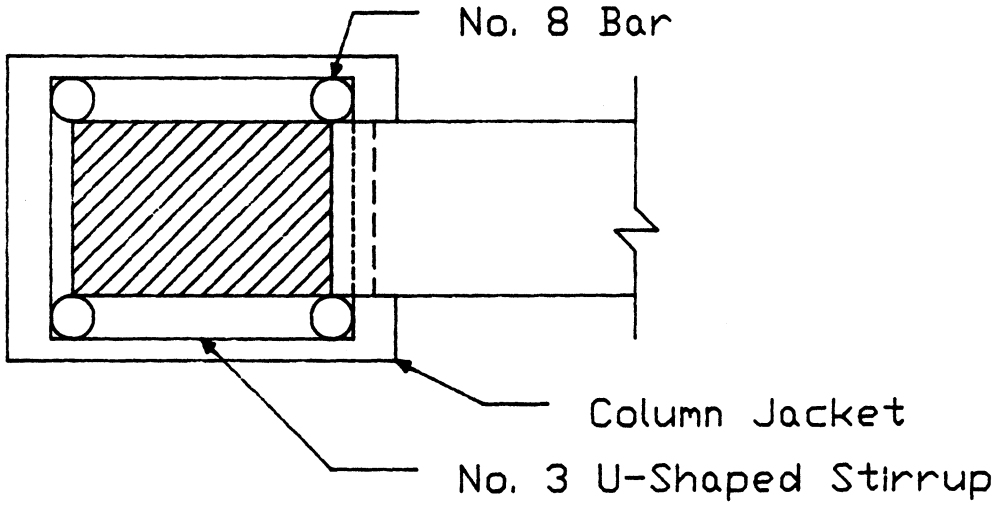

Plan Of Beam/Column Joint

Fig. 4.5 Location of Drilled Holes for Stirrups in Joint Area

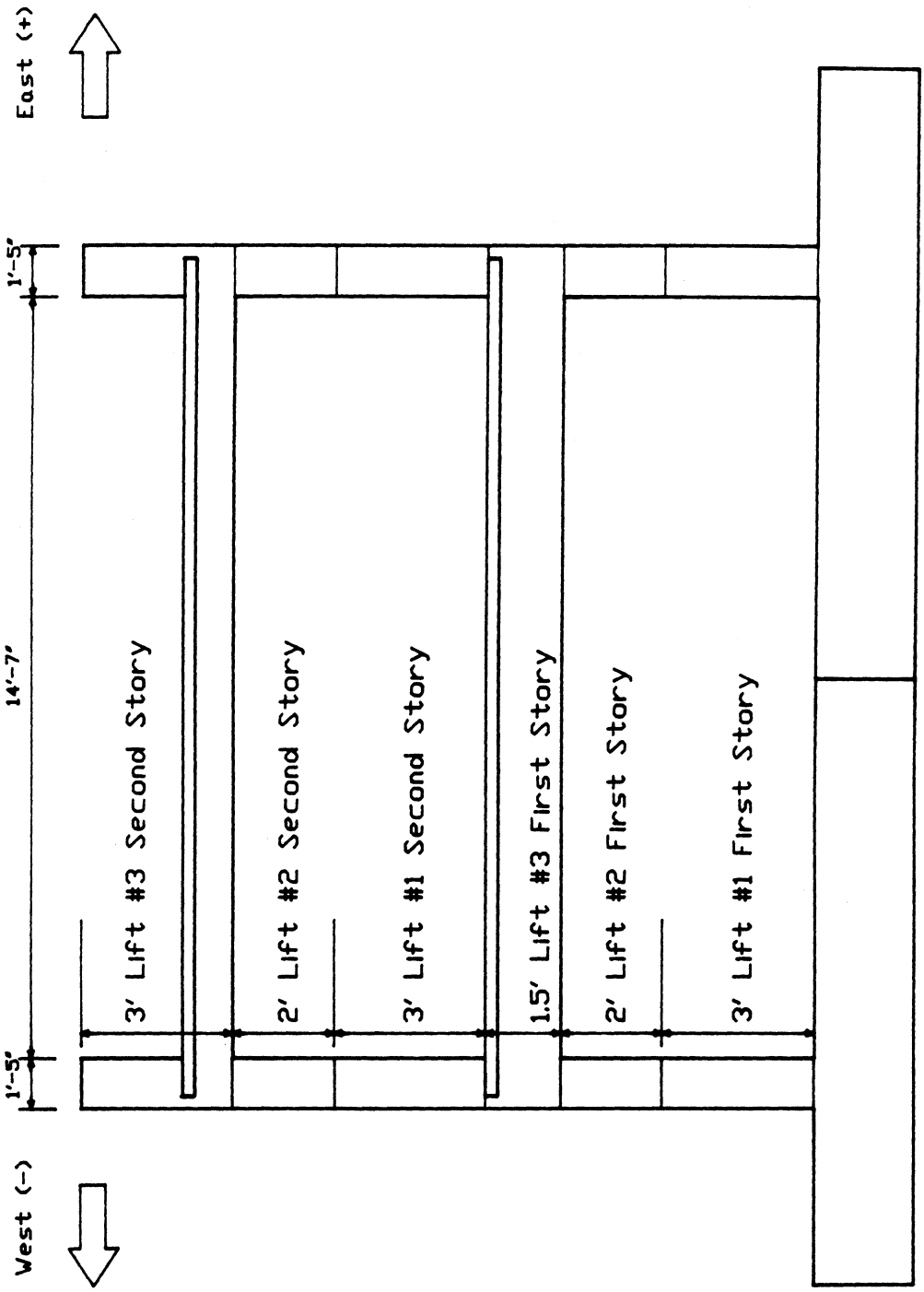

Fig. 4.6 Lift Sequence for The Reinforced Concrete Jacket

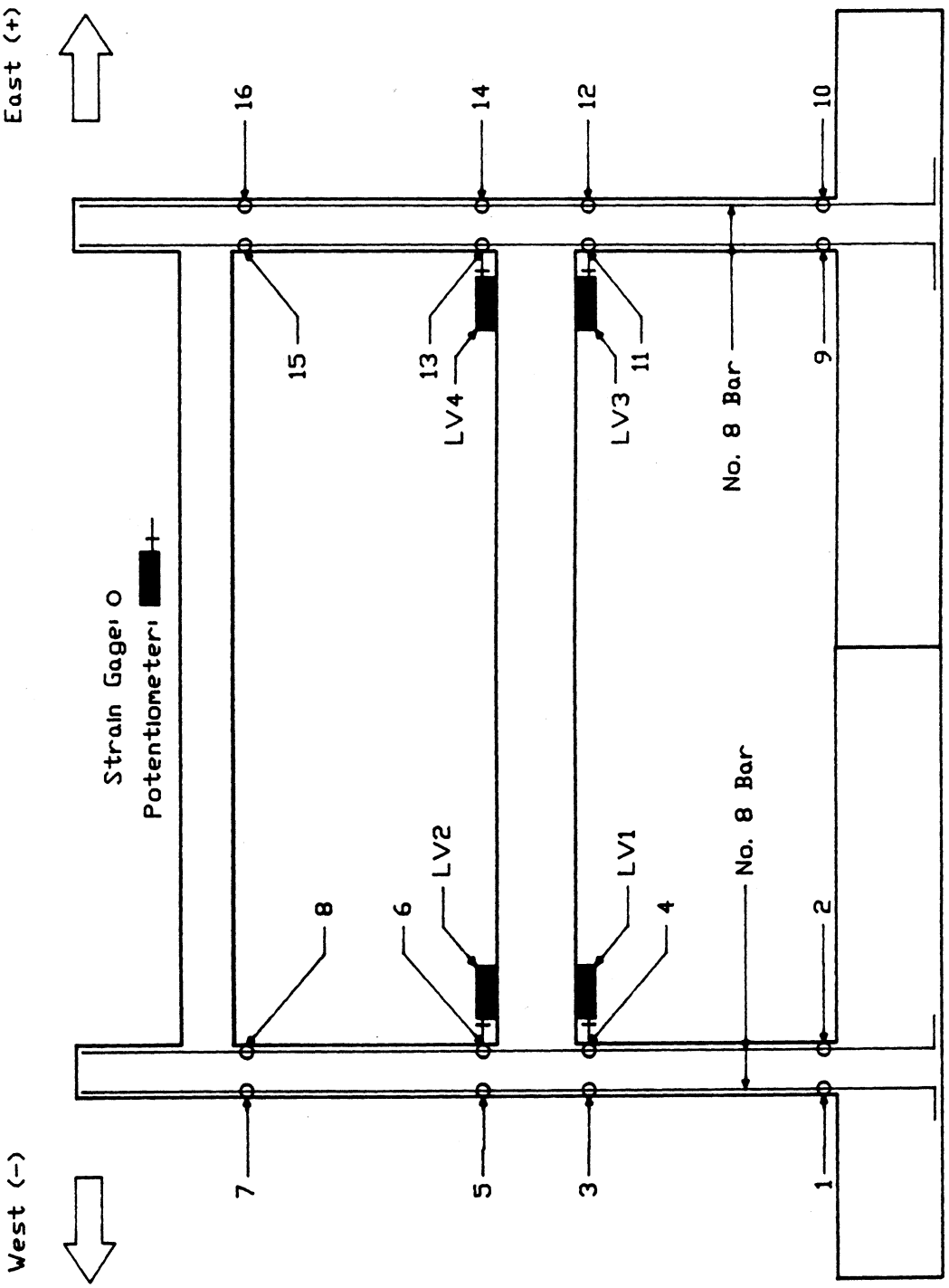

Fig. 4.7 Locations of Strain Gages and Potentiometers

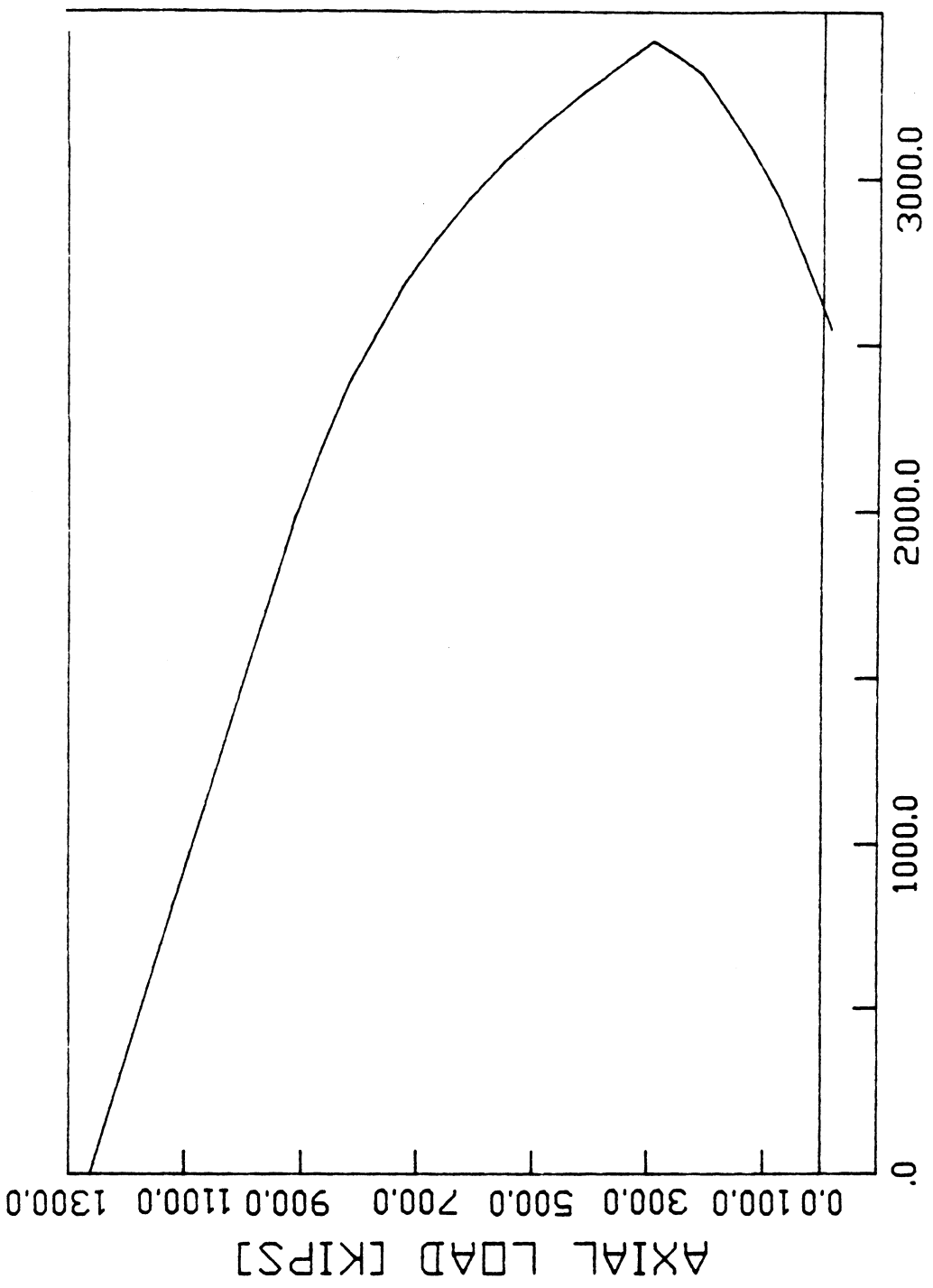

Fig. 4.8 Axial Force vs. Nominal Moment Interaction Curve for Strengthened Columns

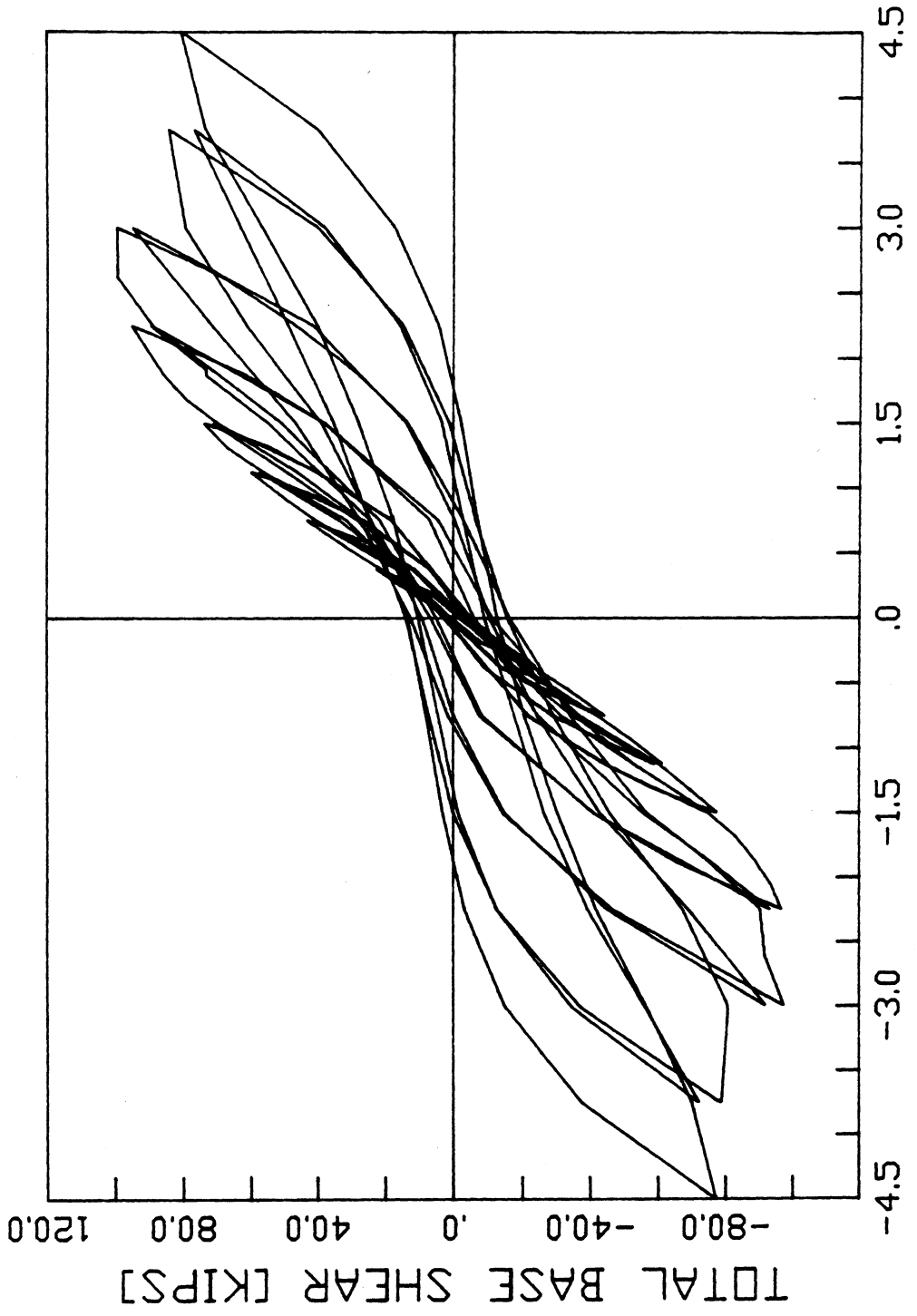

Fig. 5.1 Hysteresis Curves for Strengthened Frame Test

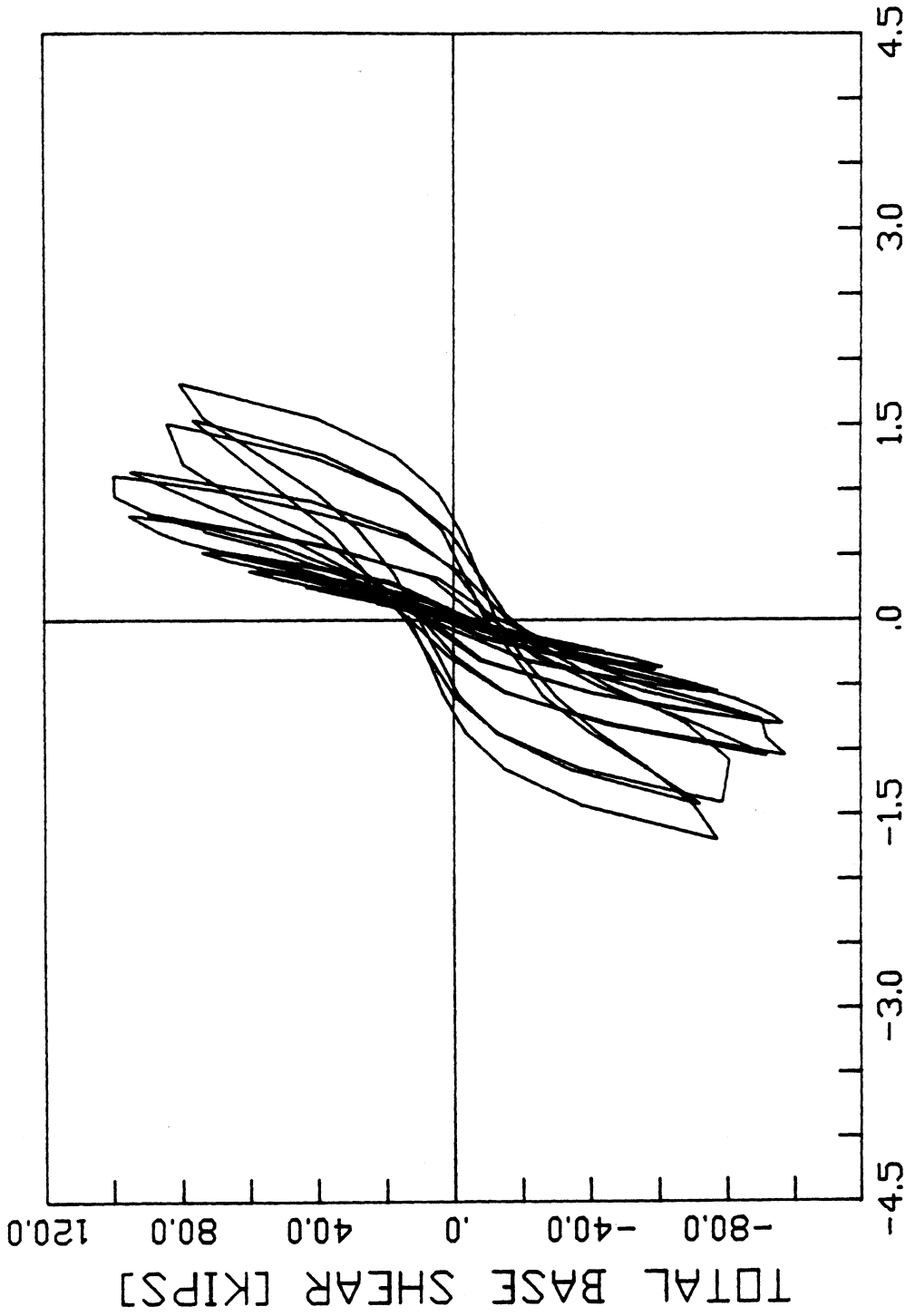

Fig. 5.2 Hysteresis Curves for Strengthened Frame Test

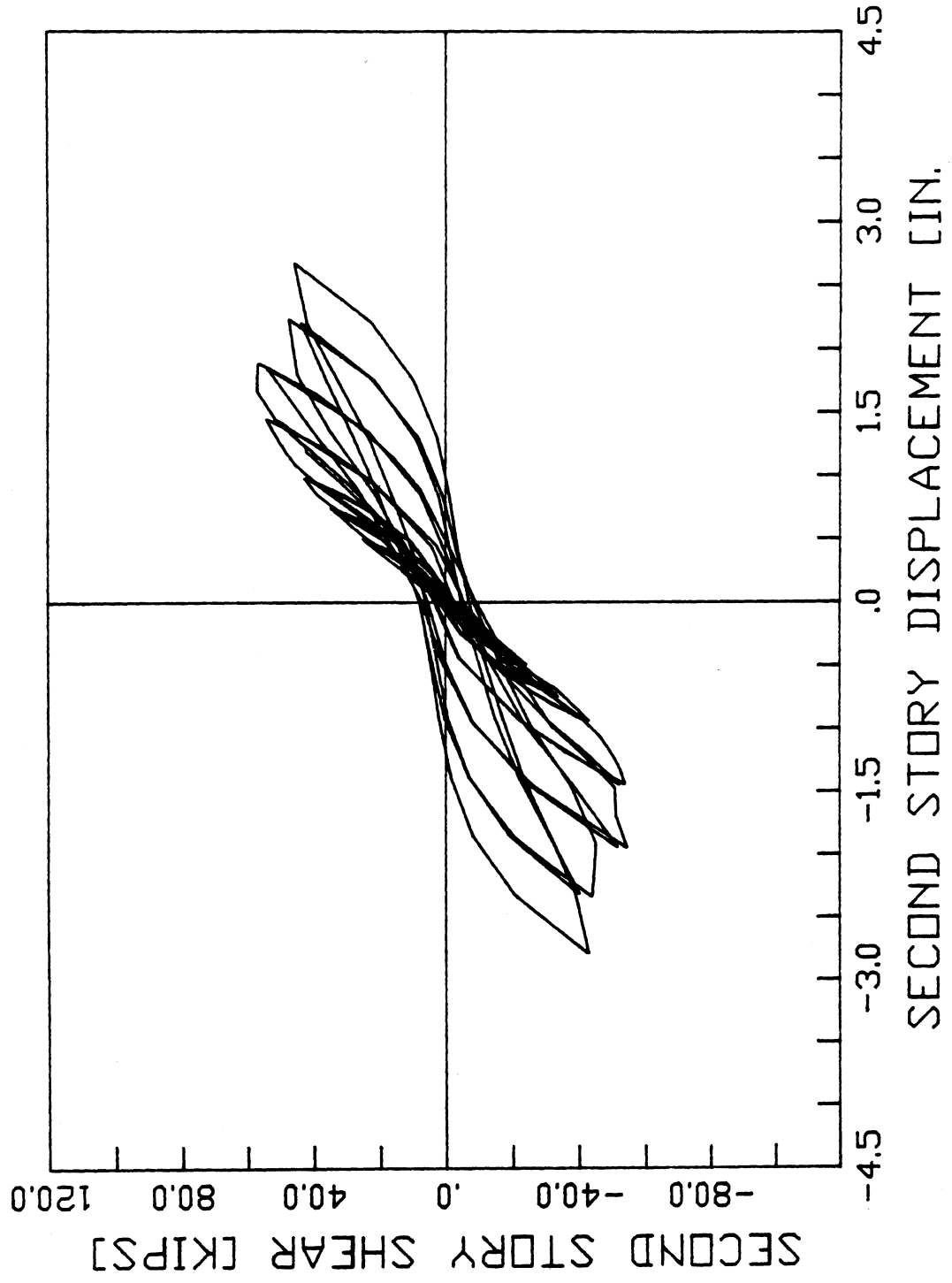

Fig. 5.3 Hysteresis Curves for Strengthened Frame Test

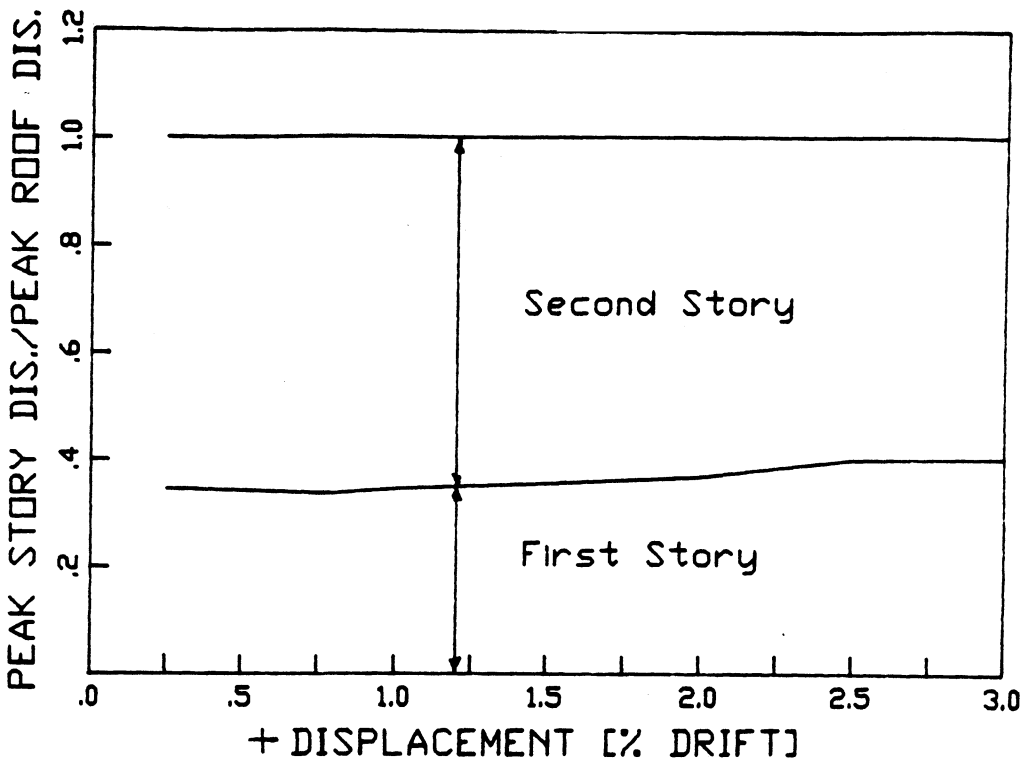

a) Positive Displacement

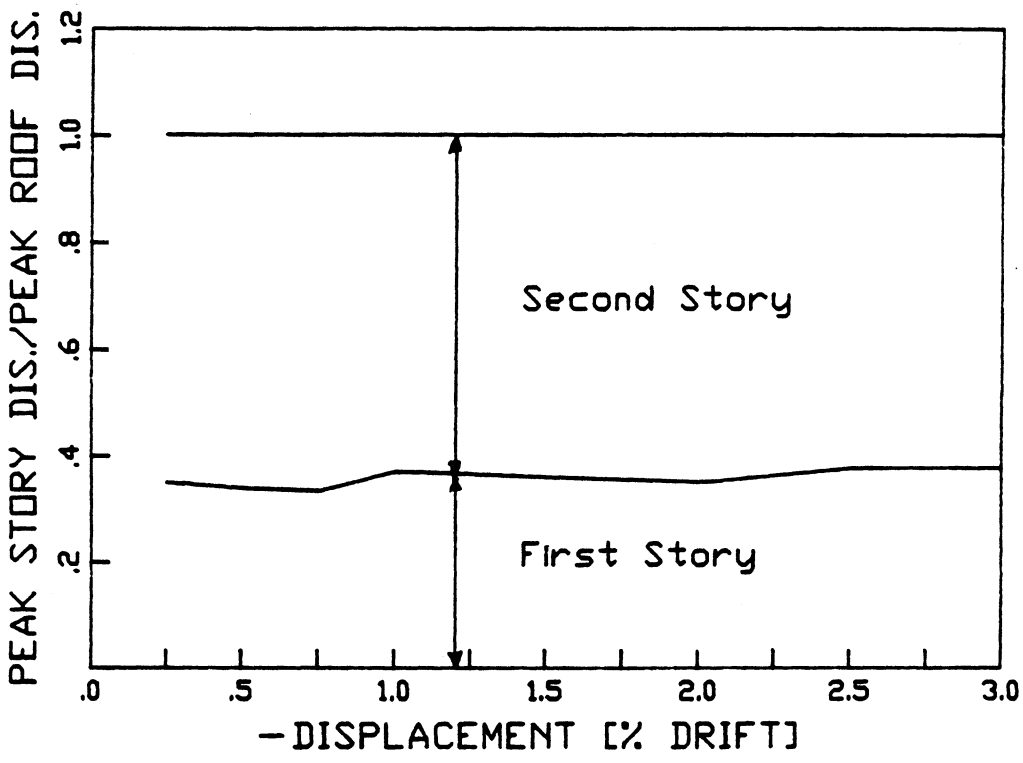

b) Negative Displacement

Fig. 5.4 Contribution of First-Story Displacement to Total Displacement

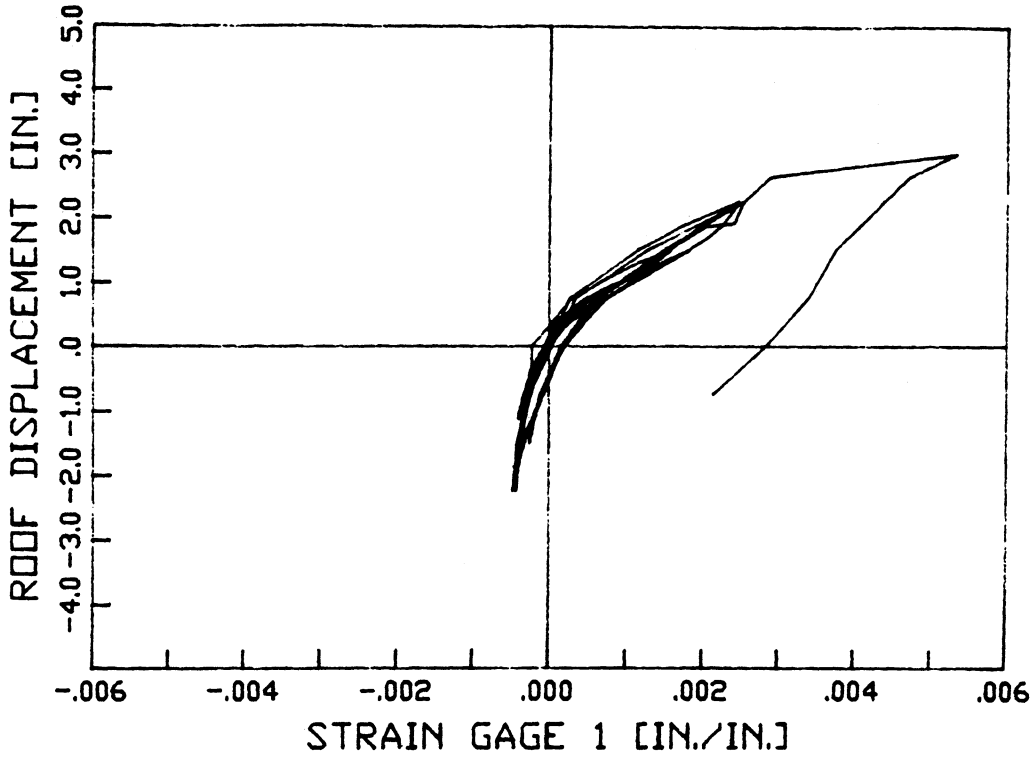

a)

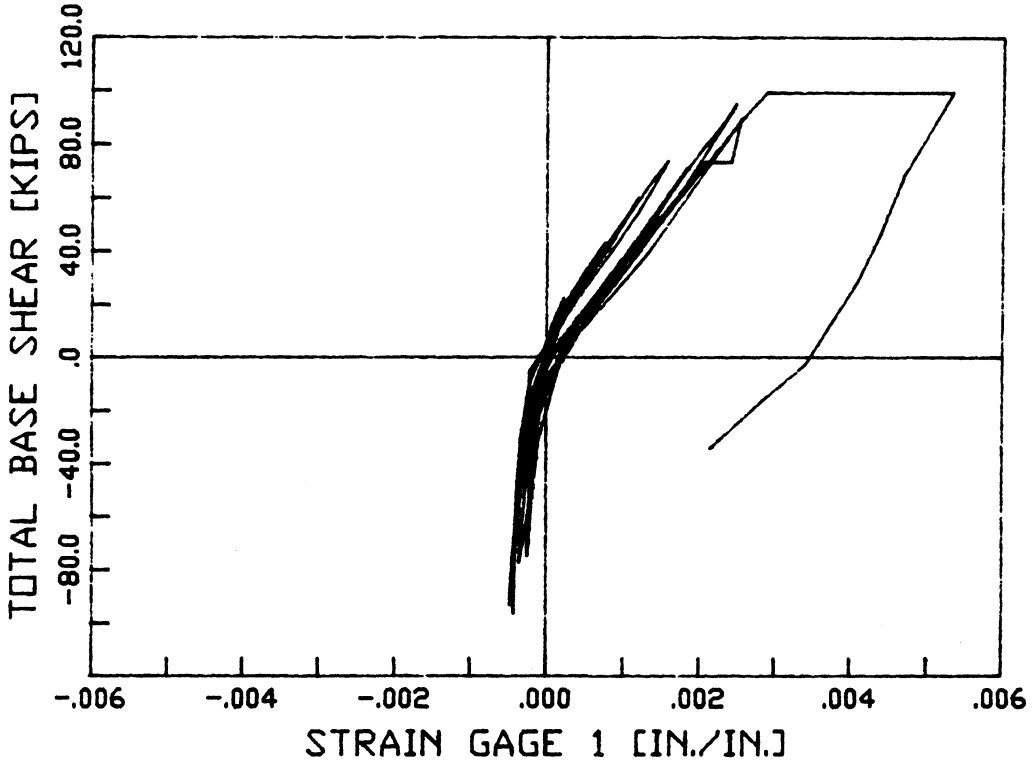

b)

Fig. 5.5 Strain Values From Gage 1 Test #3

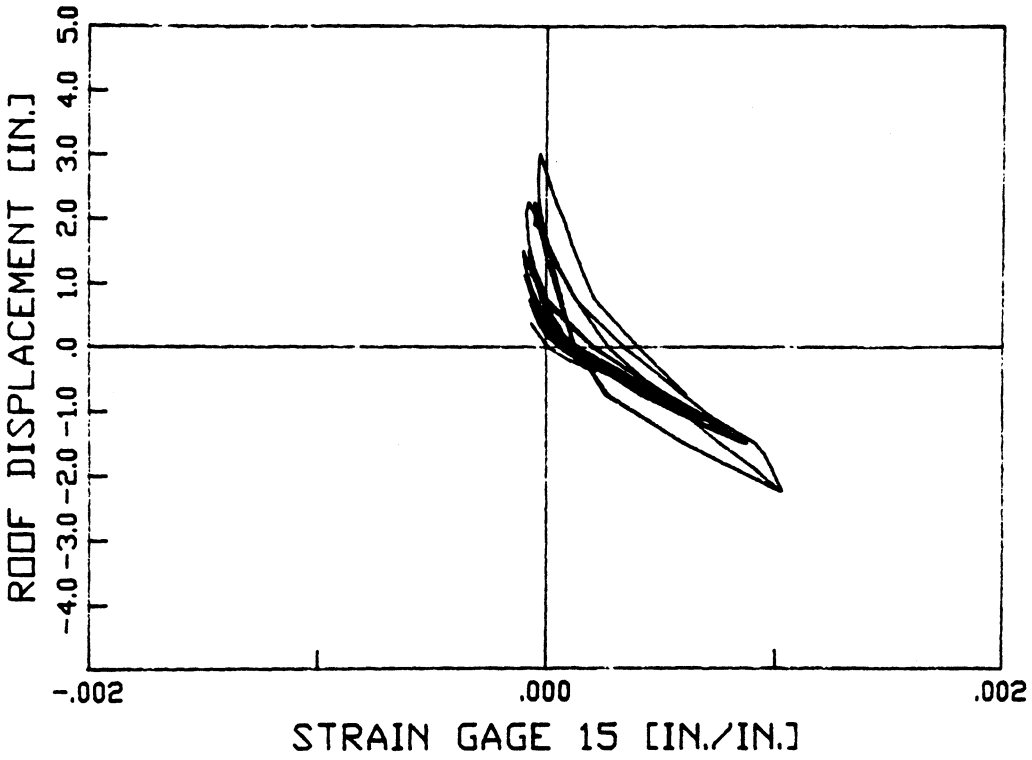

a)

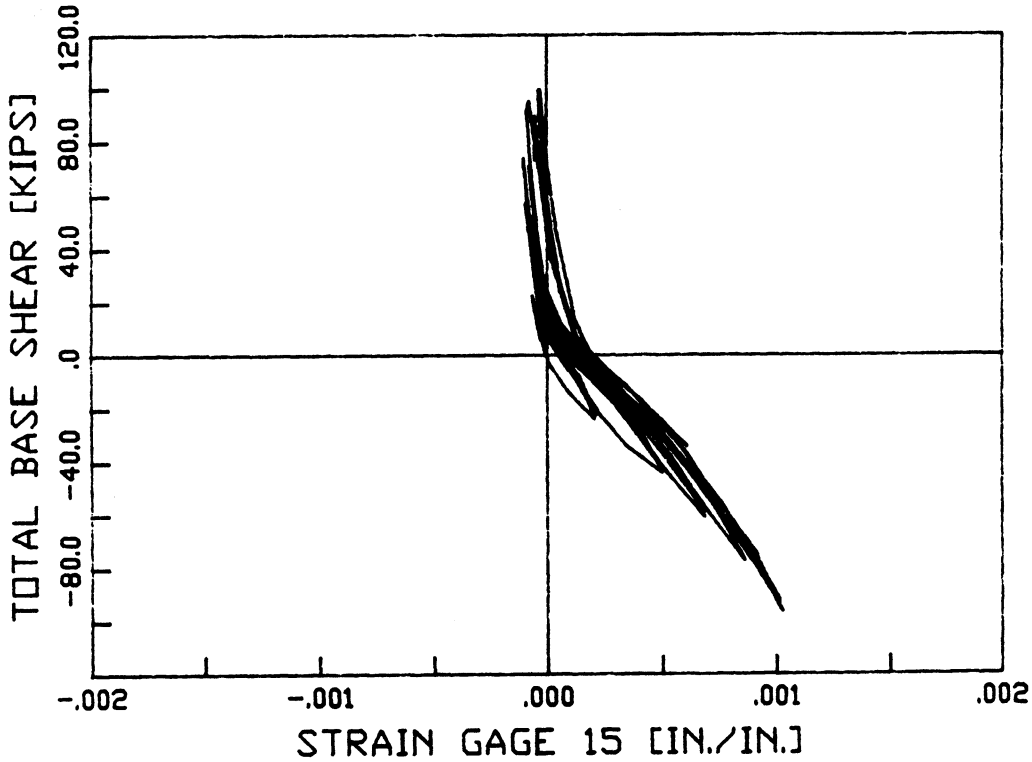

b)

Fig. 5.6 Strain Values From Gage 15 Test #3

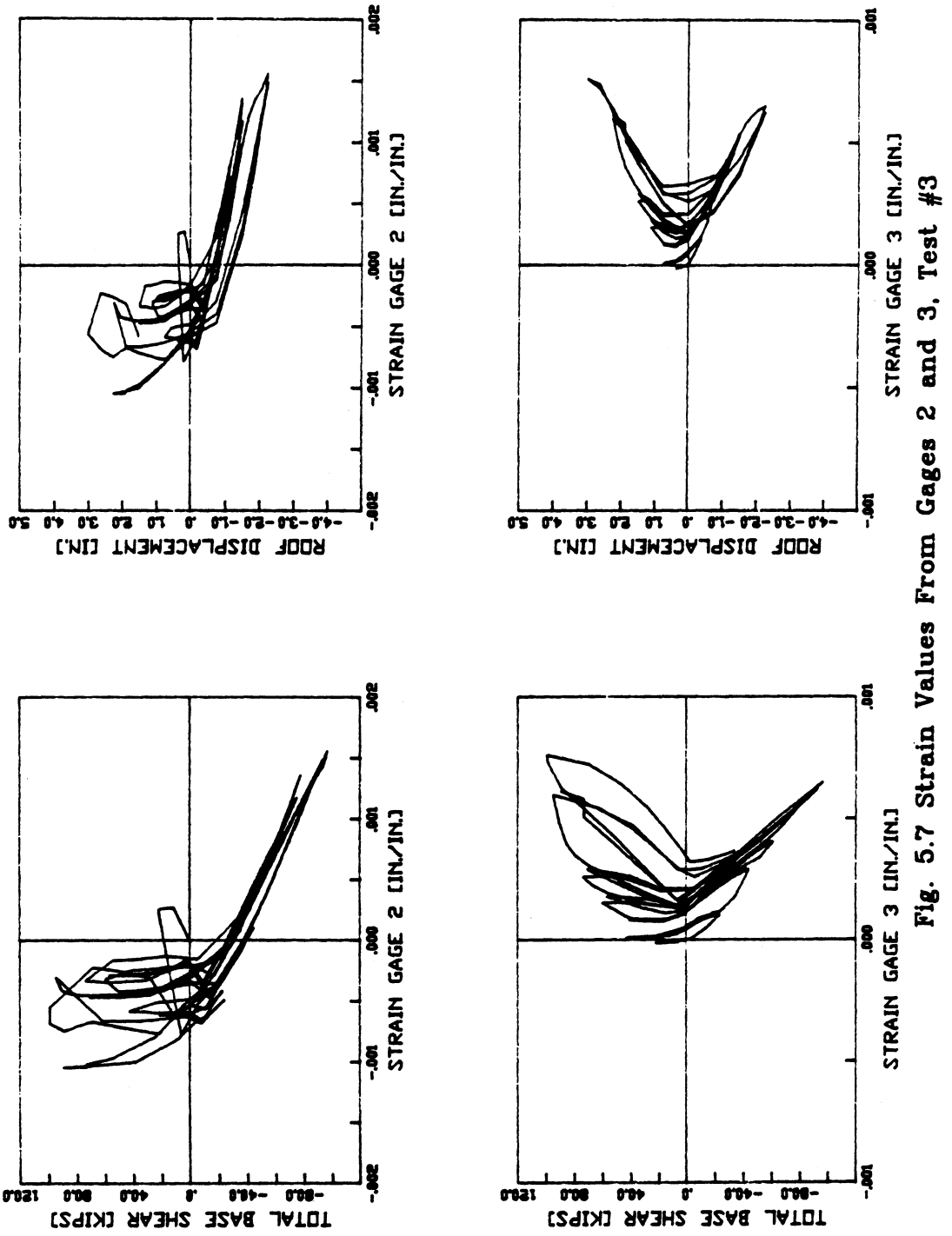

Fig. 5.7 Strain Values From Gages 2 and 3, Test #3

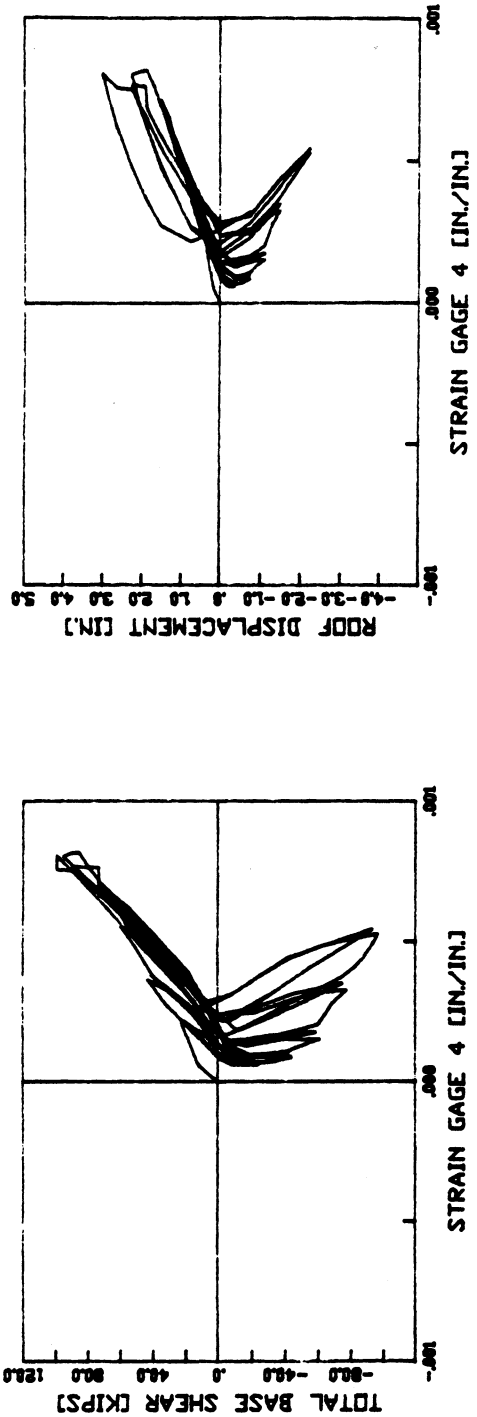

Fig. 5.8 Strain Values From Gages 4 and 5, Test #3

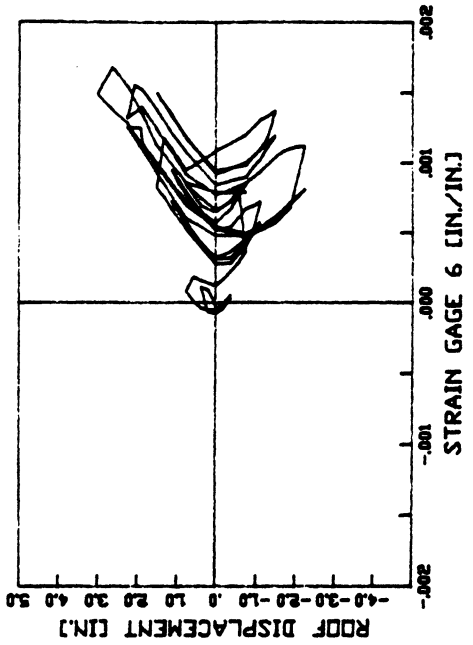

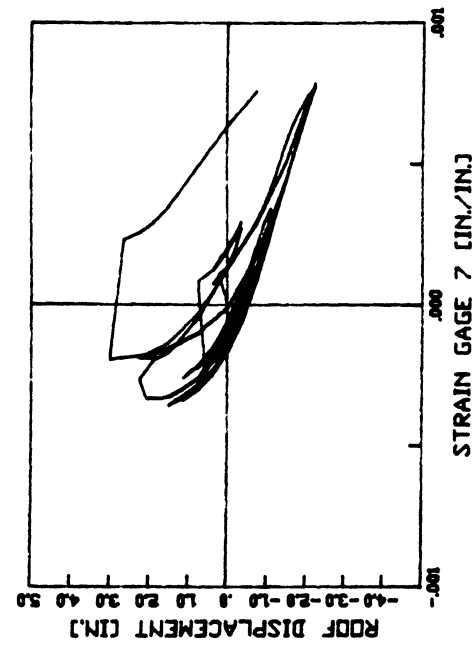

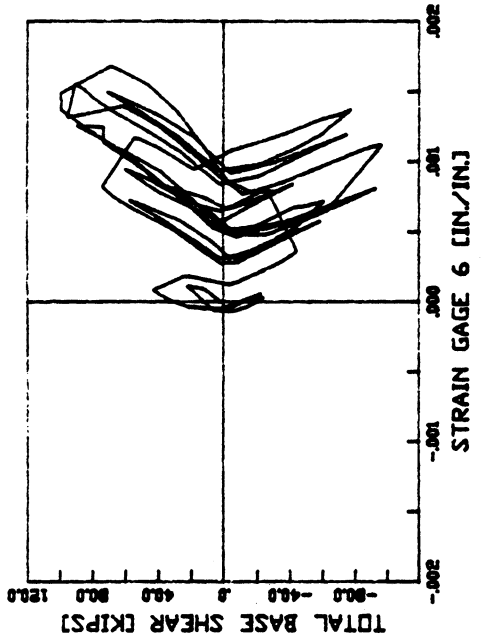

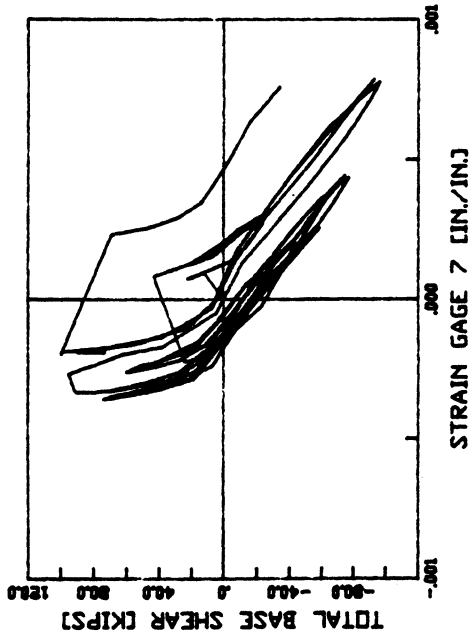

Fig. 5.9 Strain Values From Gages 6 and 7, Test #3

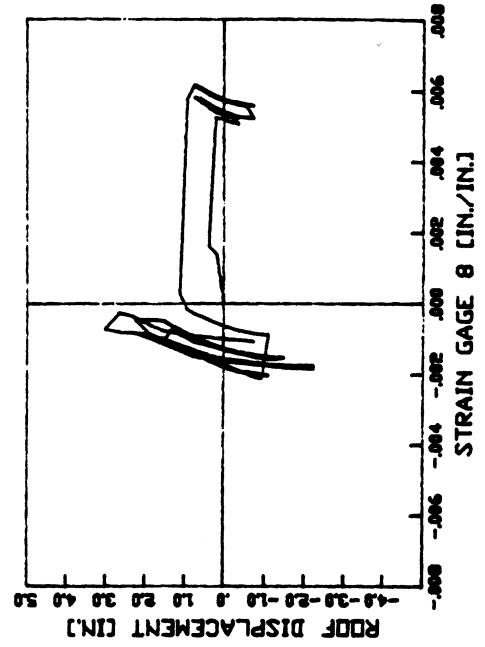

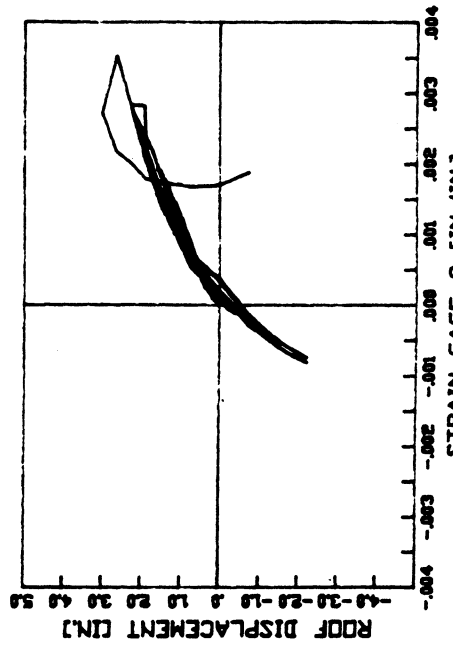

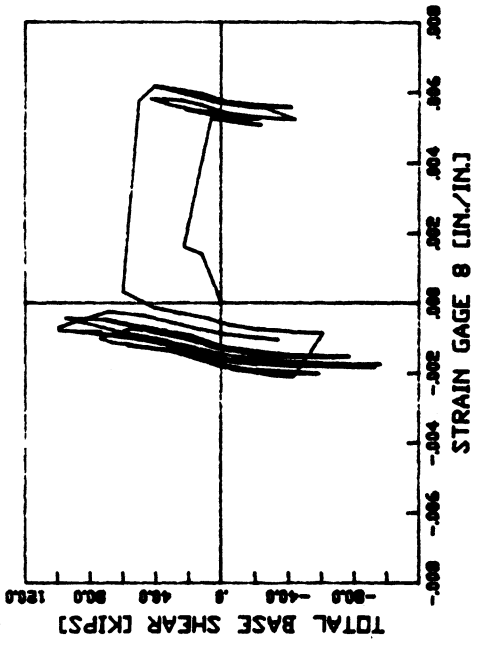

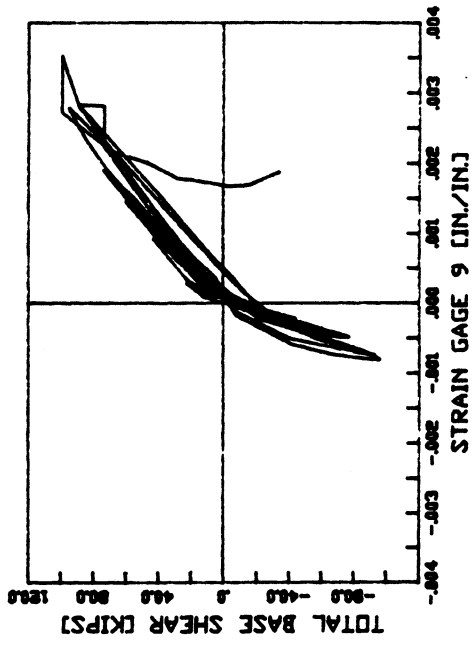

Fig. 5.10 Strain Values From Gages 8 and 9, Test #3

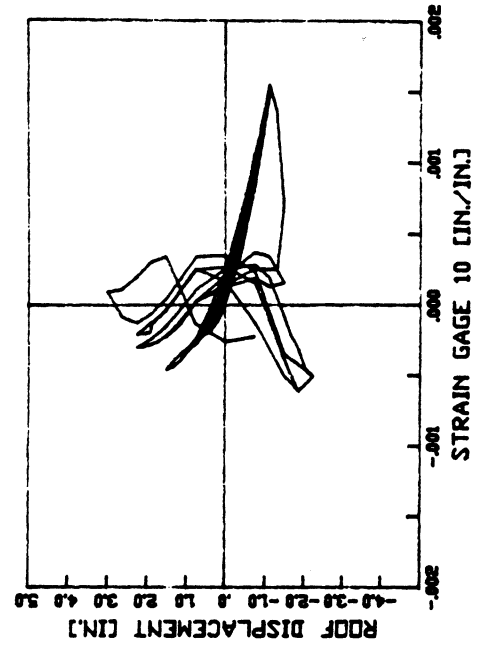

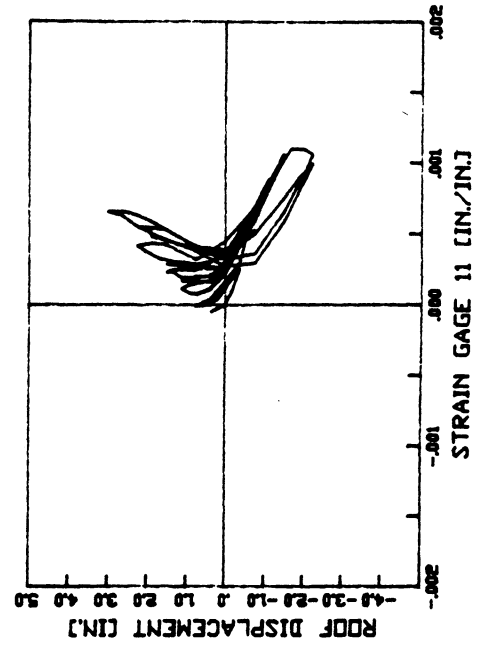

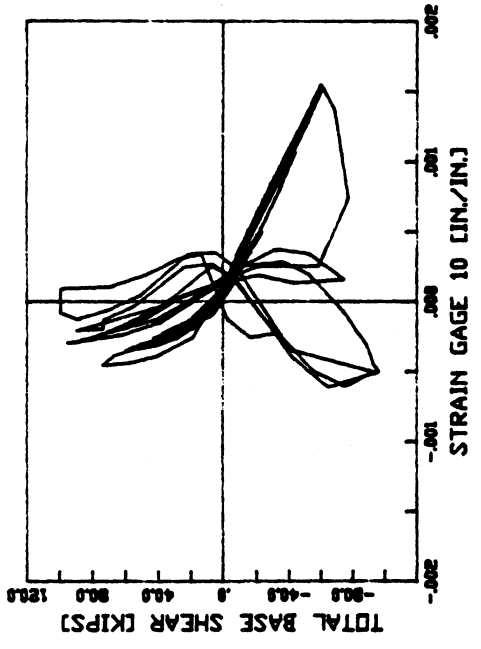

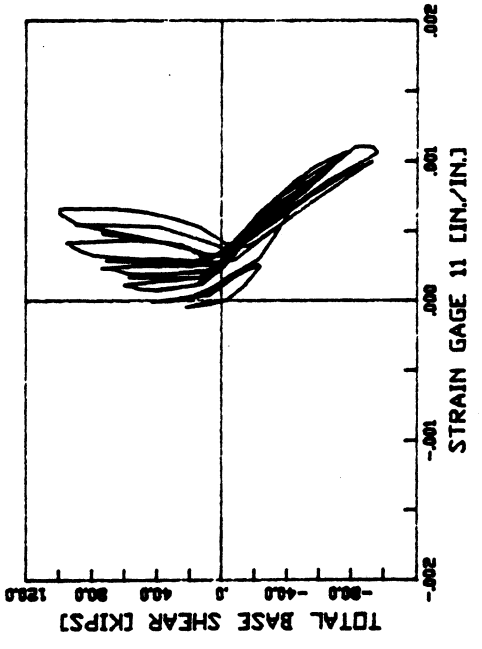

Fig. 5.11 Strain Values From Gages 10 and 11, Test #3

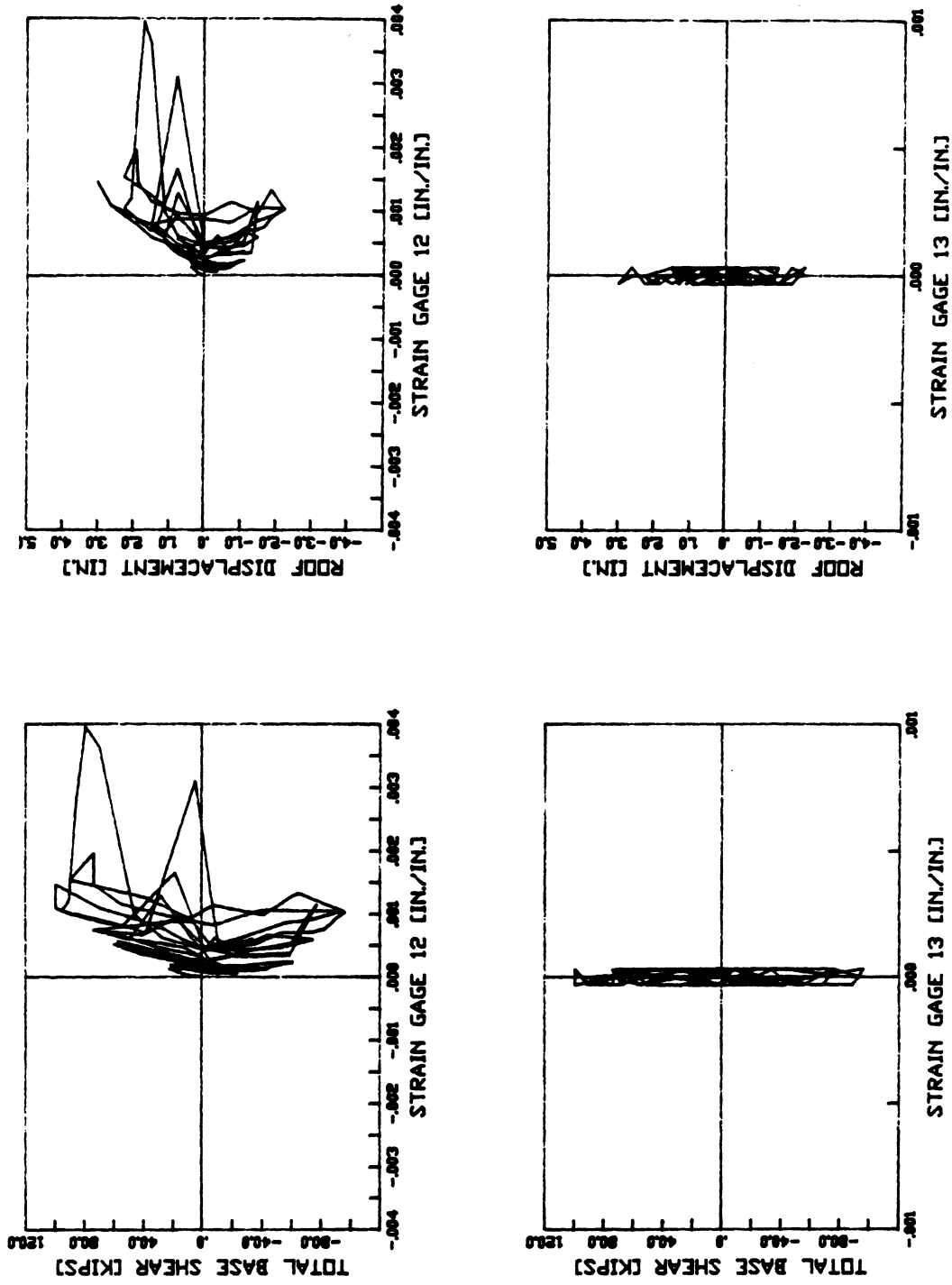

Fig. 5.12 Strain Values From Gages 12 and 13, Test #3

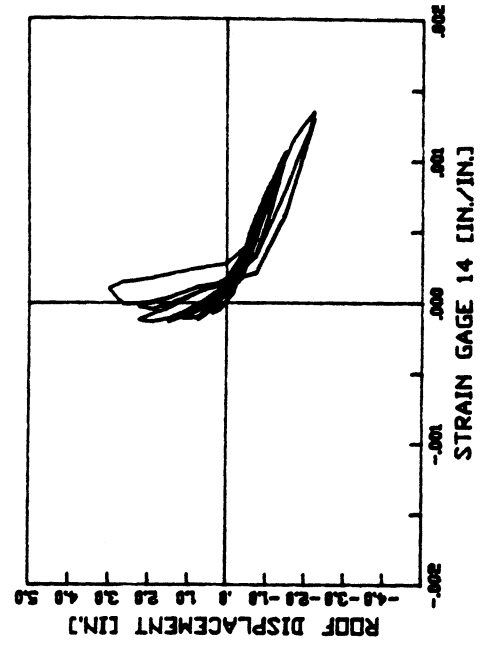

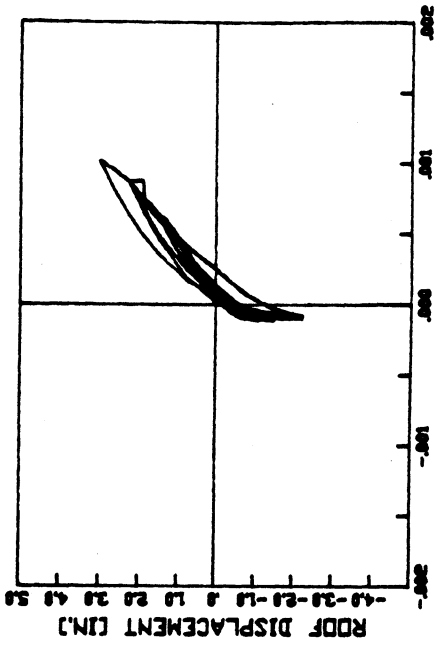

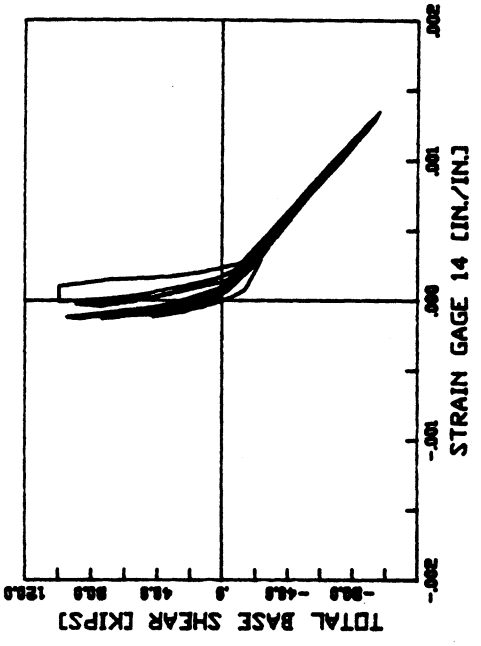

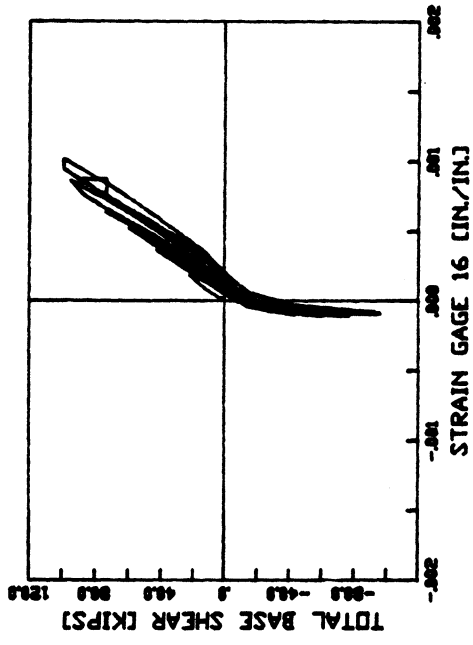

Fig. 5.13 Strain Values From Gages 14 and 16, Test #3

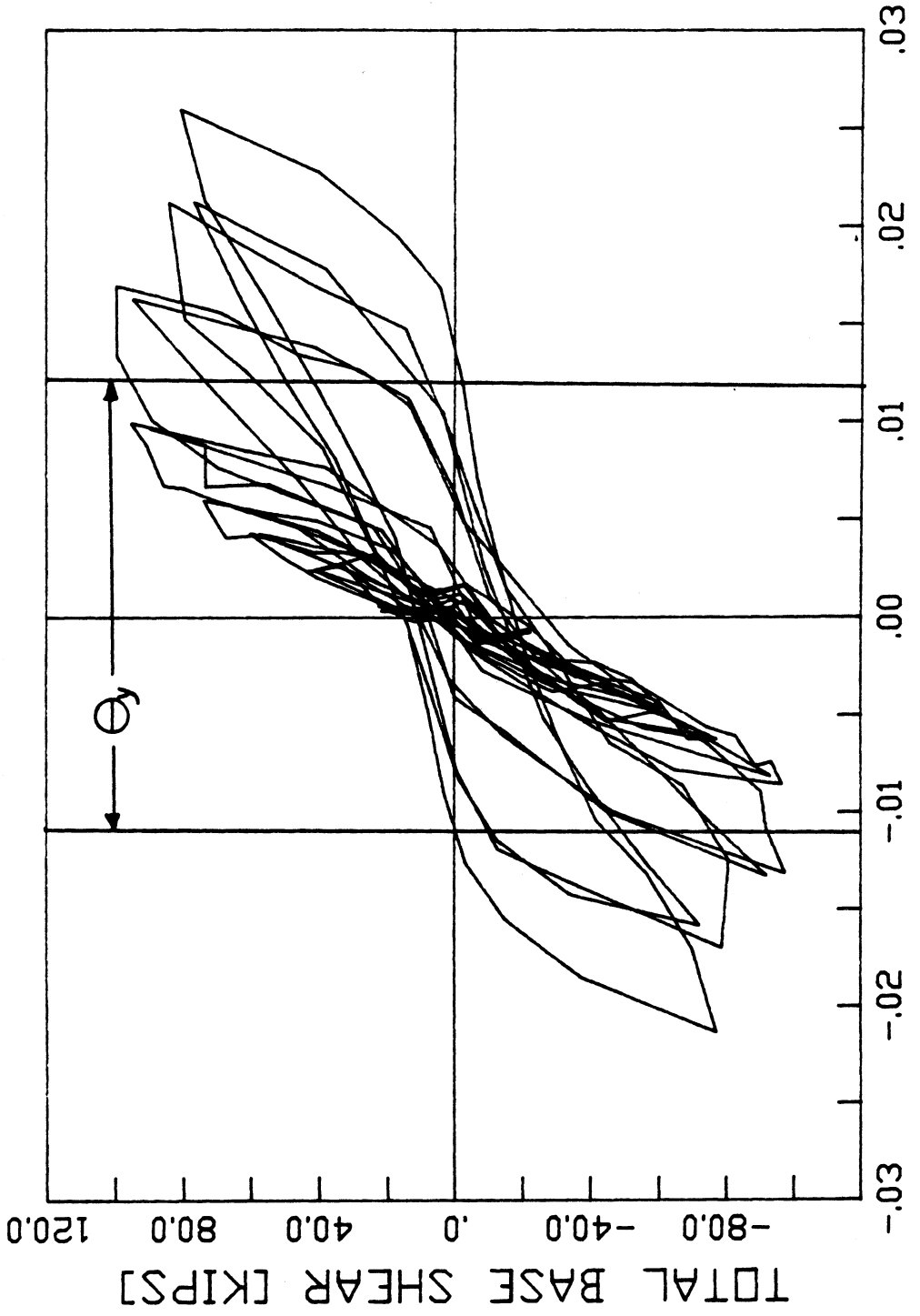

Fig. 5.14 Rotation Values for The West End of The First-Story Beam

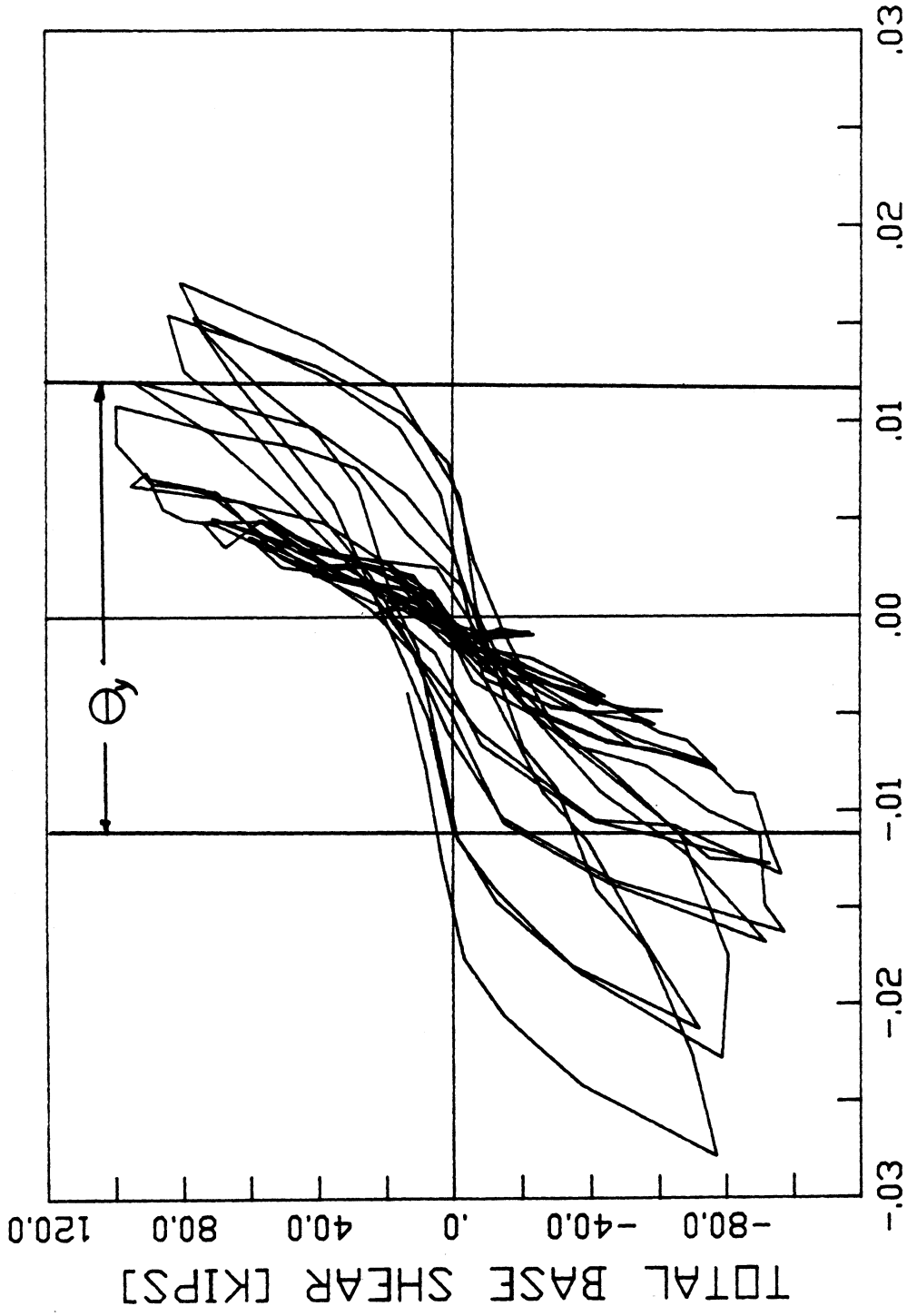

Fig. 5.15 Rotation Values for The East End of The First-Story Beam

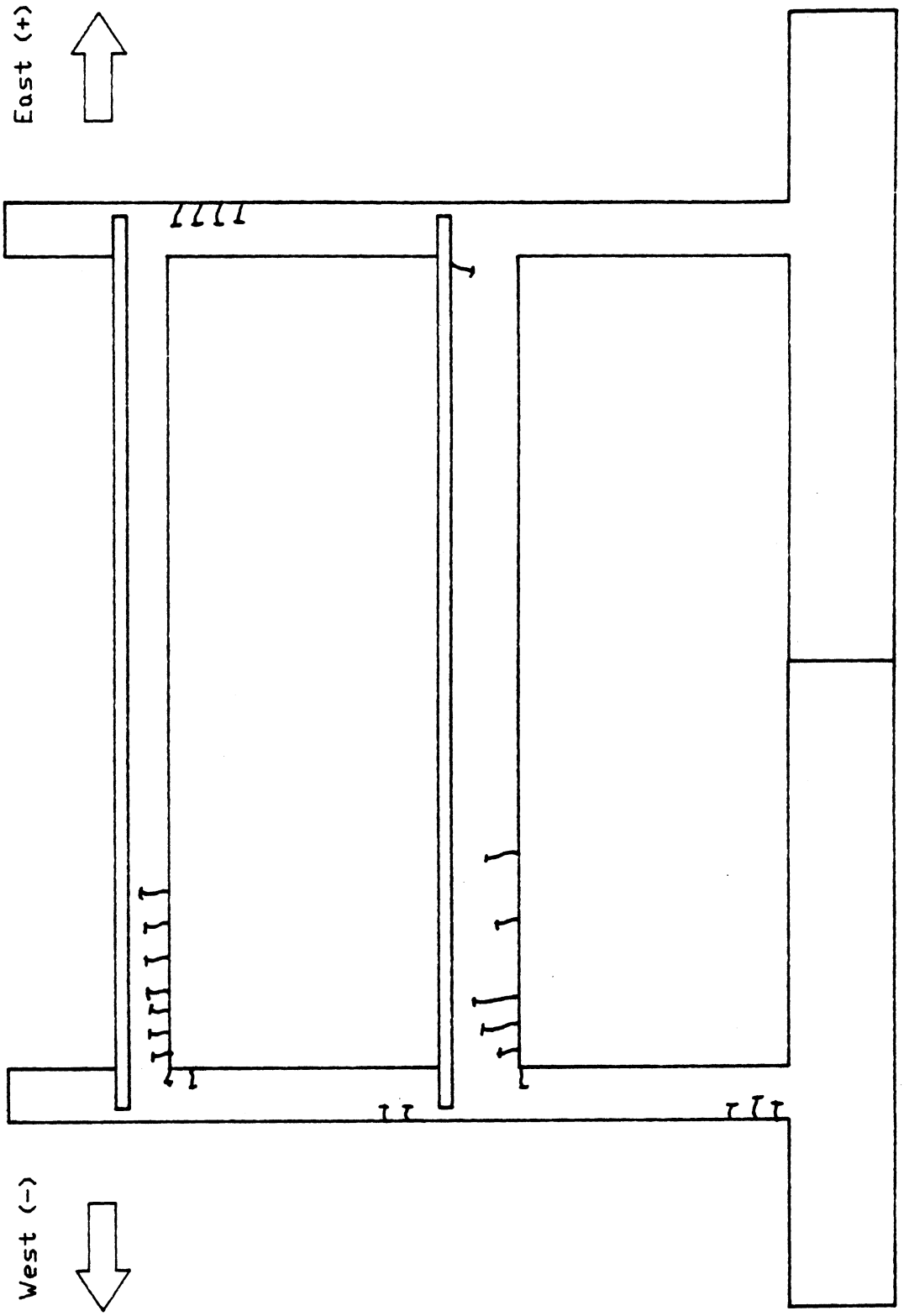

Fig. 5.16 Cracking Patterns Cycle 1, East, Test #3

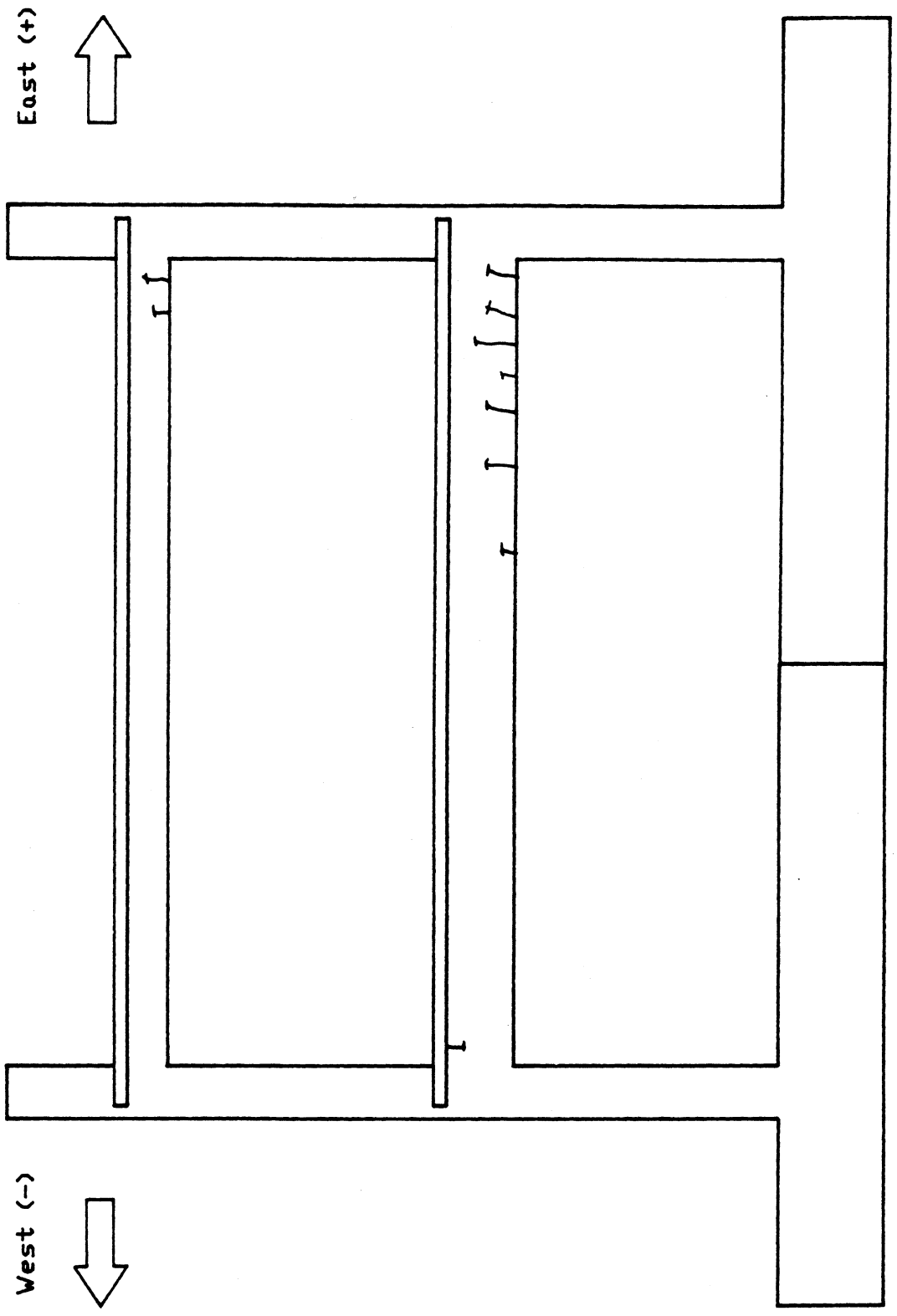

Fig. 5.17 Cracking Patterns Cycle 1, West, Test #3

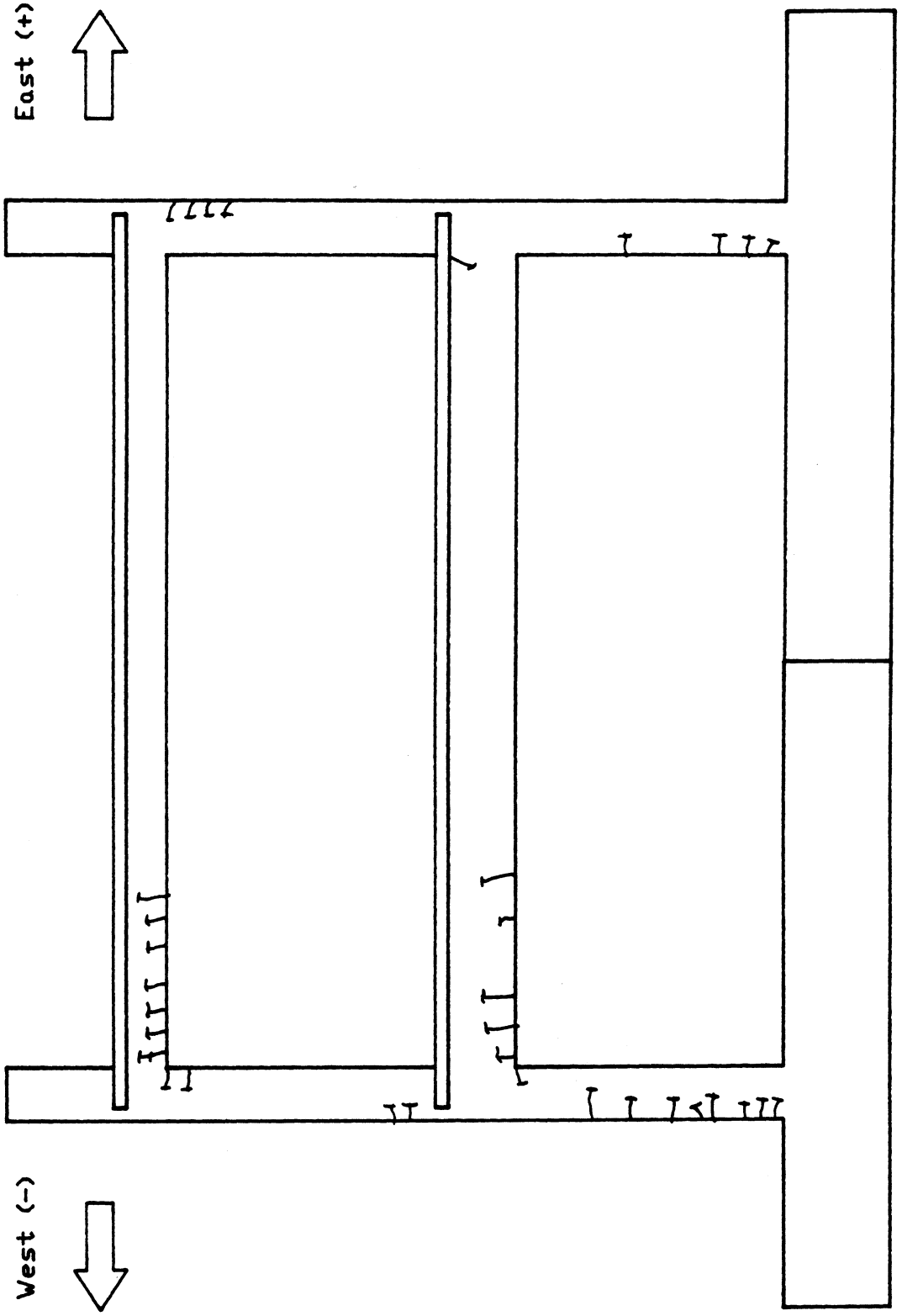

Fig. 5.18 Cracking Patterns Cycle 3, East, Test #3

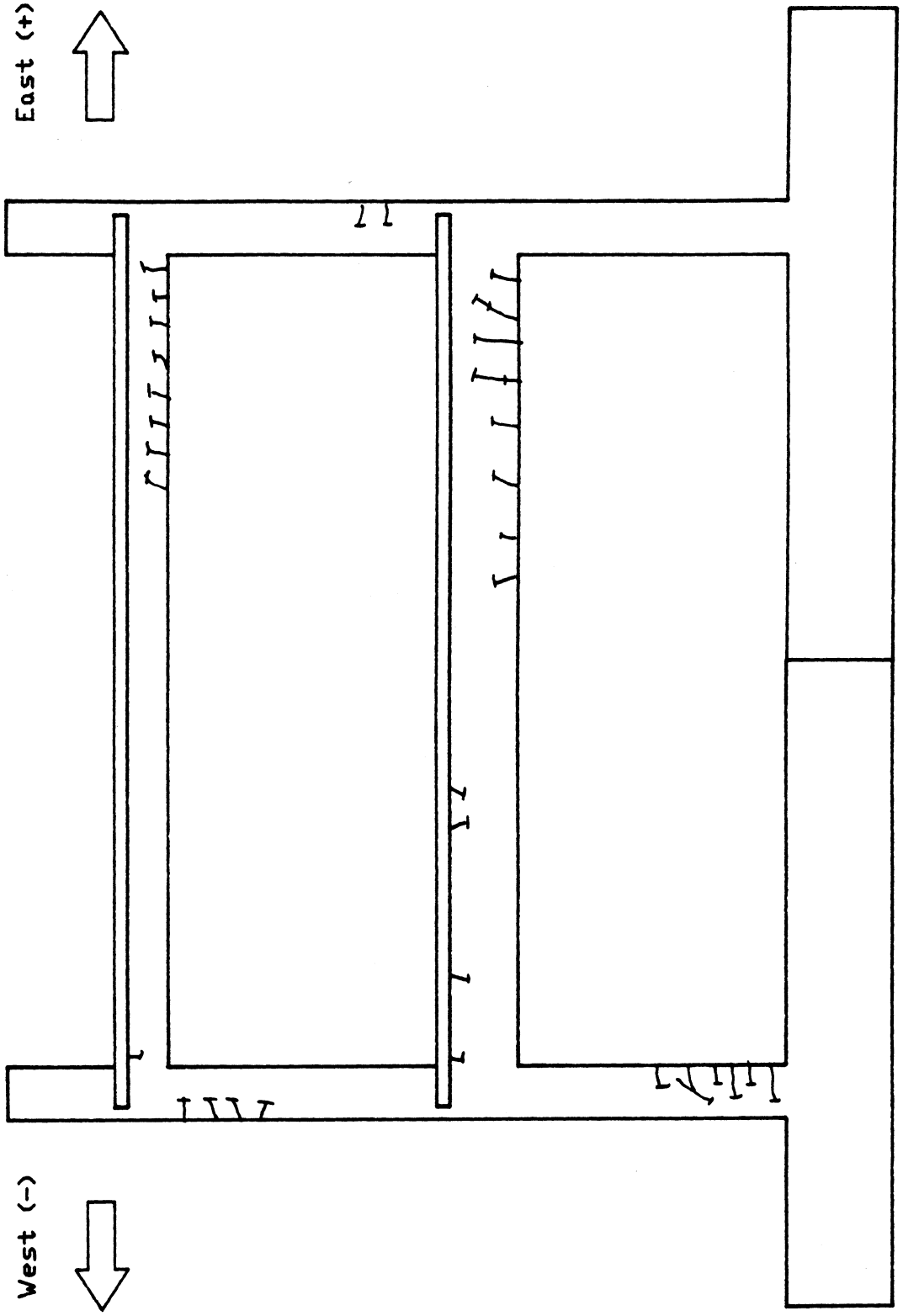

Fig. 5.19 Cracking Patterns Cycle 3, West, Test #3

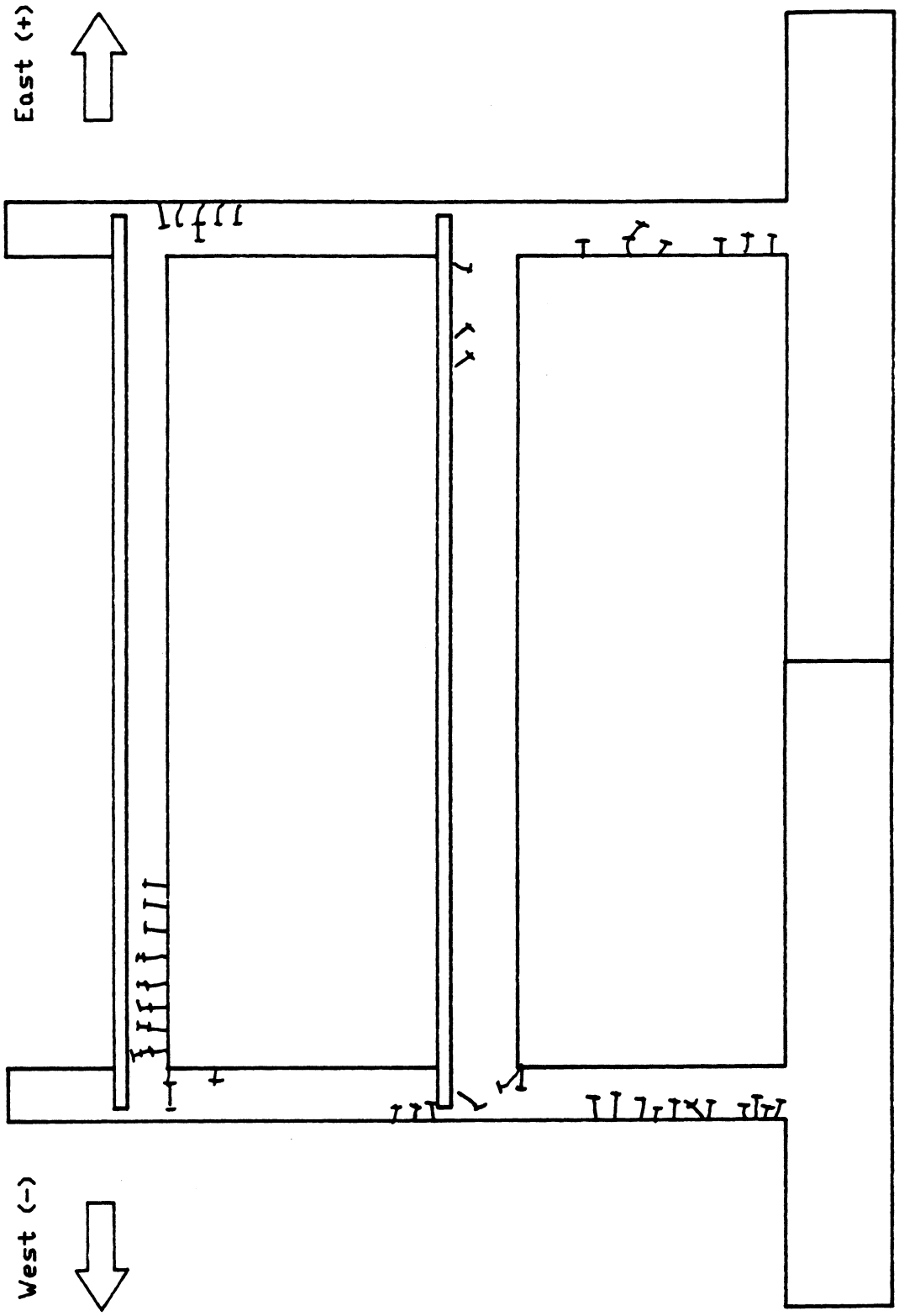

Fig. 5.20 Cracking Patterns Cycle 5, East, Test #3

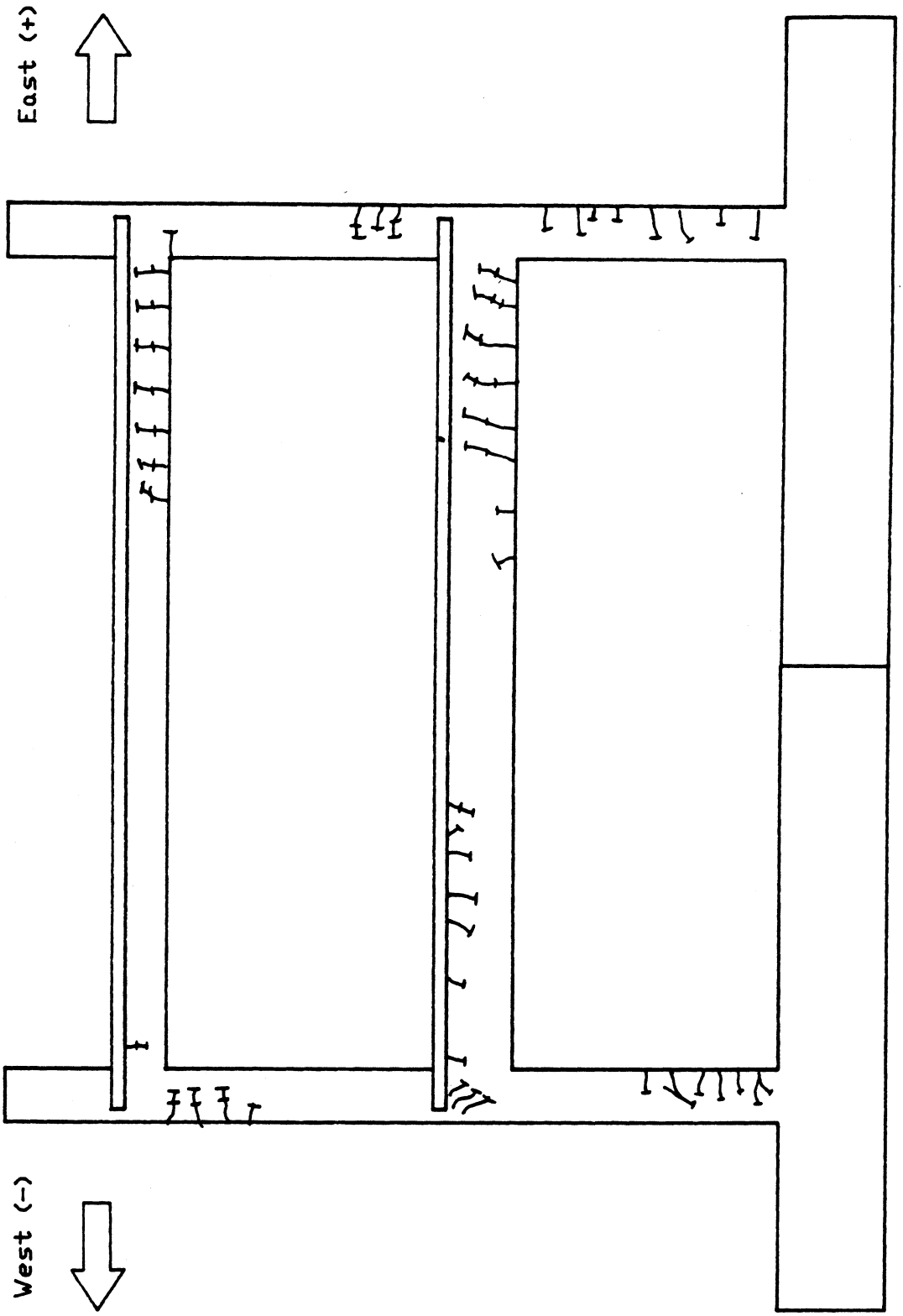

Fig. 5.21 Cracking Patterns Cycle 5, West, Test #3

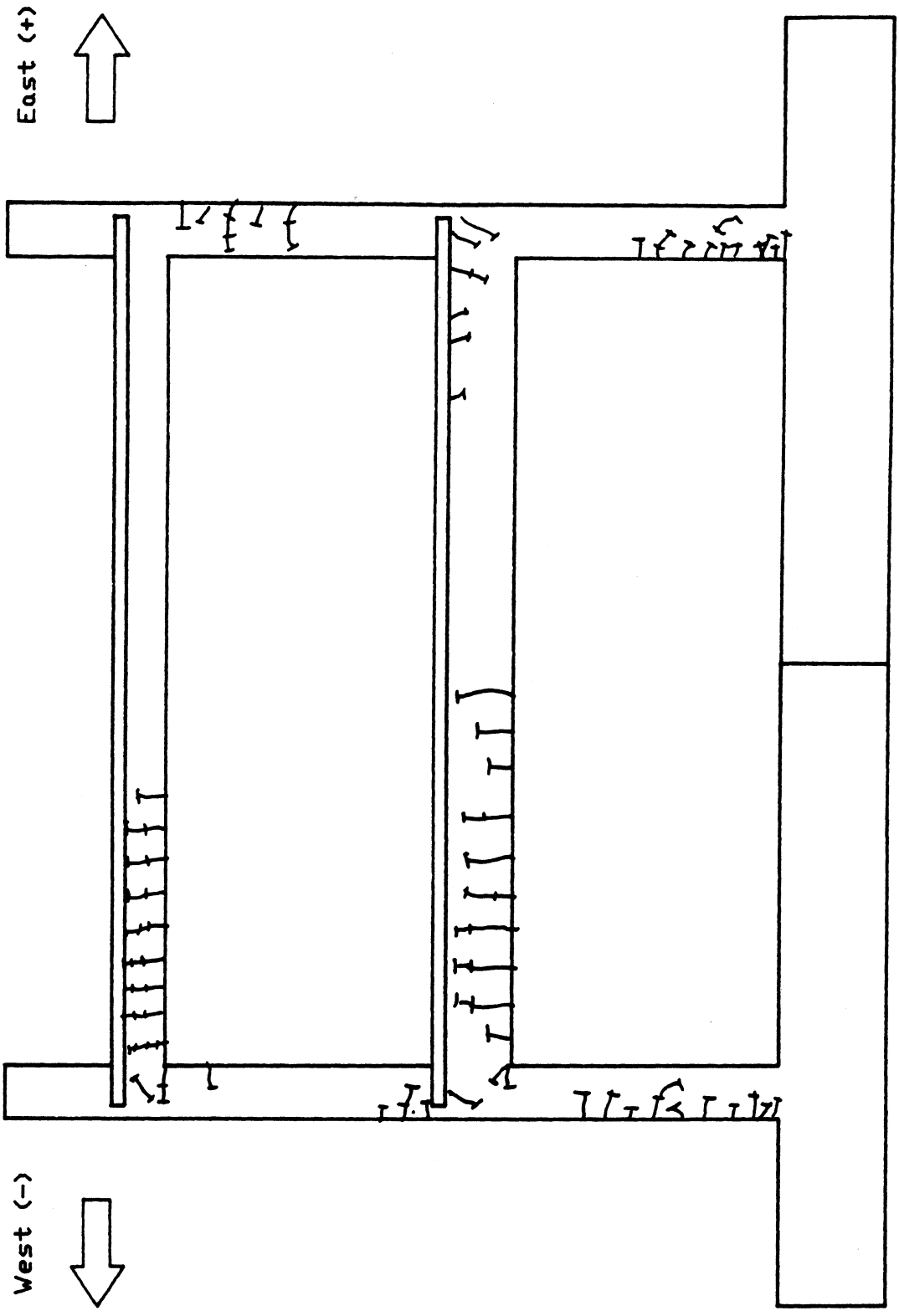

Fig. 5.22 Cracking Patterns Cycle 7, East, Test #3

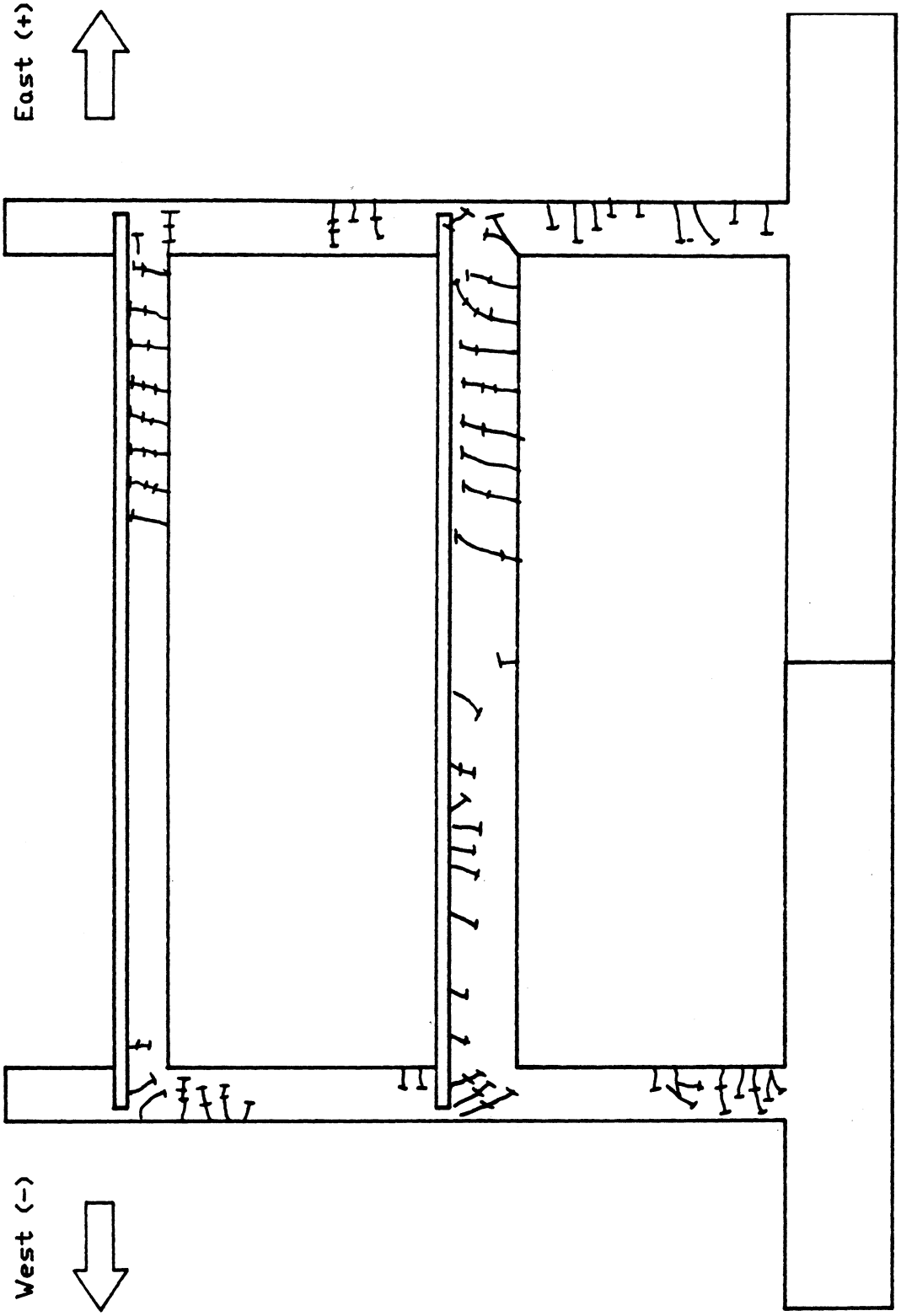

Fig. 5.23 Cracking Patterns Cycle 7, West, Test #3

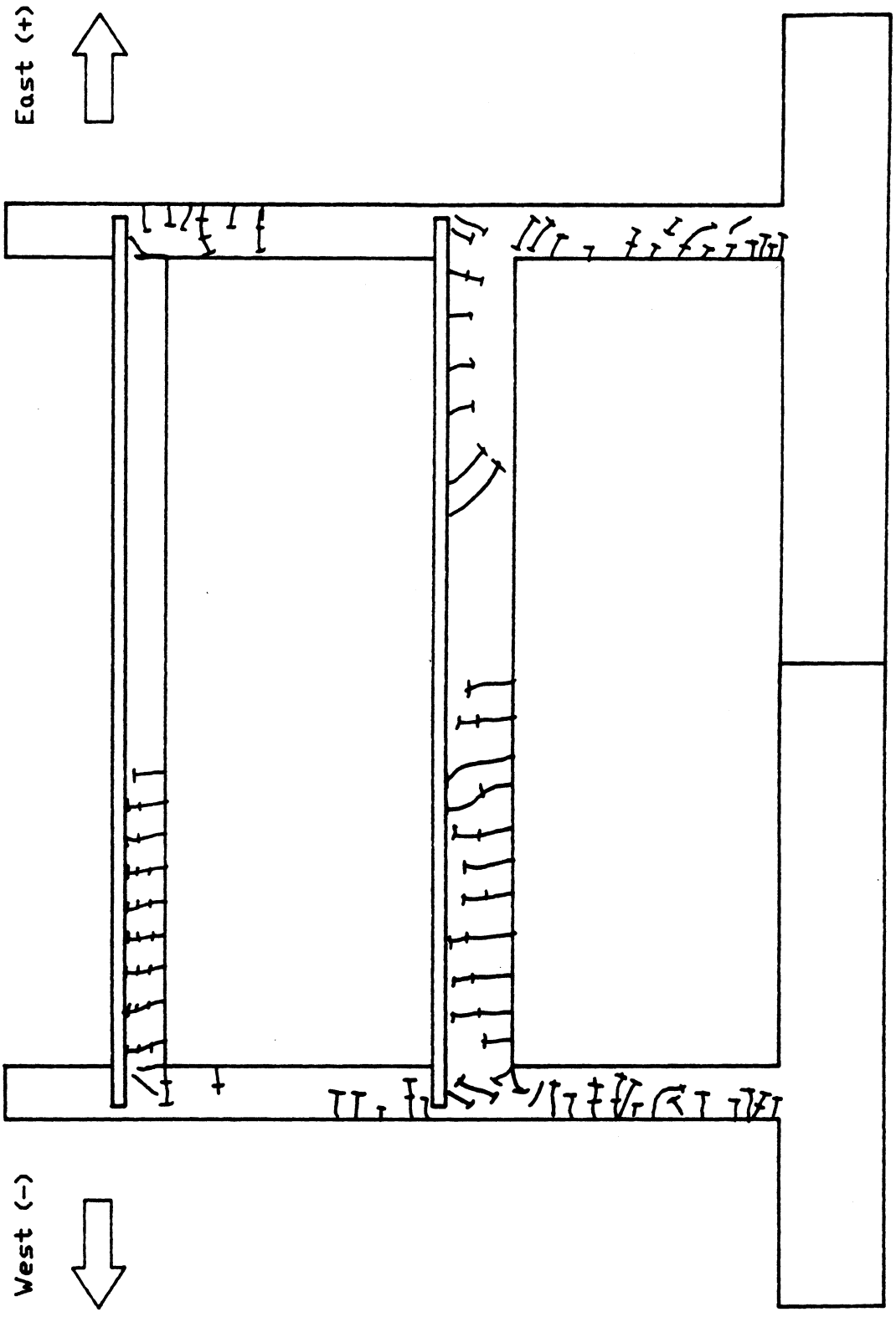

Fig. 5.24 Cracking Patterns Cycle 9, East, Test #3

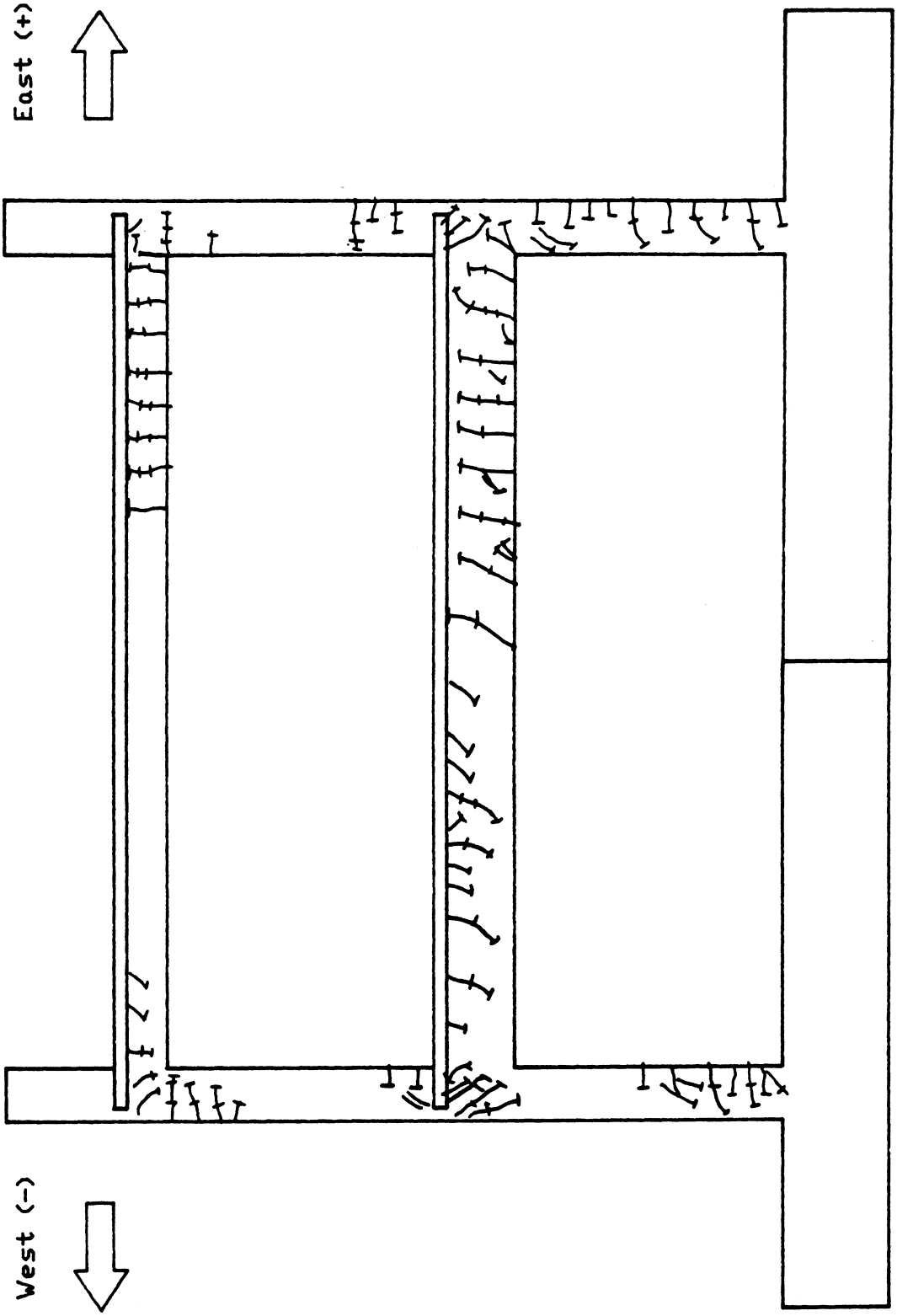

Fig. 5.25 Cracking Patterns Cycle 9, West, Test #3

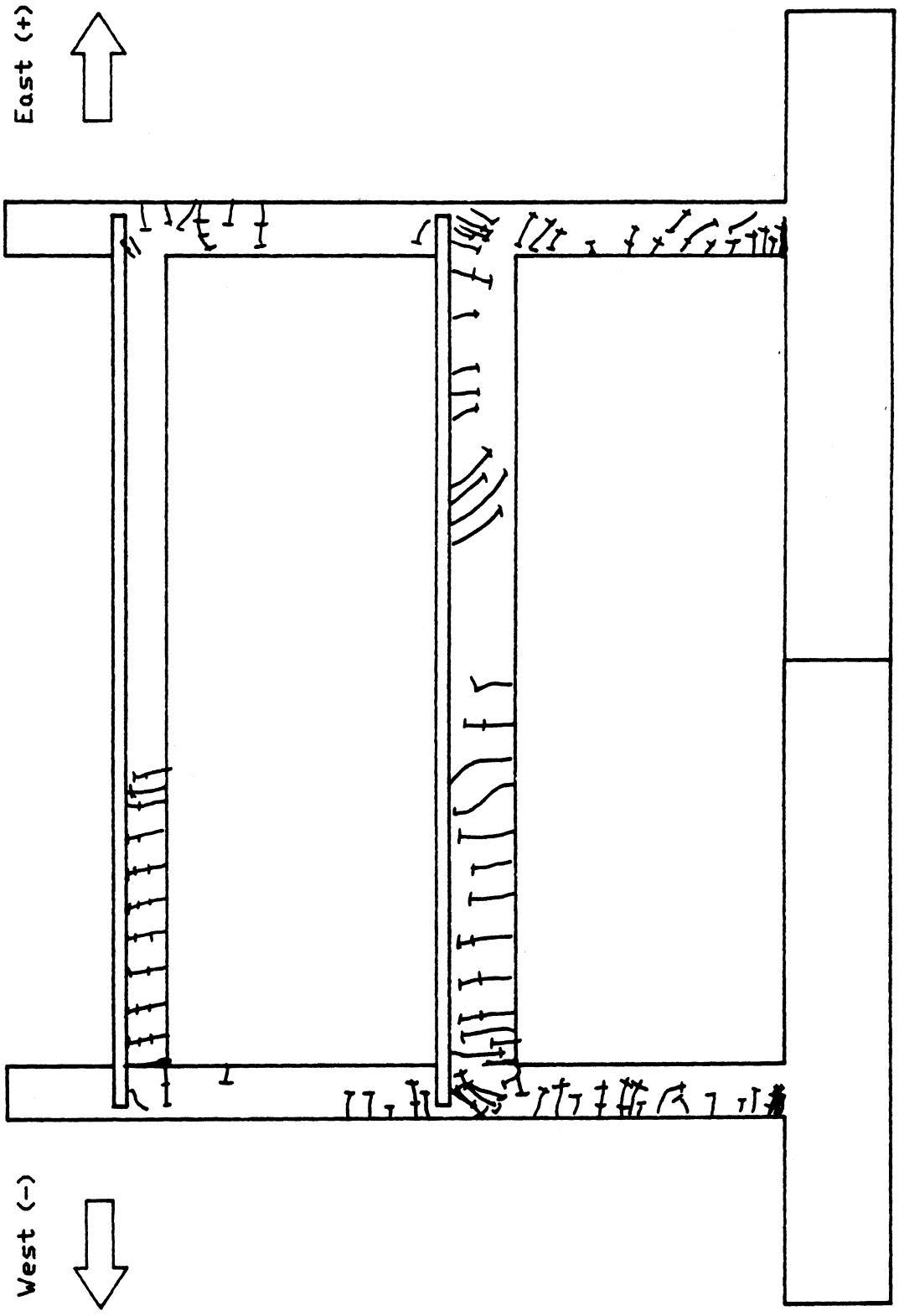

Fig. 5.26 Cracking Patterns Cycle 11, East, Test #3

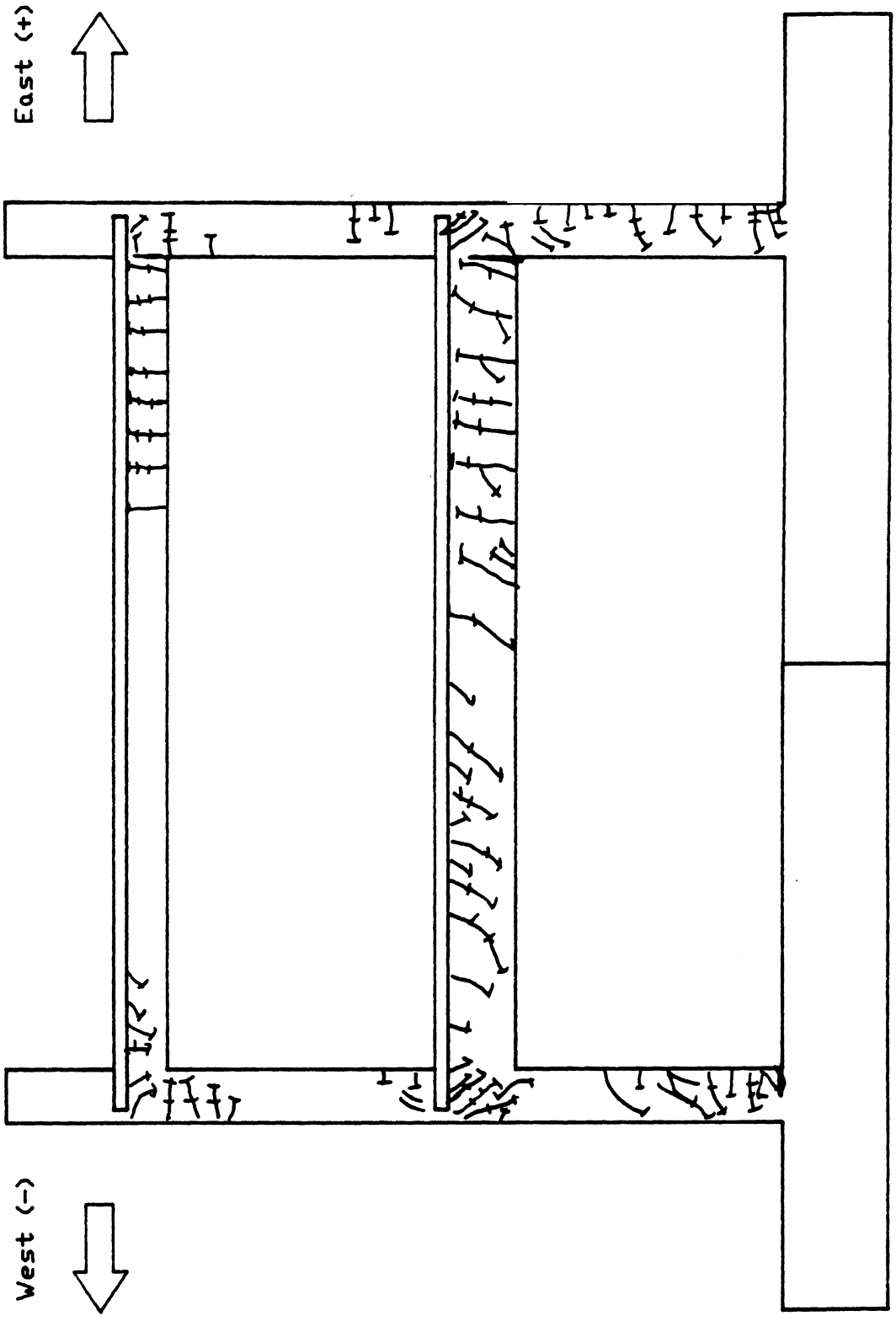

Fig. 5.27 Cracking Patterns Cycle 11, West, Test #3

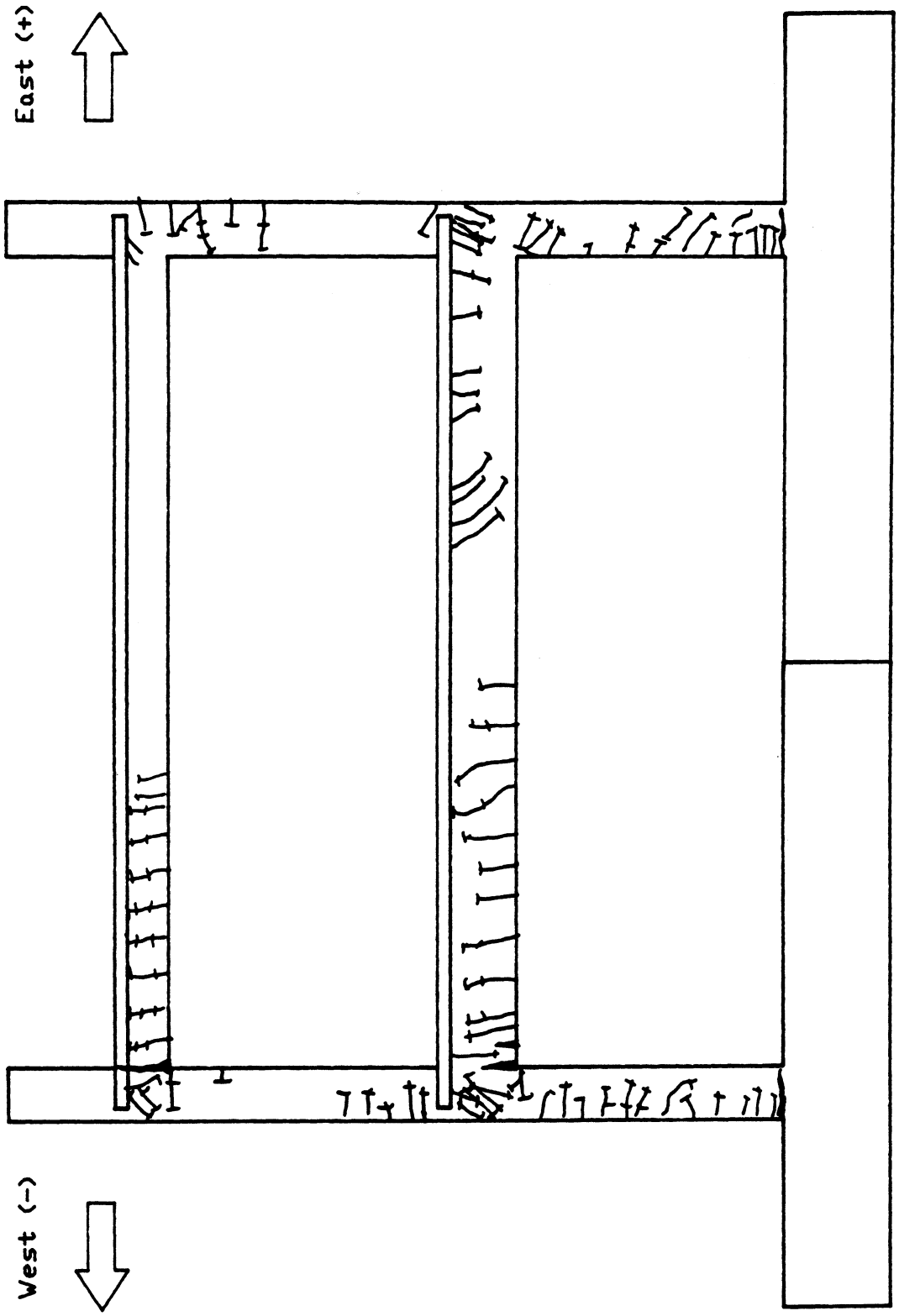

Fig. 5.28 Cracking Patterns Cycle 13, East, Test #3

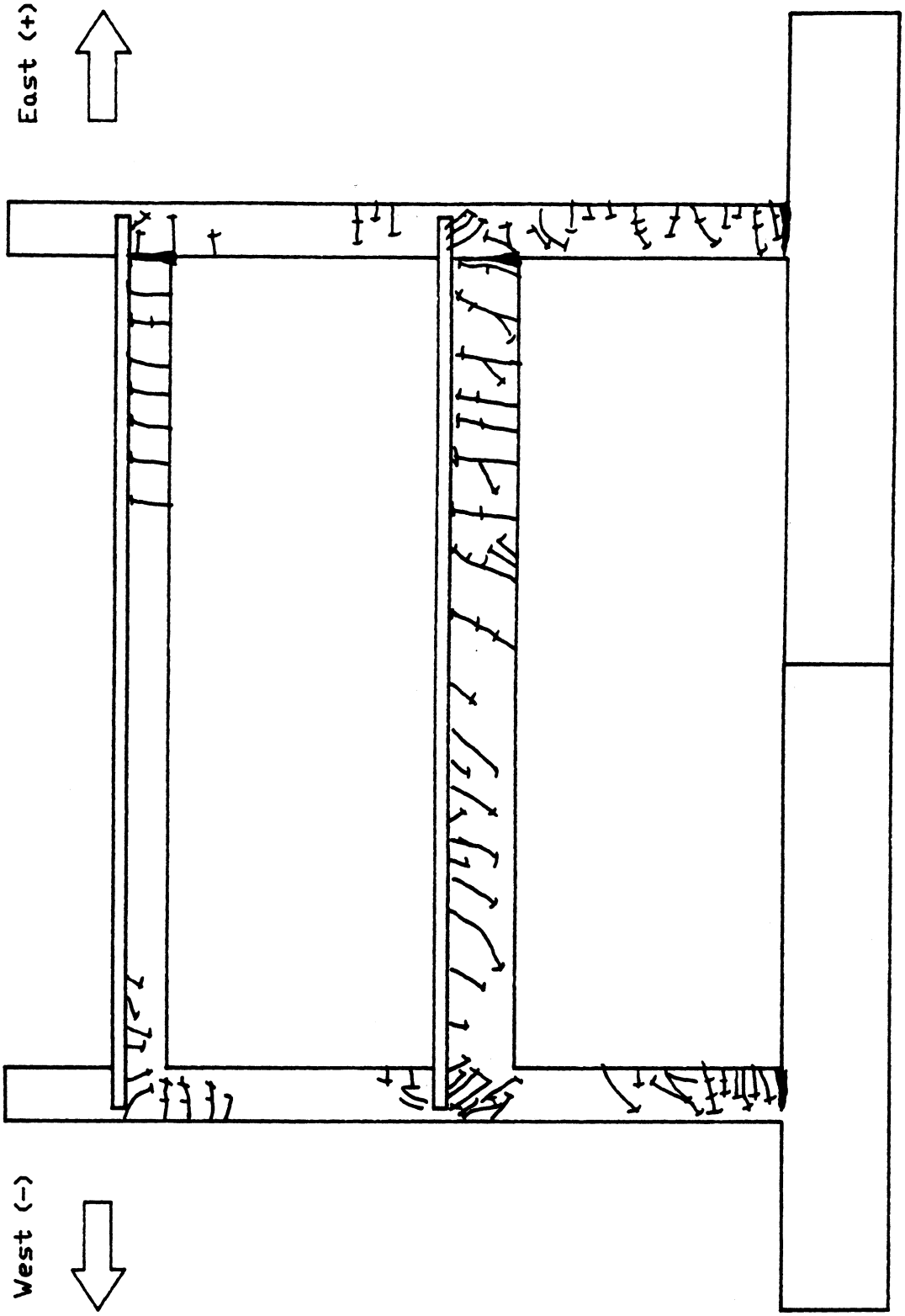

Fig. 5.29 Cracking Patterns Cycle 13, West, Test #3

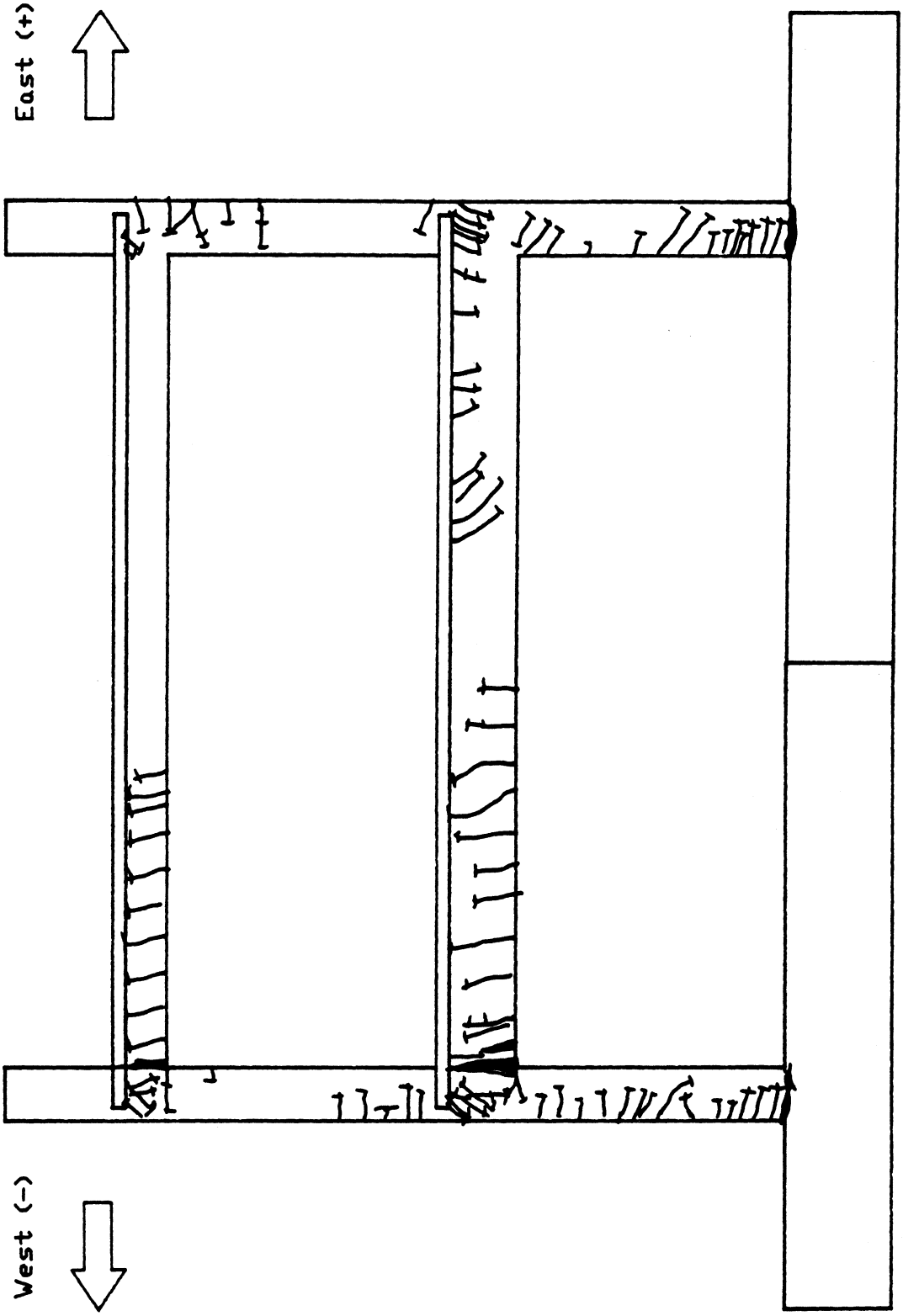

Fig. 5.30 Cracking Patterns Cycle 15, East, Test #3

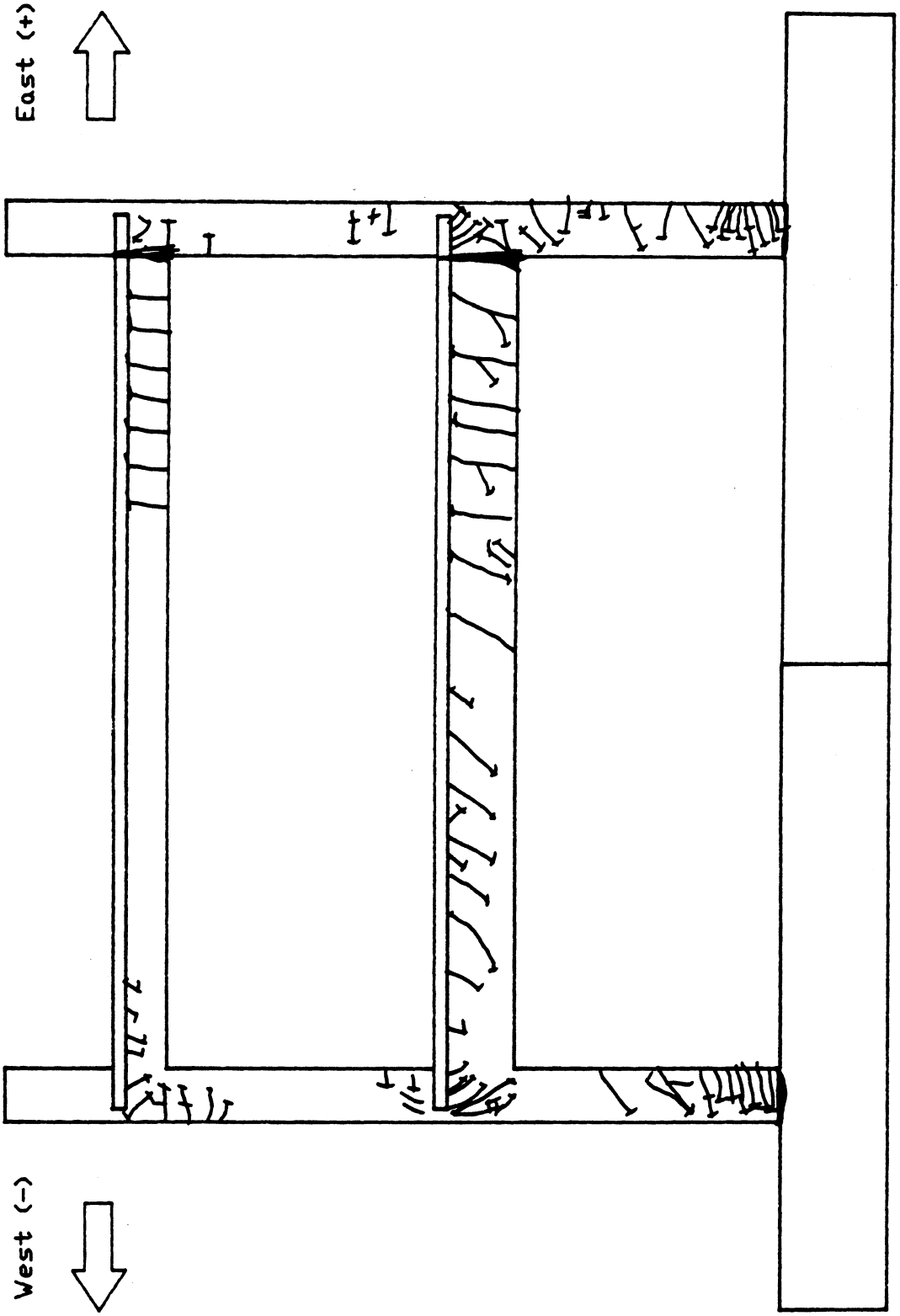

Fig. 5.31 Cracking Patterns Cycle 15, West, Test #3

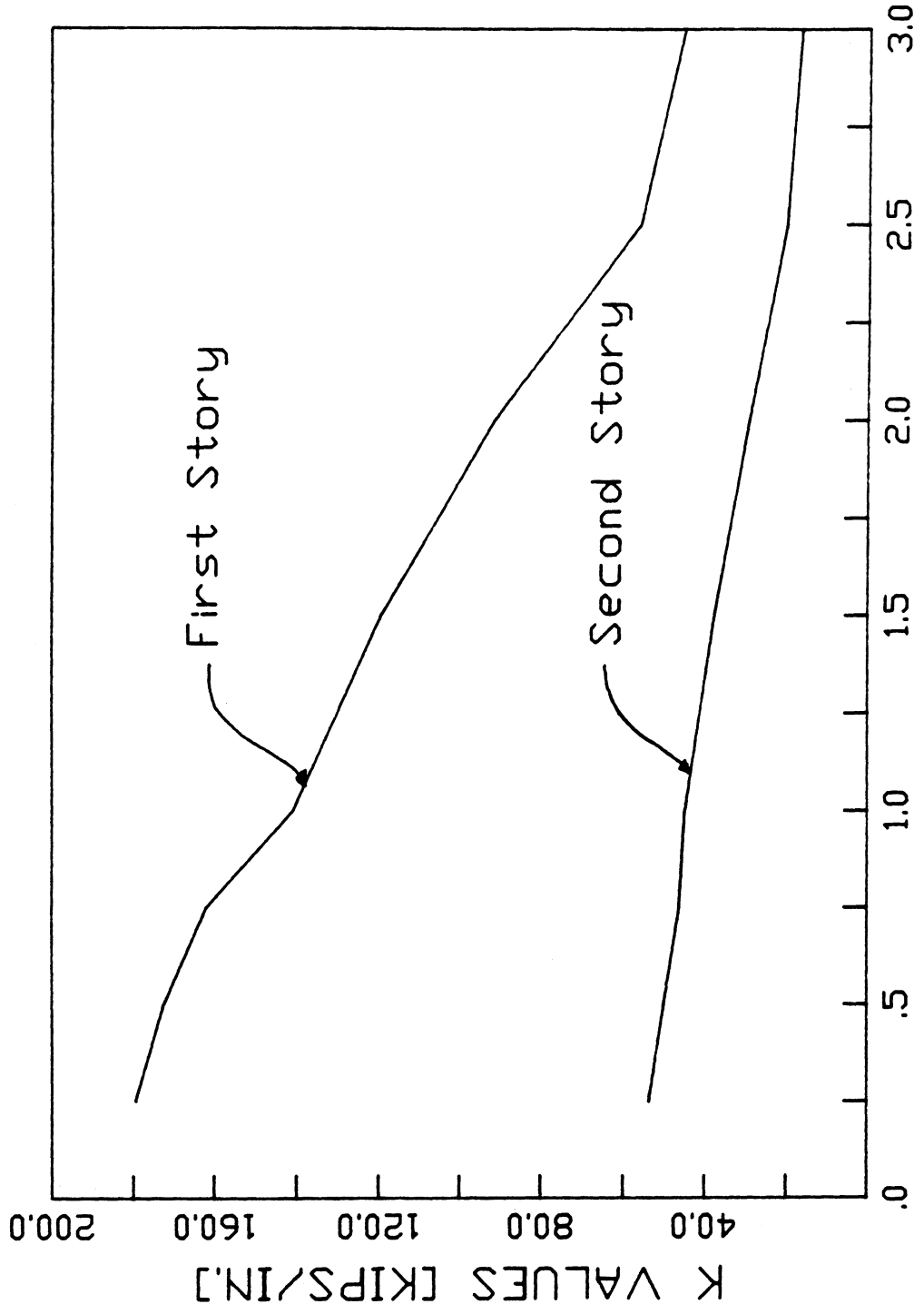

Fig. 5.32 Stiffness Degradation Curves for Test #3

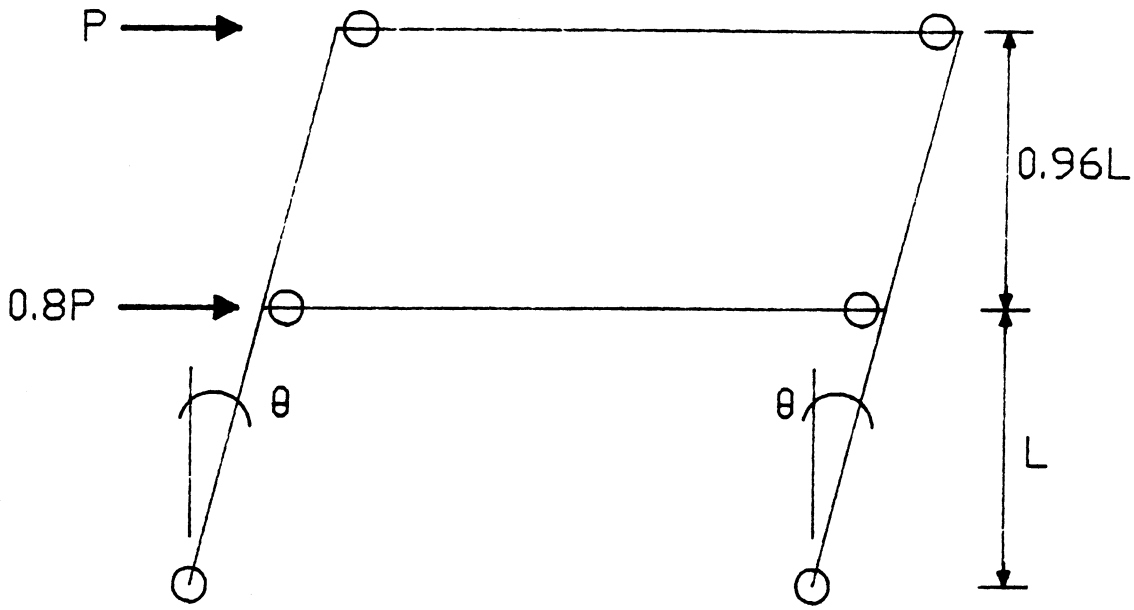

$$L = 69''$$

$$I.W. = 2\theta M_{col.} + 2\theta M_{bm1} + 2\theta M_{bm2}$$

$$E.W. = P\theta(1.96L) + 0.8P\theta L$$

$$P = 50.0 \text{ kips}$$

Fig. 6.1 Failure Mechanism Test #3

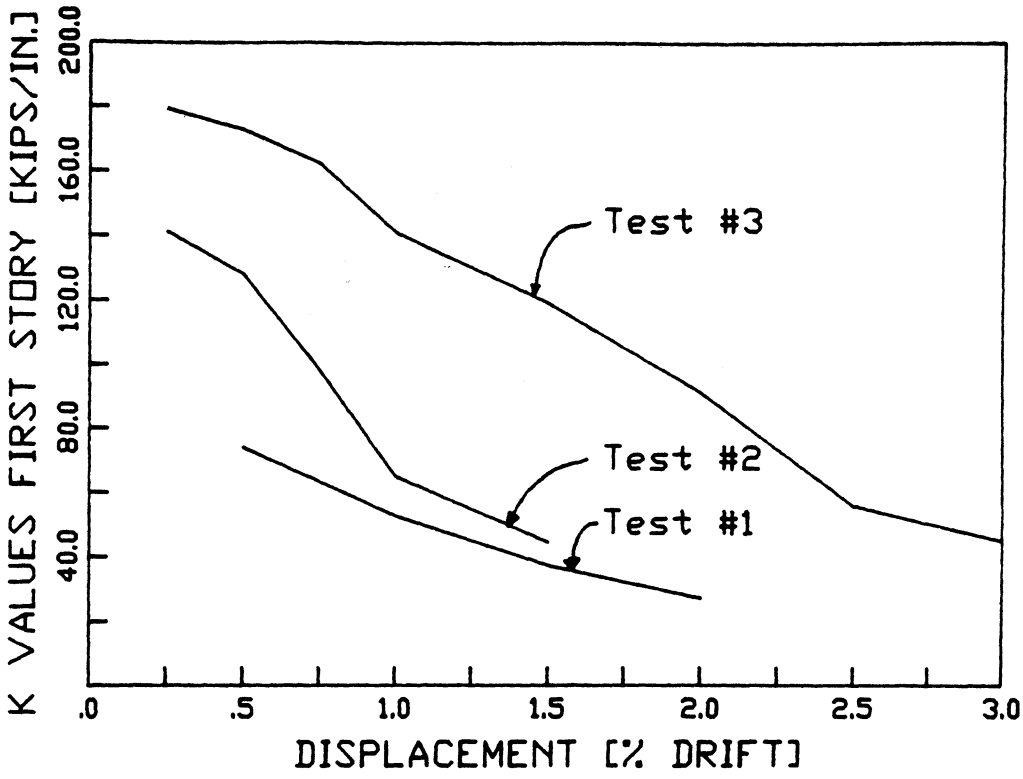

a) First-Story Stiffness

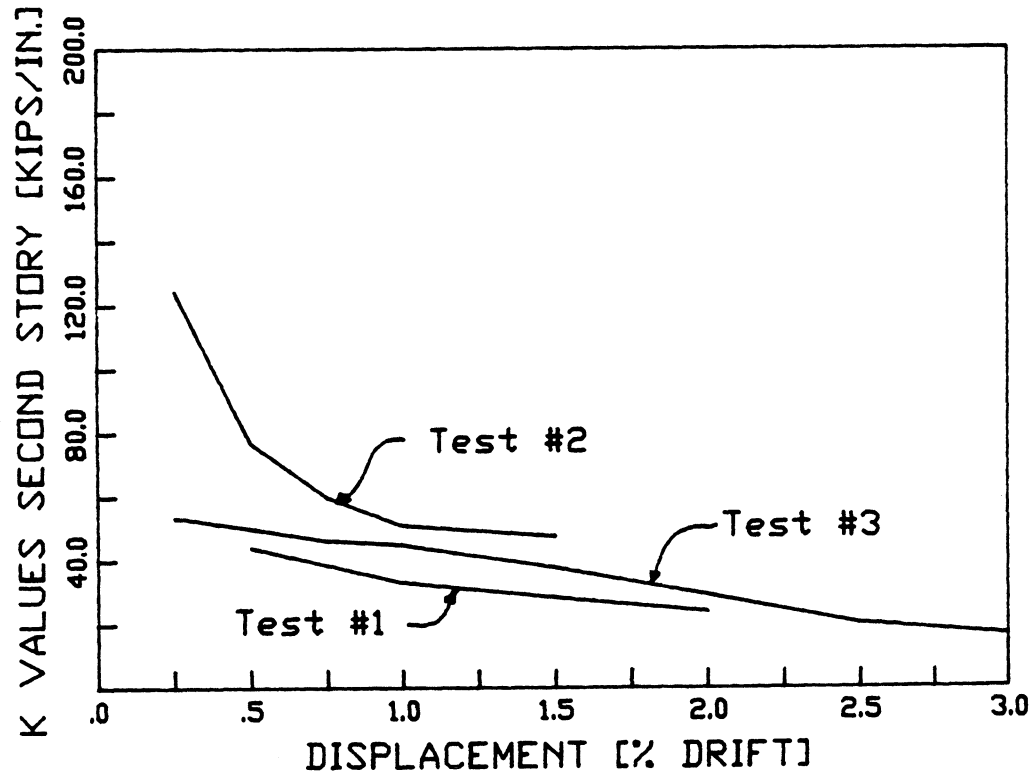

b) Second-Story Stiffness

Fig. 6.2 Comparison of Stiffness in Tests #1, #2, and #3

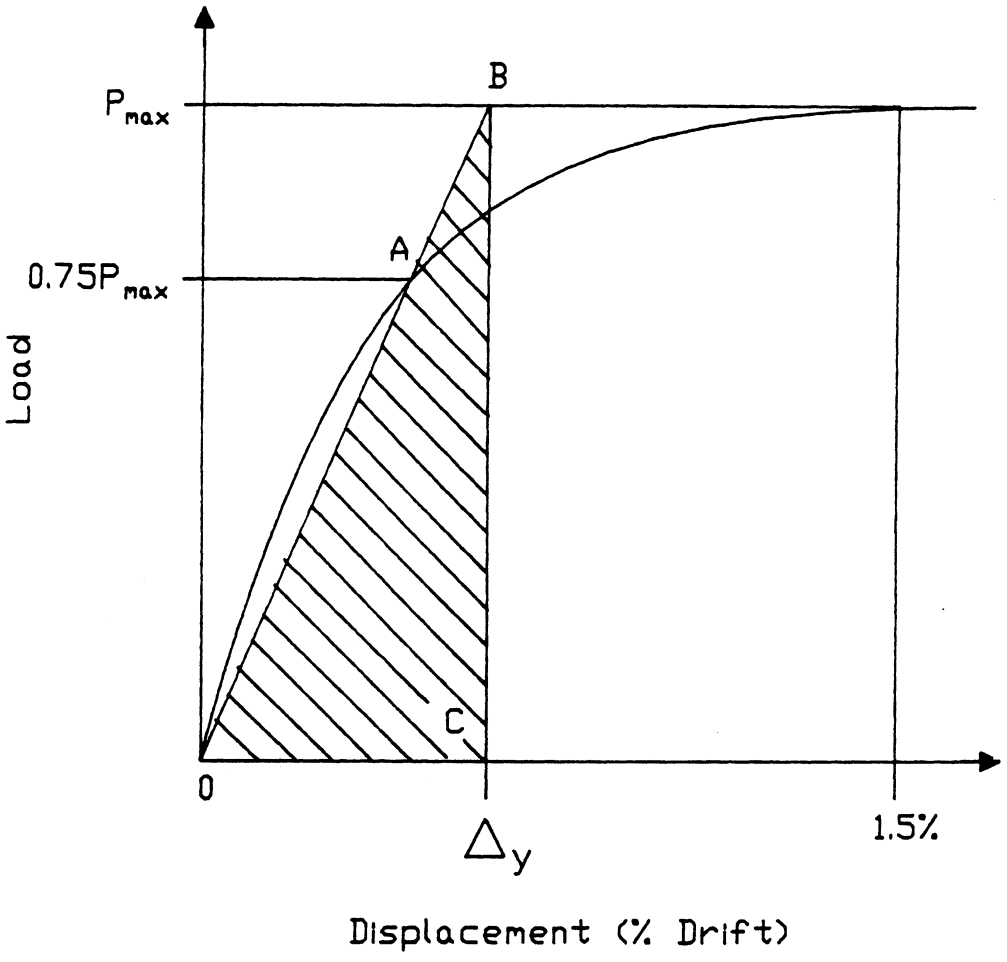

Fig. 6.3 Calculation of Energy Dissipated at Yield Point

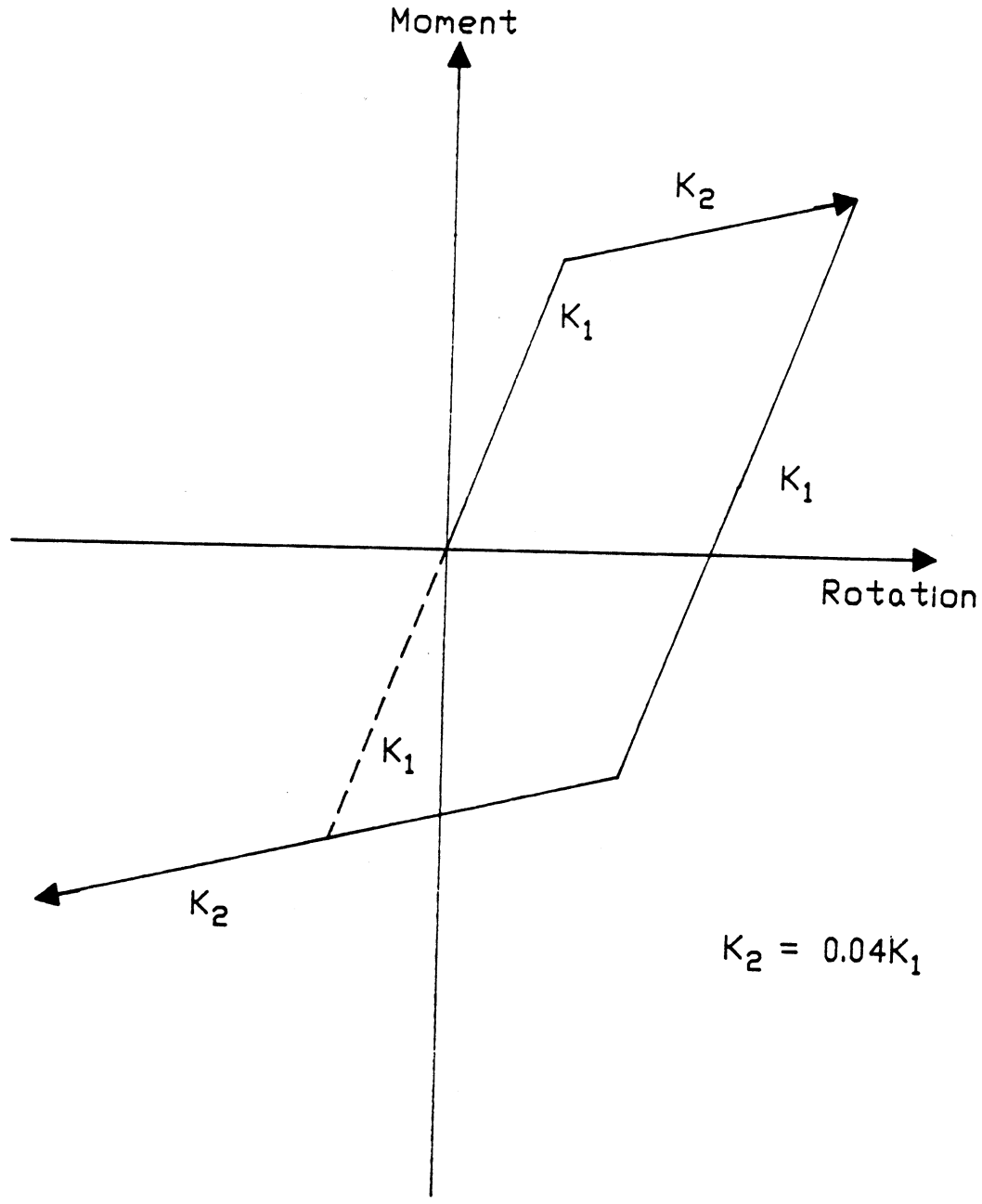

oment vs. Rotation Model for Element 5

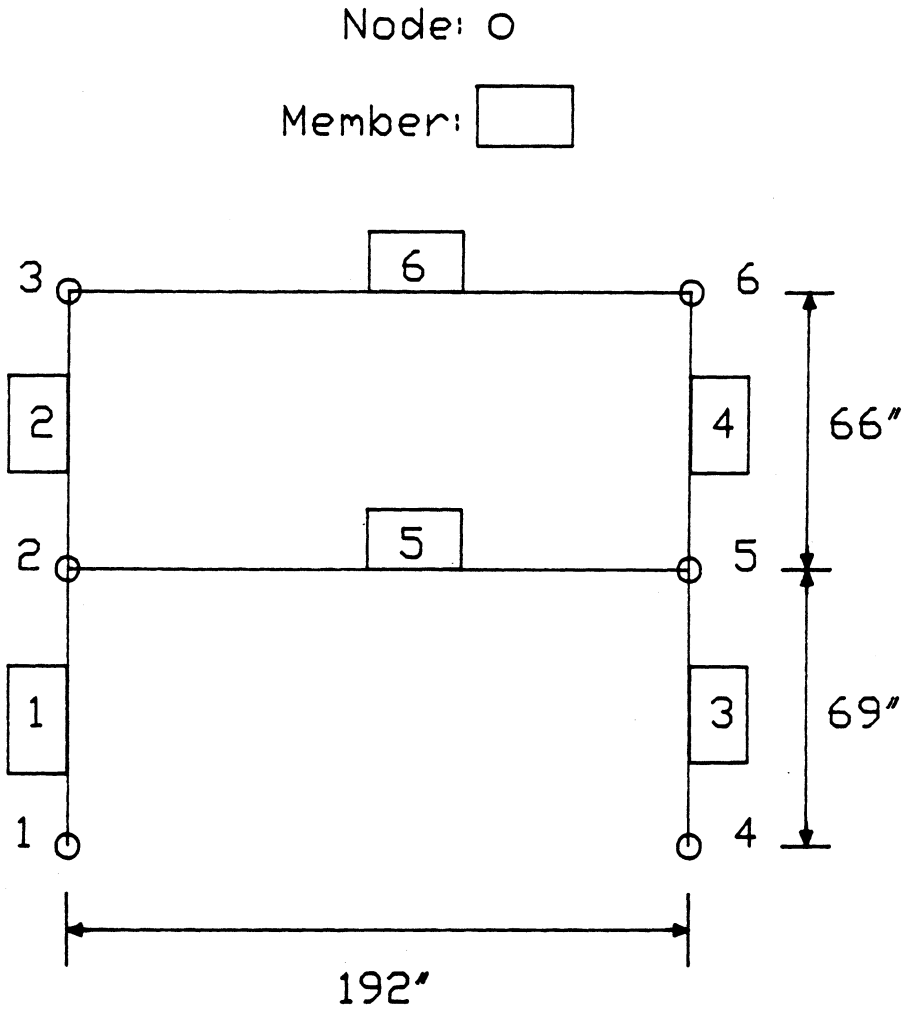

Fig. 7.2 Computer Model of Test Frame

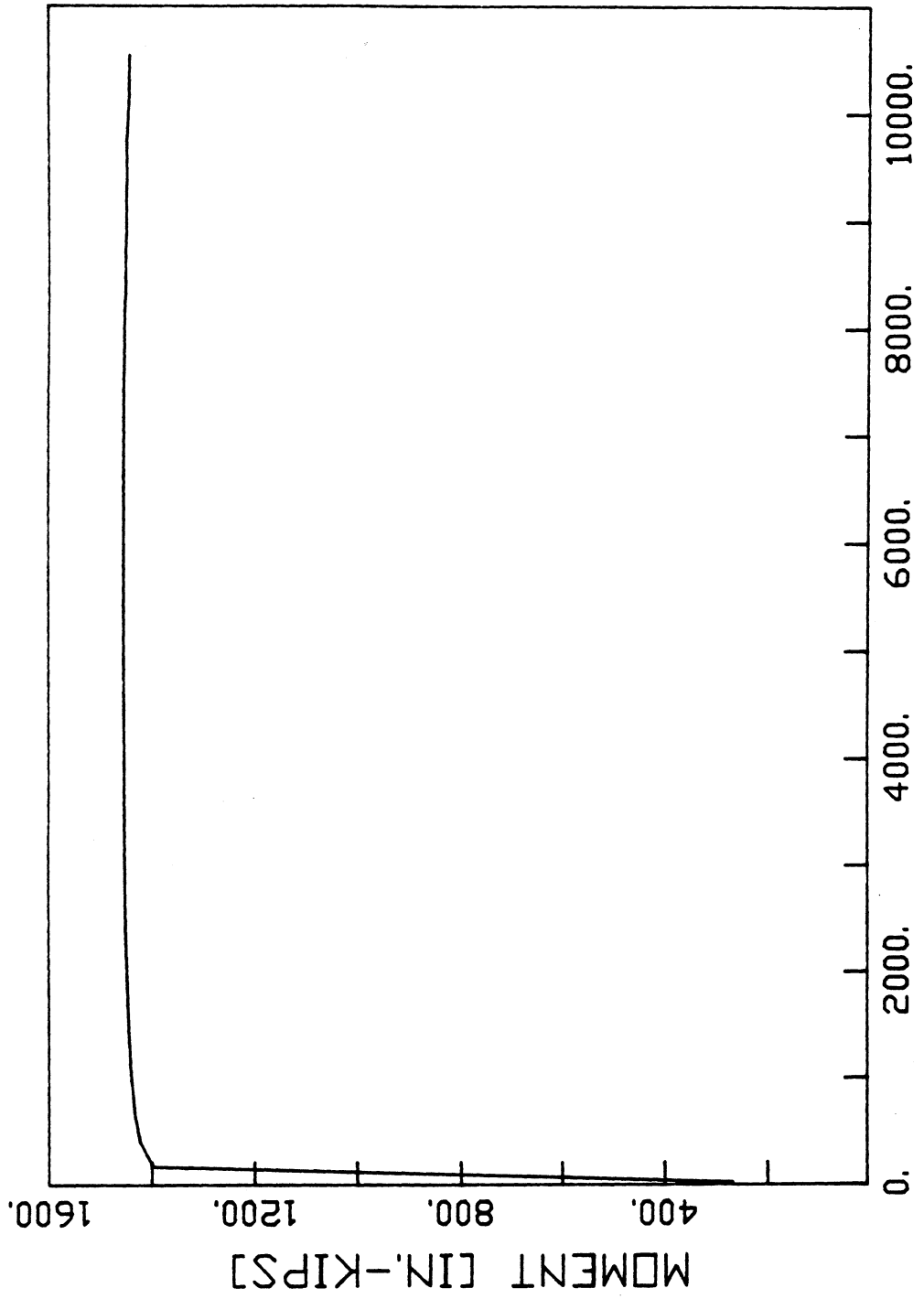

Fig. 7.3 Moment vs. Curvature Diagram for The First-Story Beam

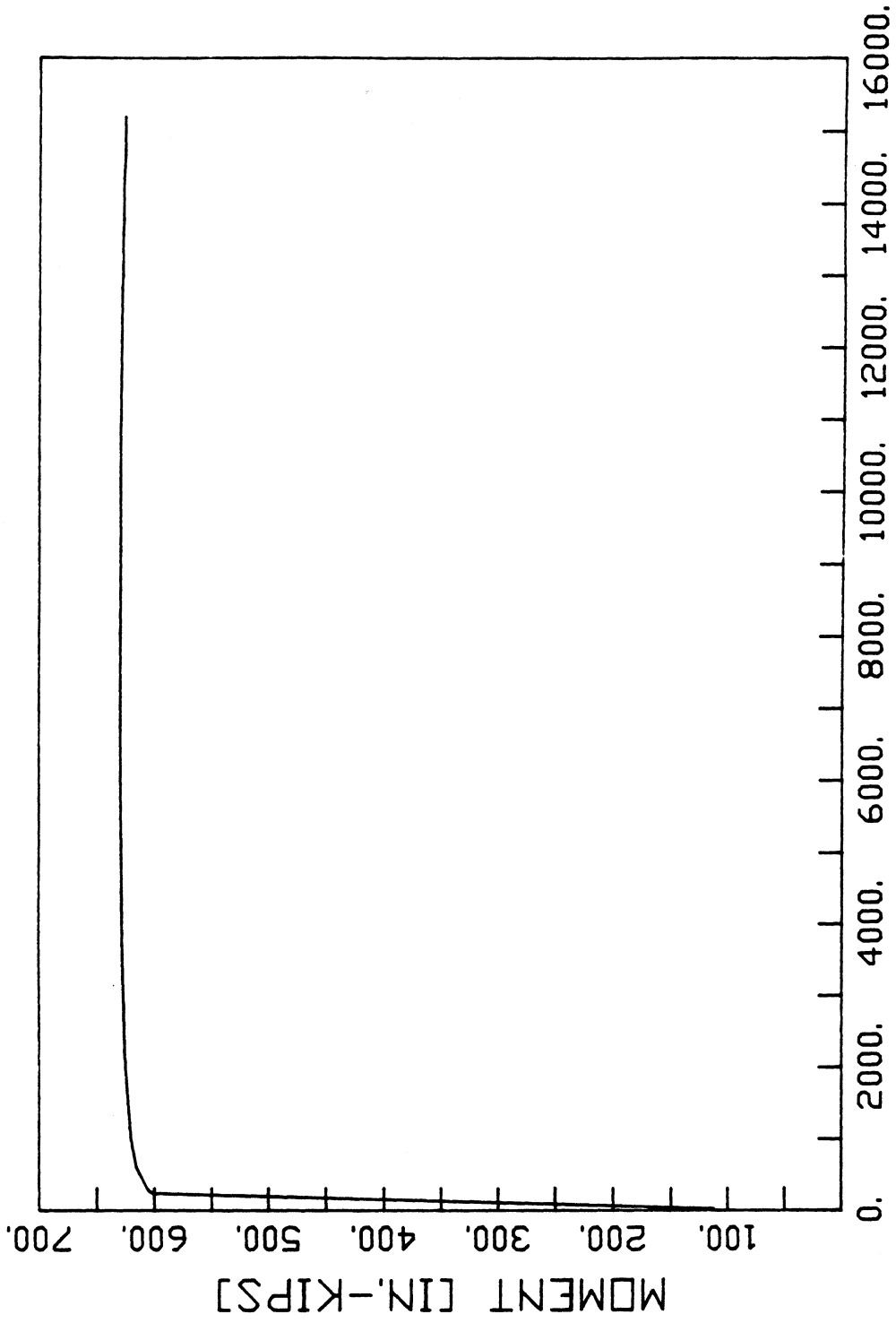

Fig. 7.4 Moment vs. Curvature Diagram for The Second-Story Beam

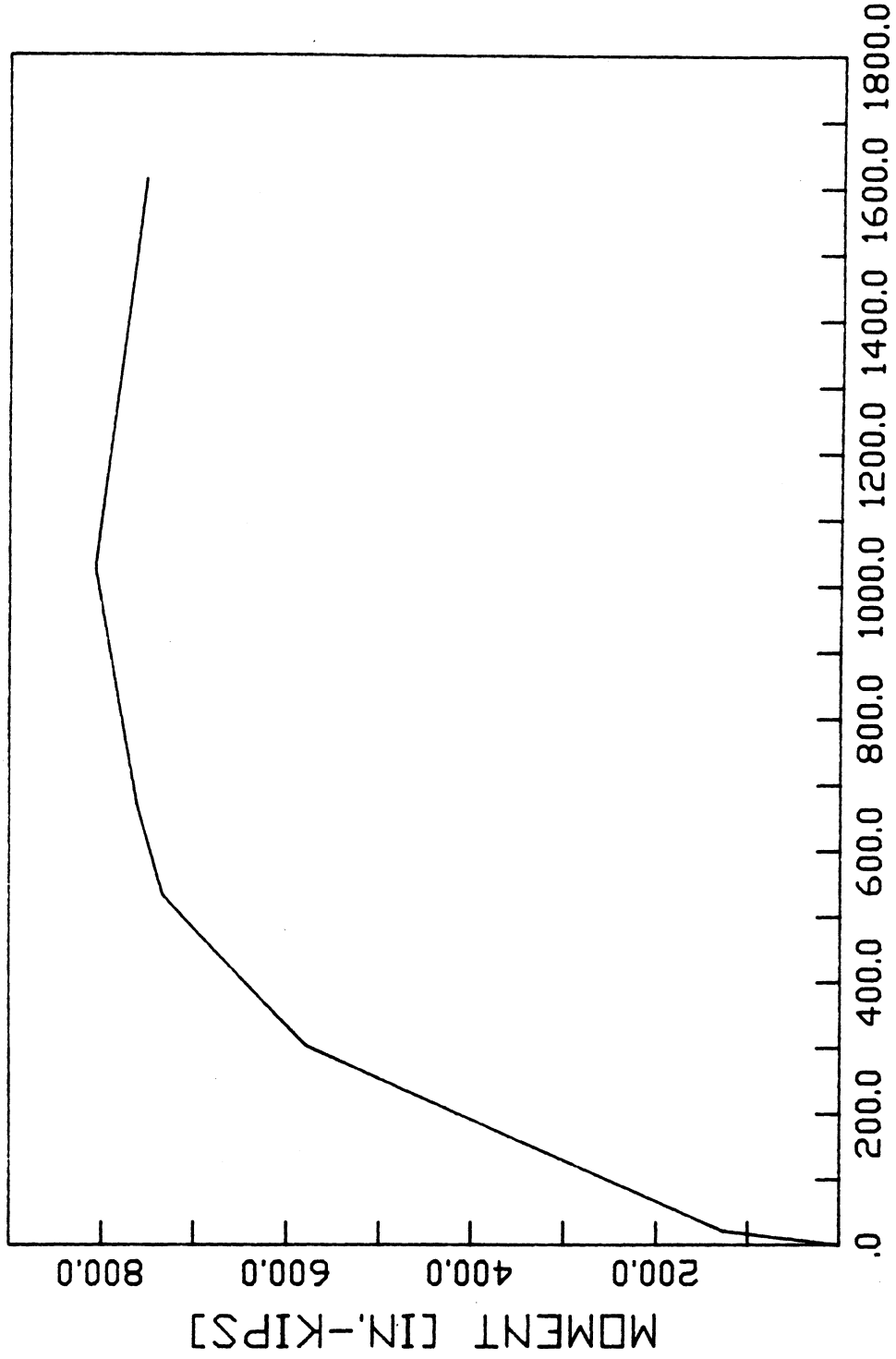

Fig. 7.5 Moment vs. Curvature Diagram for The Original Column

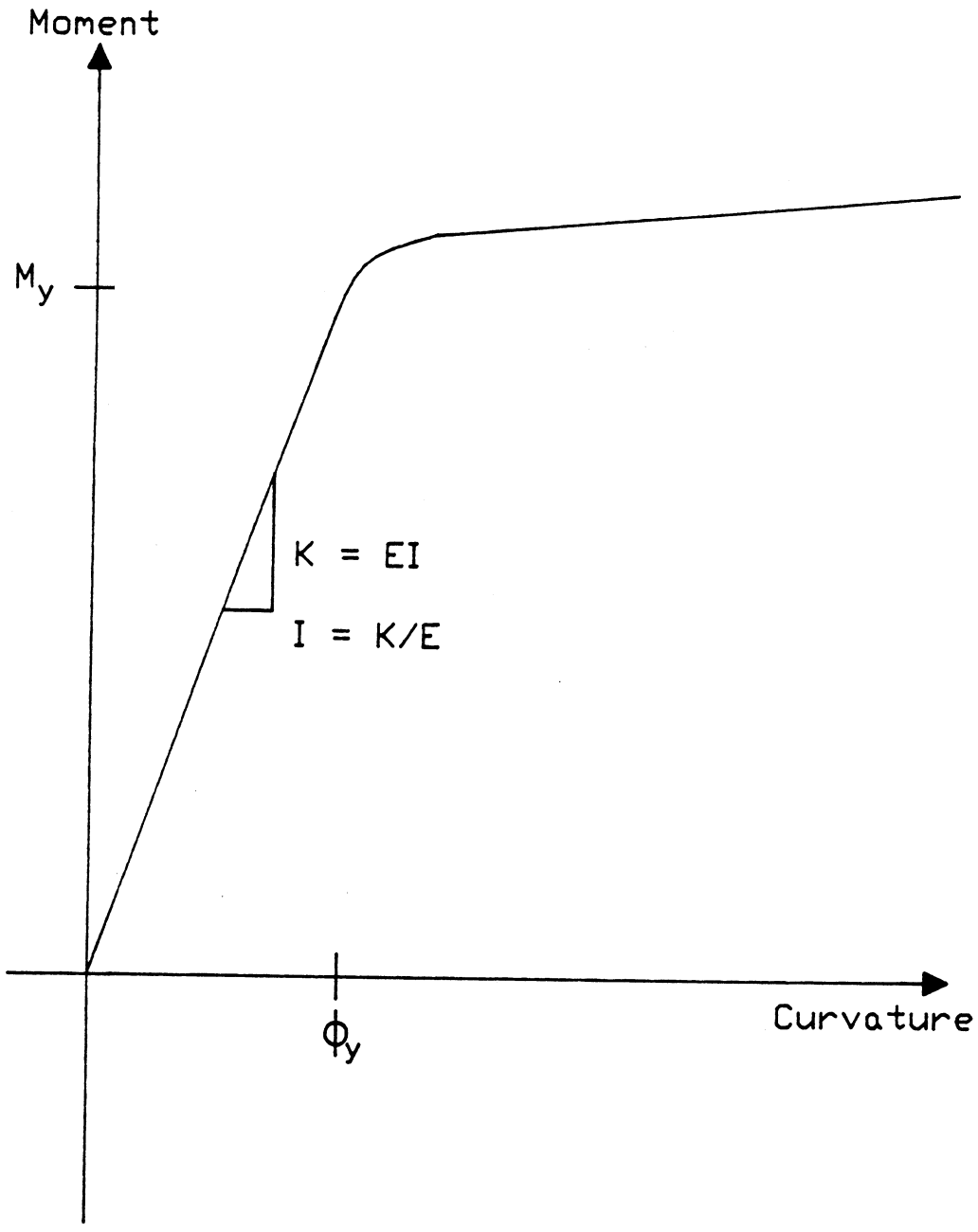

Fig. 7.6 Calculation of Input Values for Computer Model

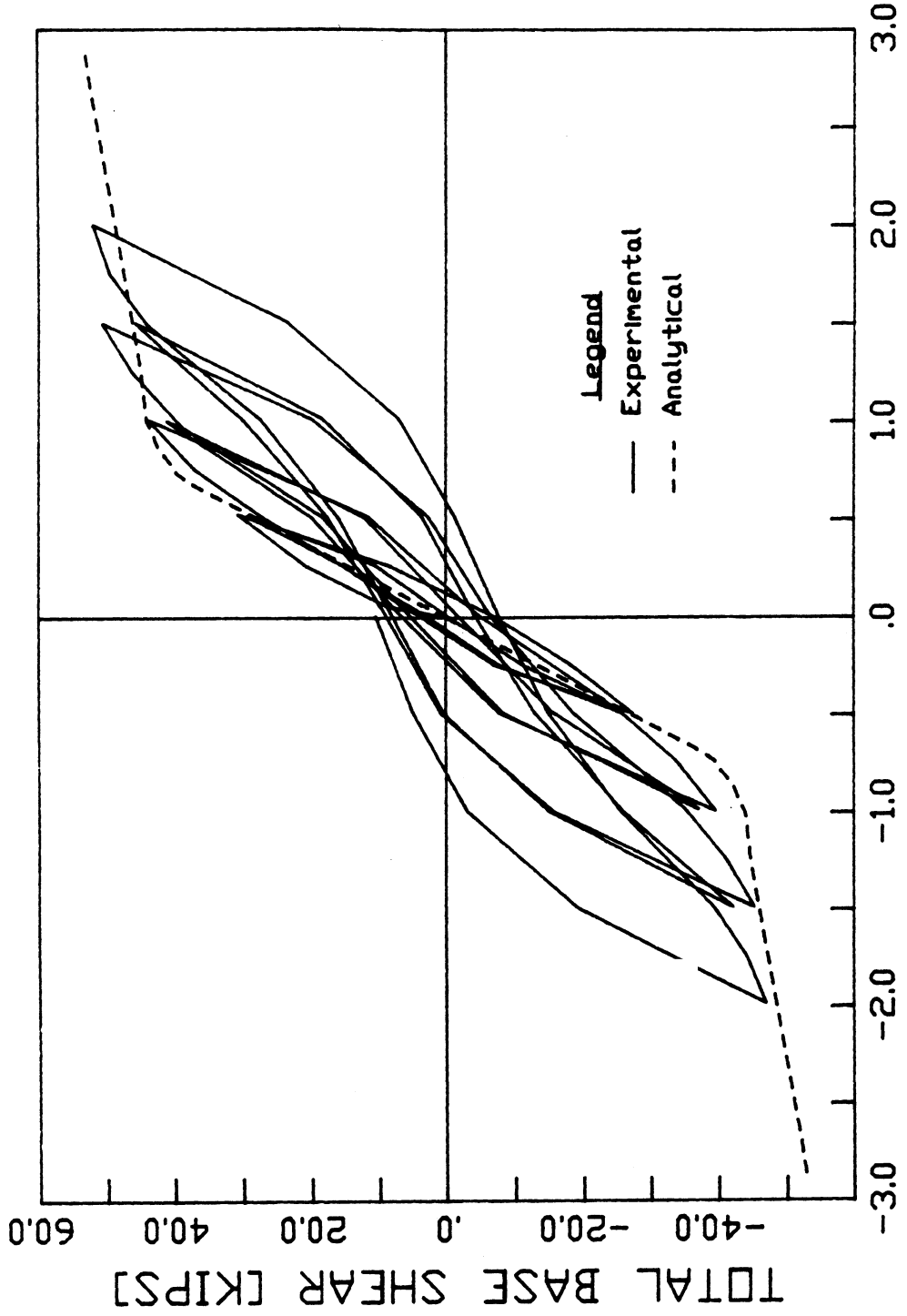

Fig. 7.7 Comparison of Analytical and Experimental Results for The Original Frame

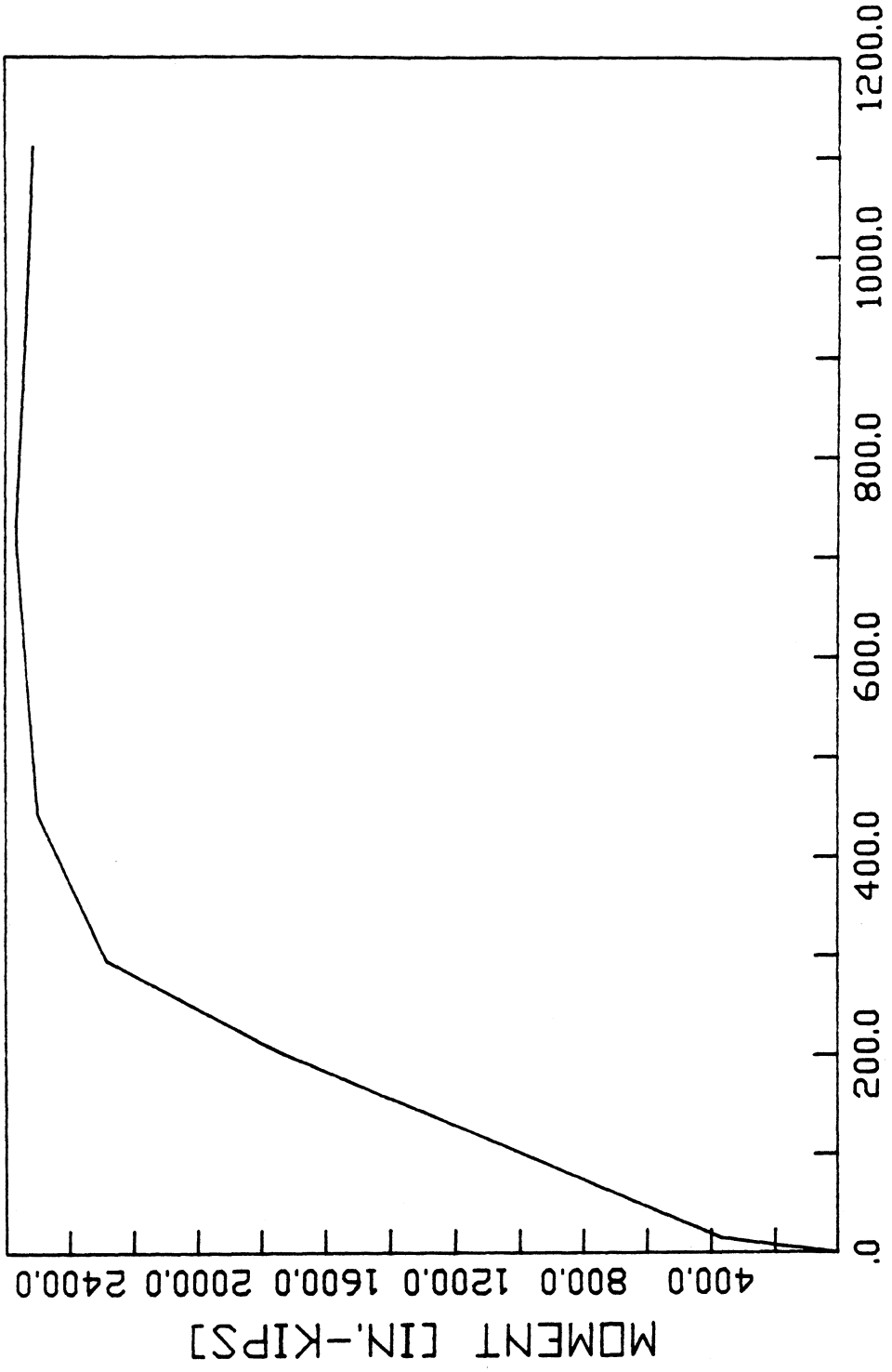

Fig. 7.8 Moment vs. Curvature Diagram for The Strengthened Column

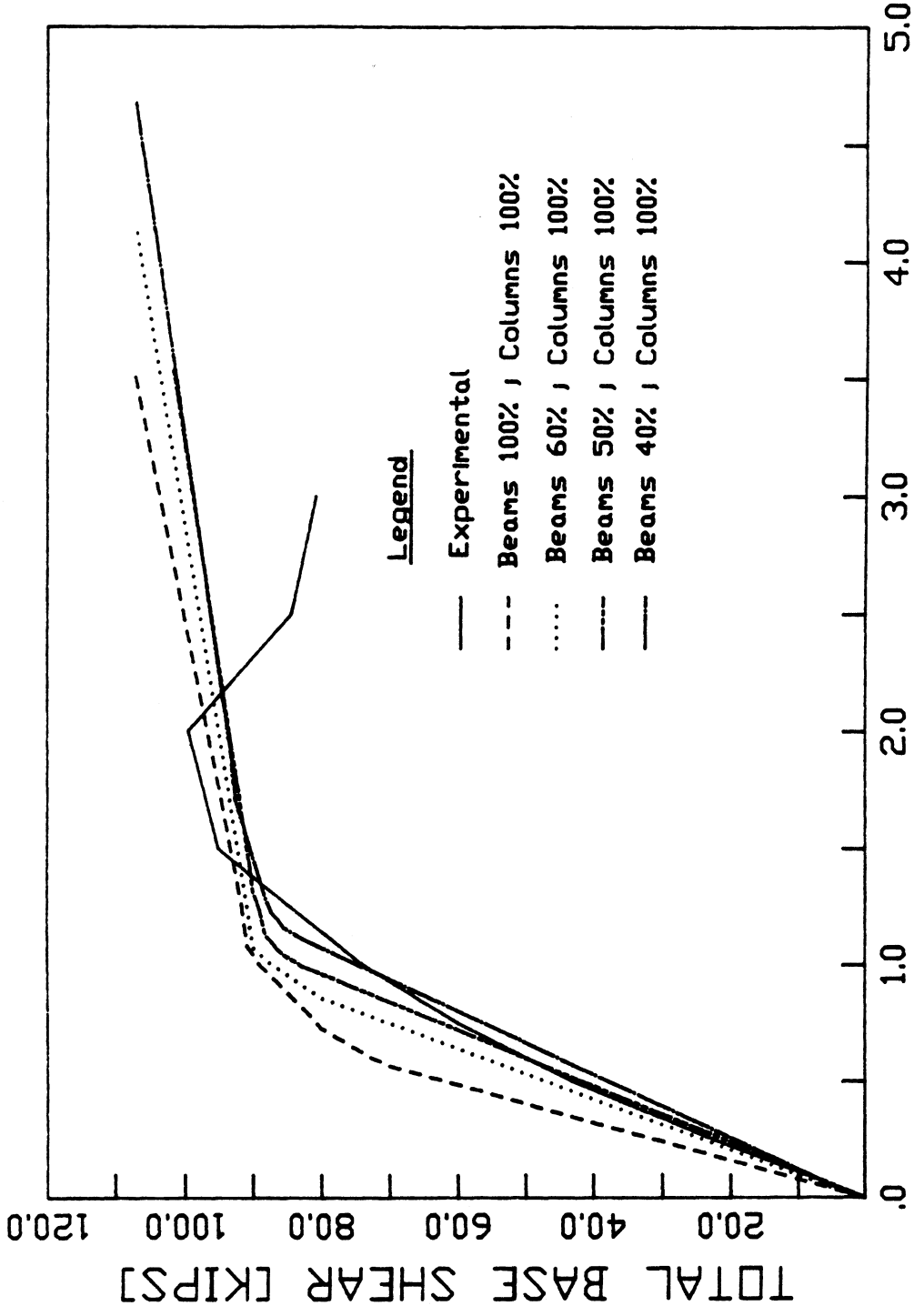

Fig. 7.9 Parametric Study of The Effect of Beam Stiffness on Model Behavior

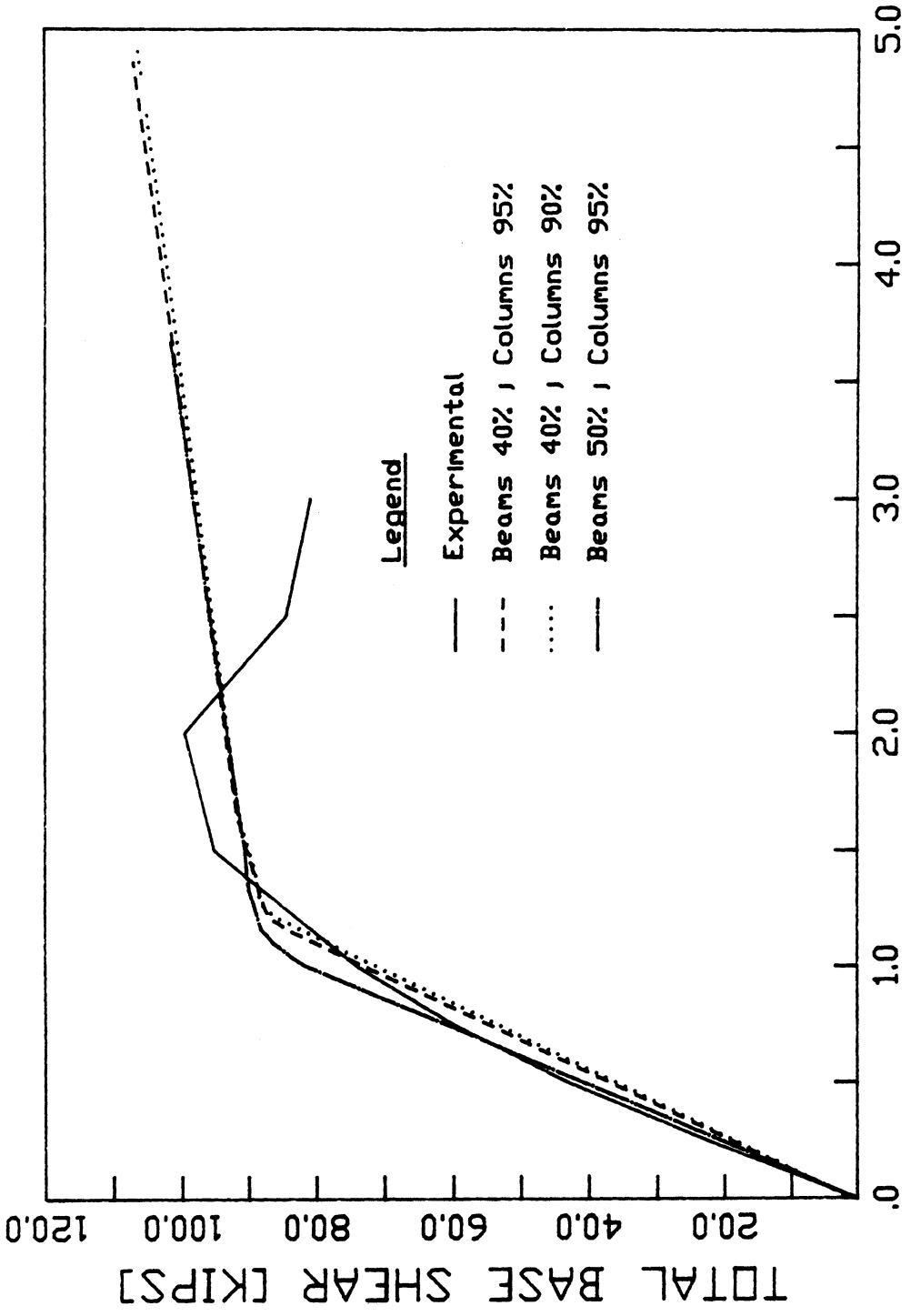

Fig. 7.10 Parametric Study of The Effect of Column Stiffness on Model Behavior

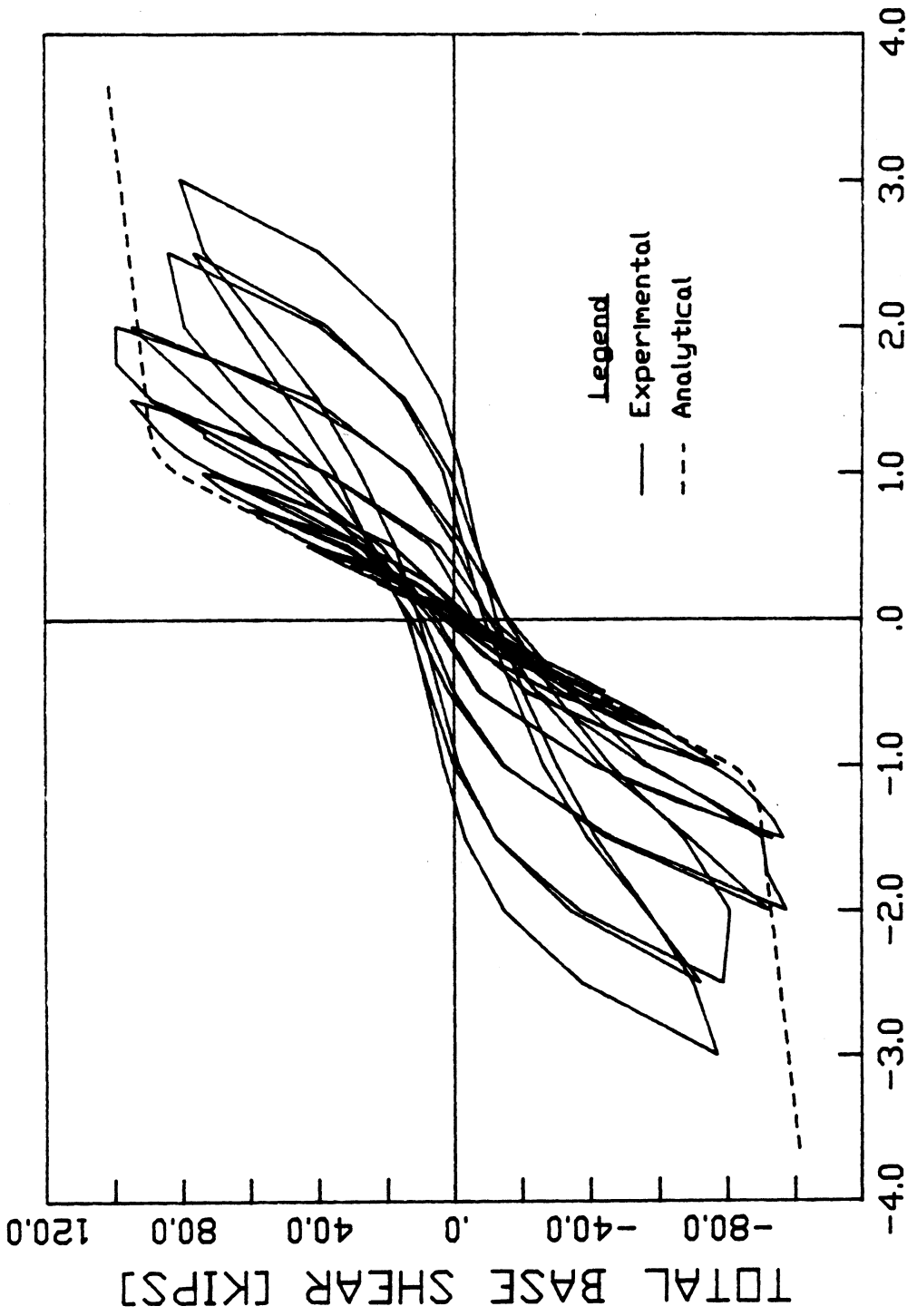

Fig. 7.11 Comparison of Analytical and Experimental Results for The Strengthened Frame

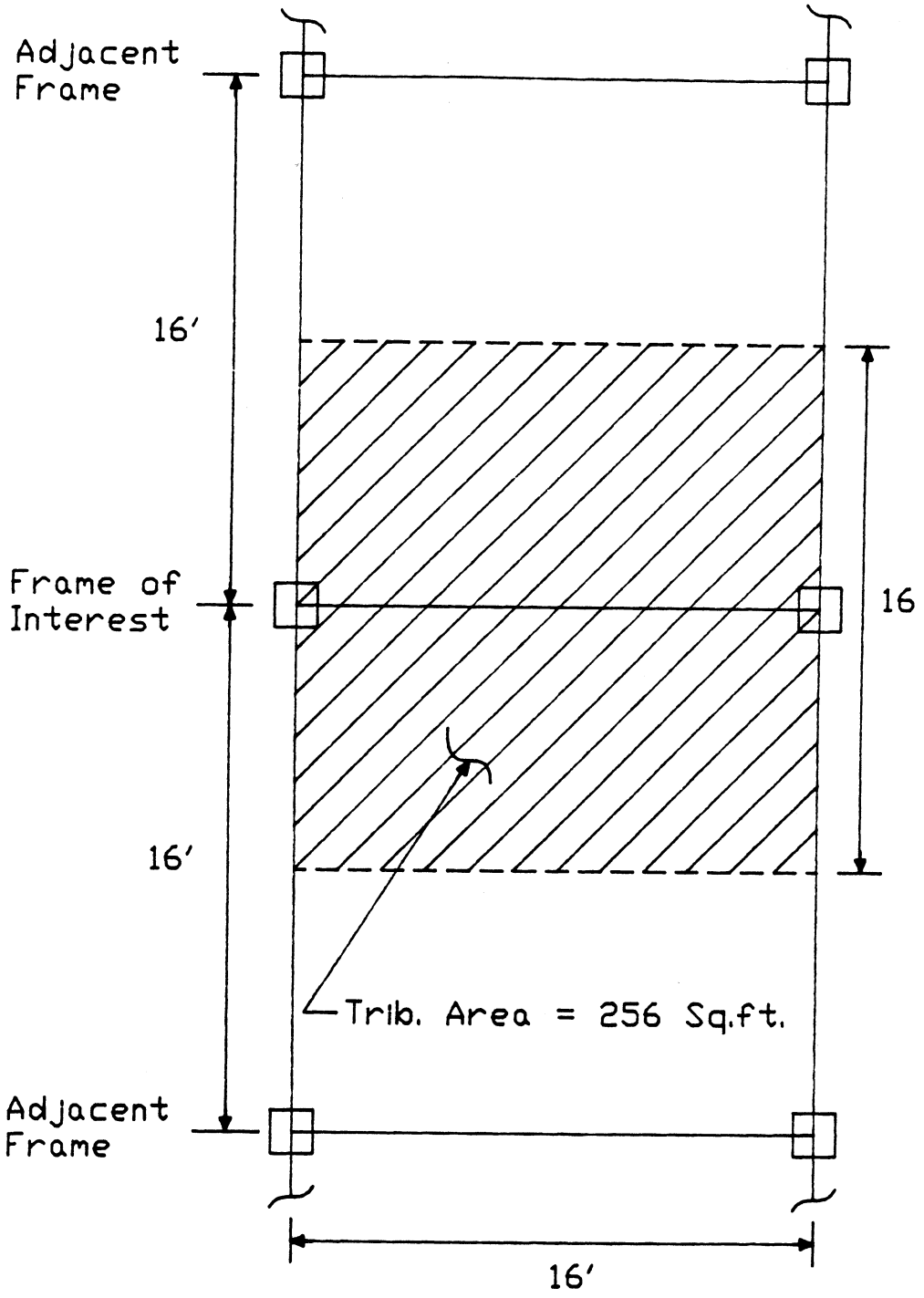

Fig. 7.12 Tributary Area of Model Frame for Mass Calculations

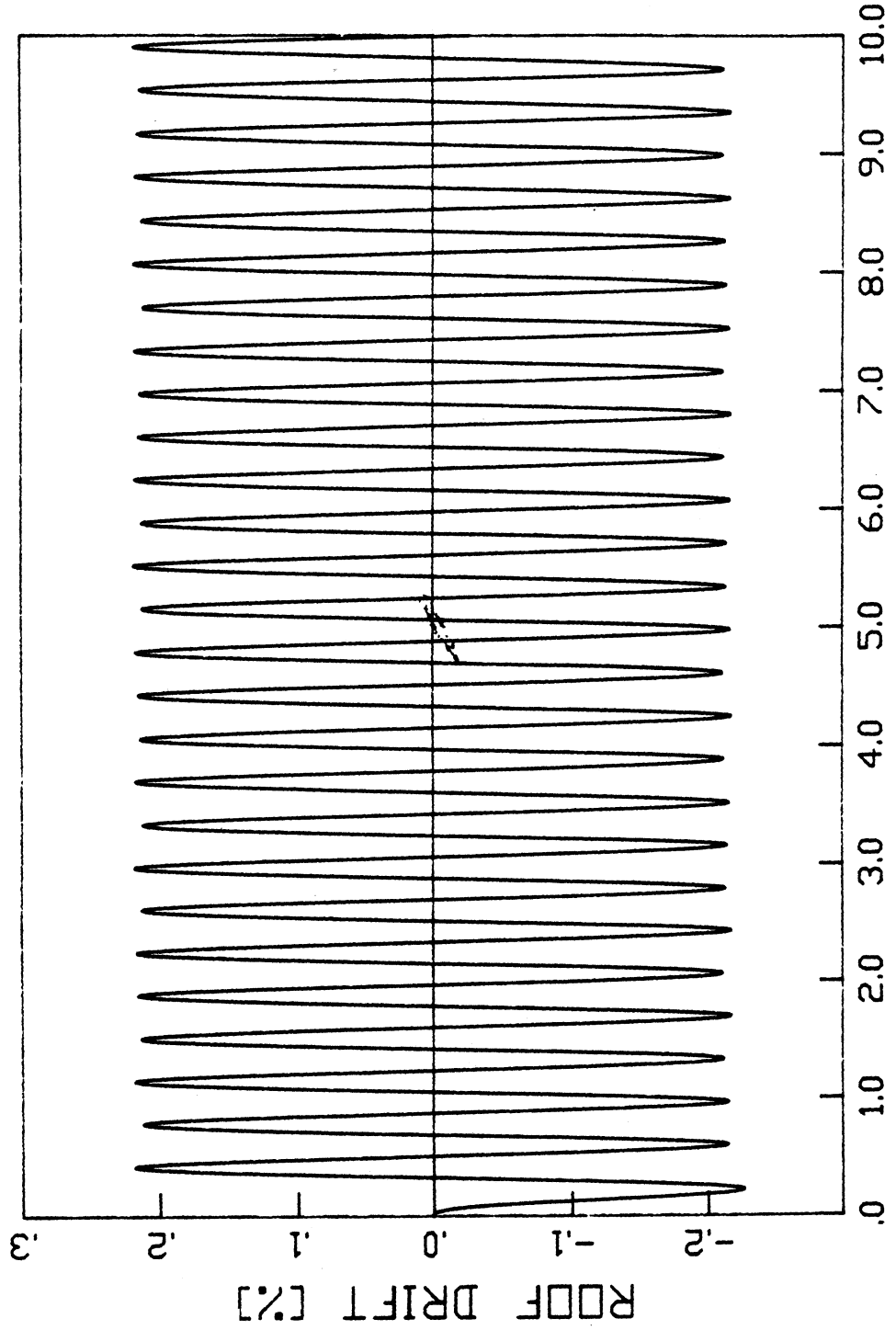

Fig. 7.13 Response of The Original Frame Model to a Pulse Load

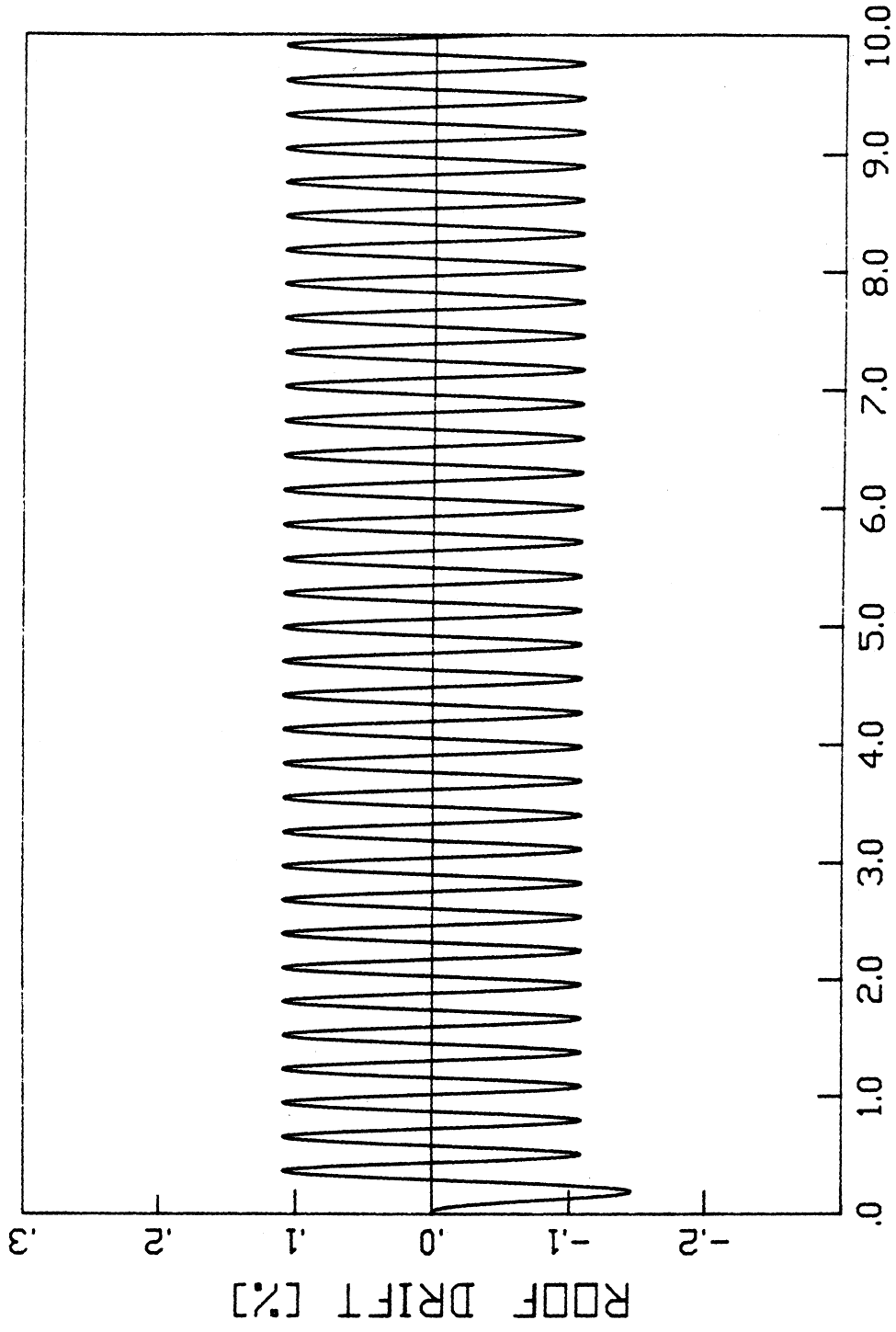

Fig. 7.14 Response of The Strengthened Frame Model to a Pulse Load

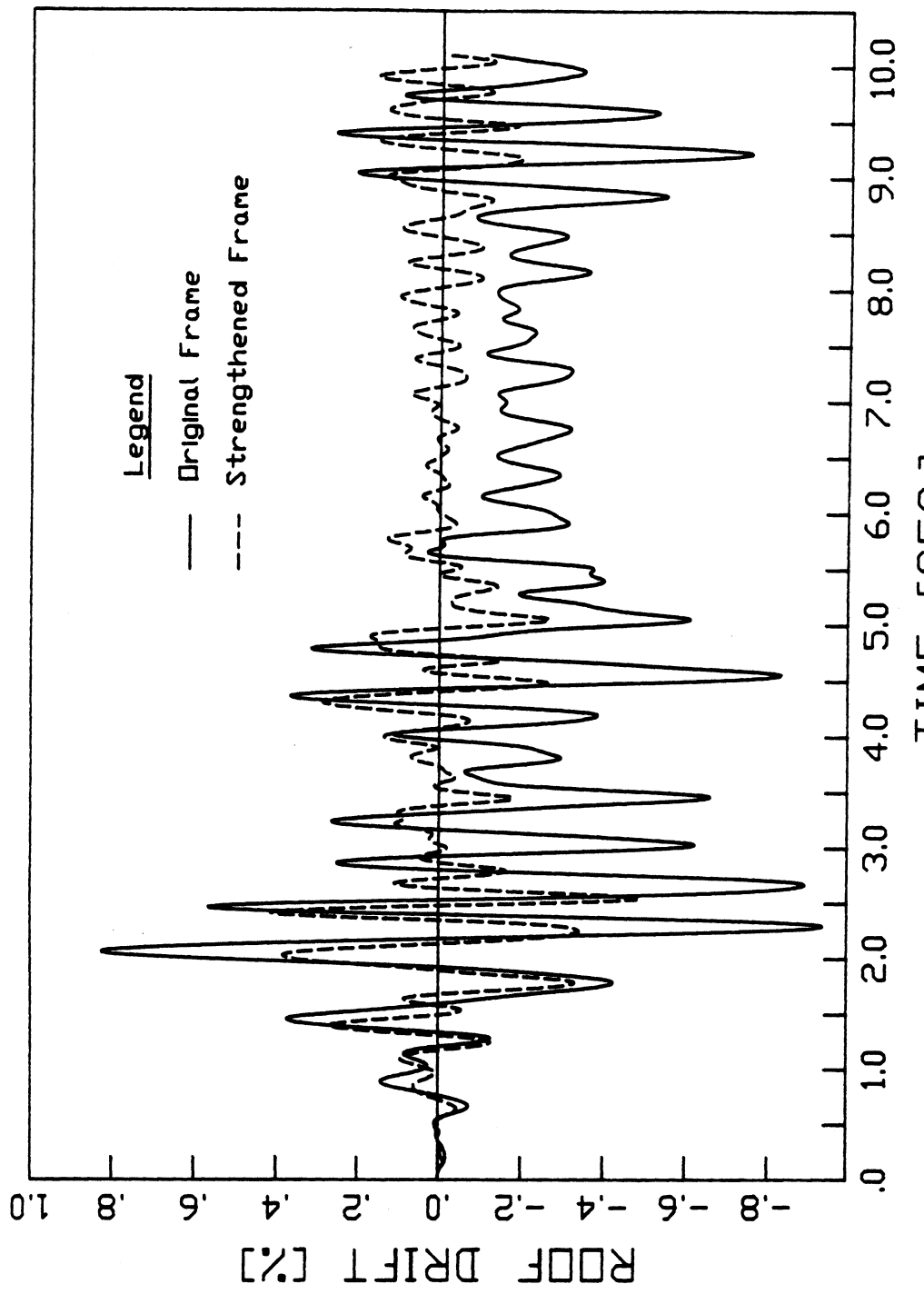

Fig. 7.15 Response of The Original and Strengthened Frame Models to The El Centro Record

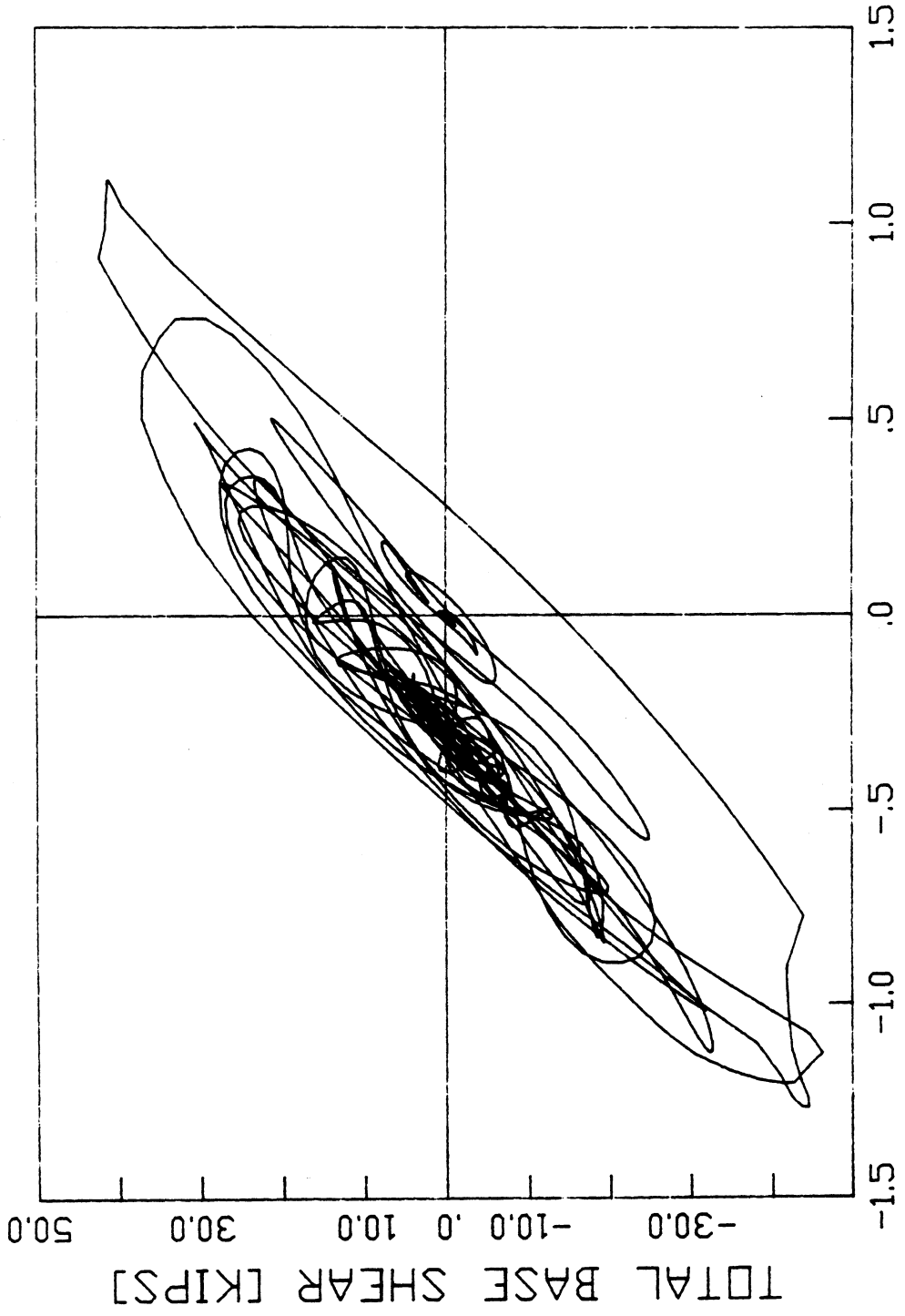

Fig. 7.16 Hysteresis Curves for The Original Frame Model, El Centro Record

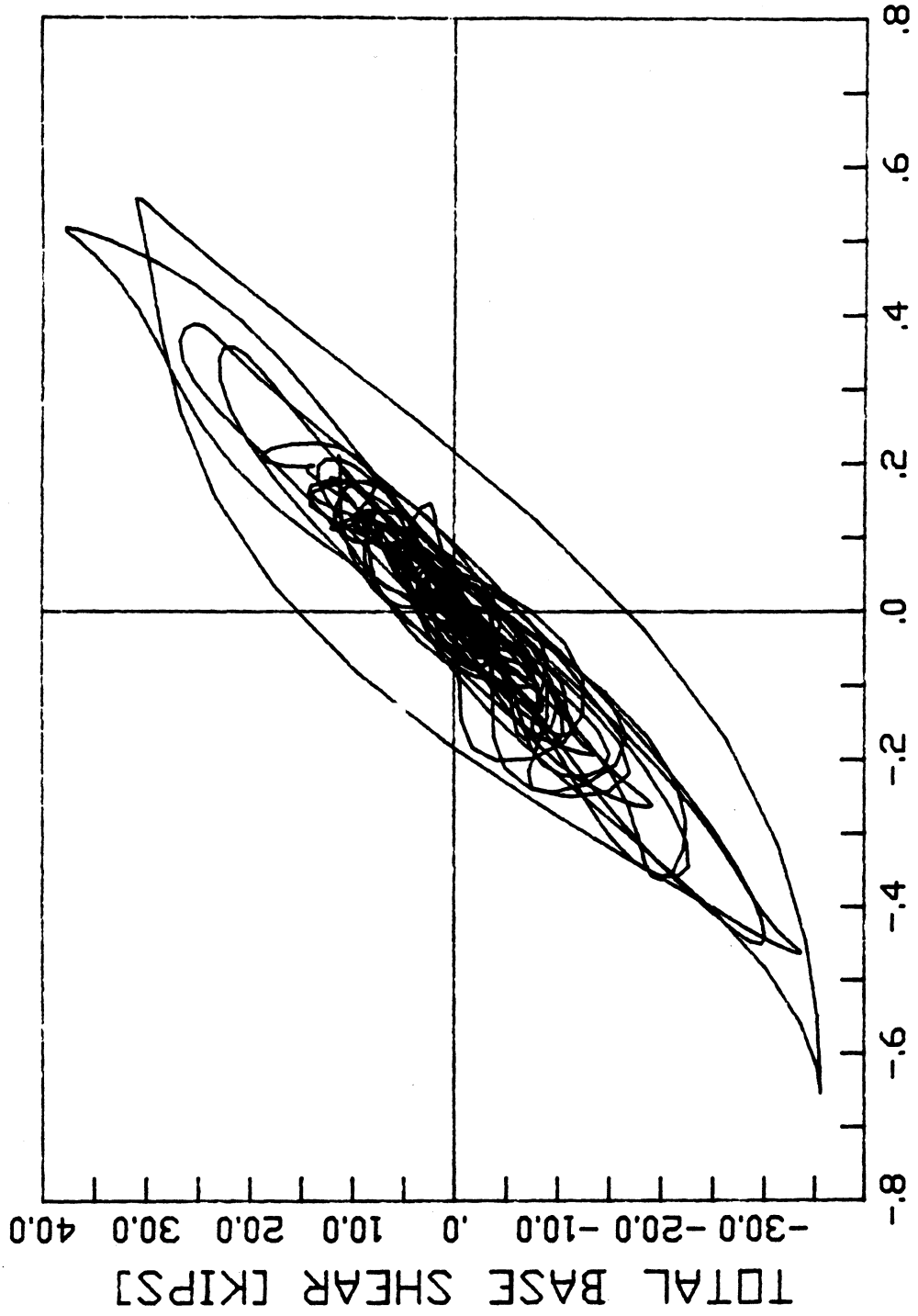

Fig. 7.17 Hysteresis Curves for The Strengthened Frame Model, El Centro Record

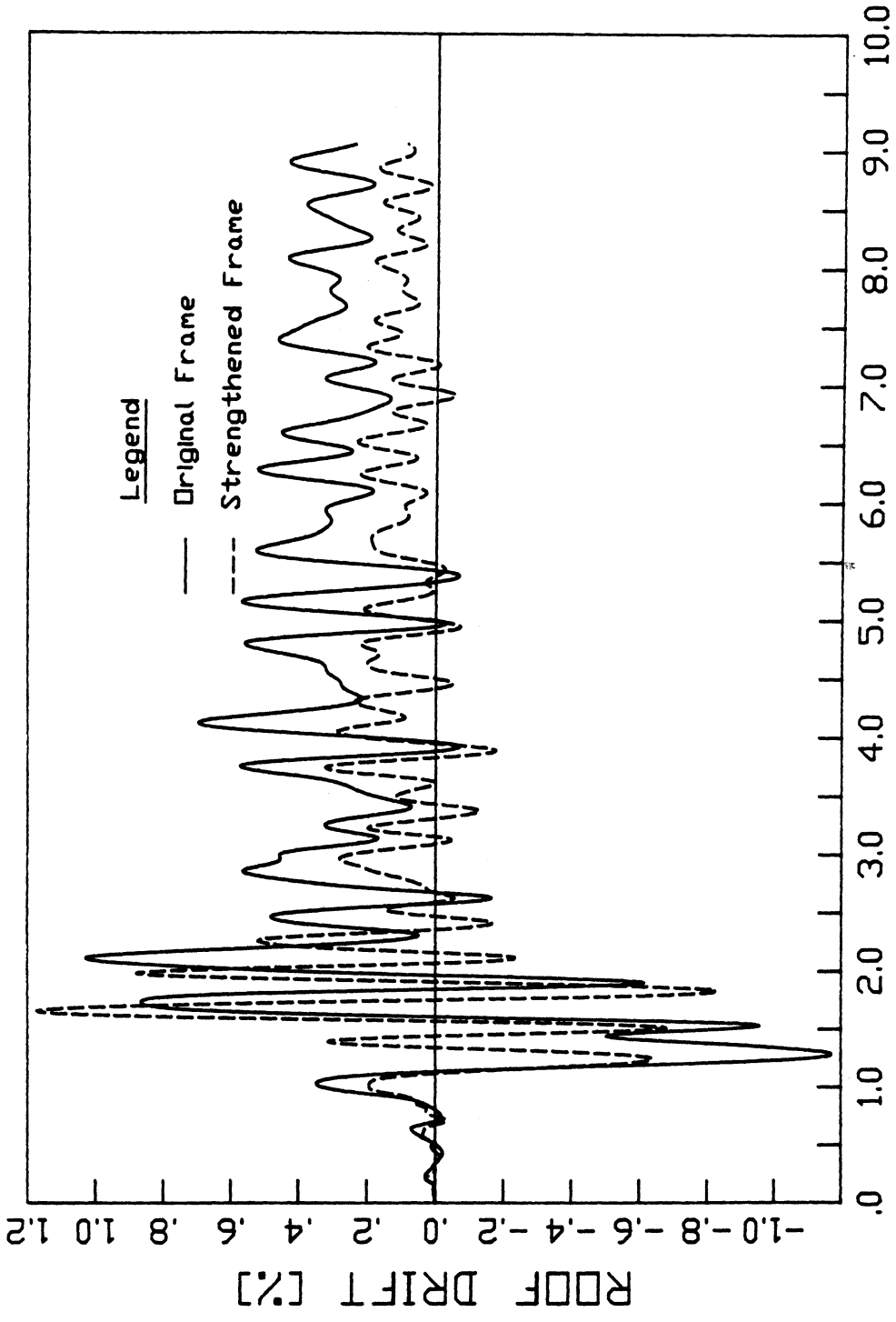

Fig. 7.18 Response of The Original and Strengthened Frame Models to The San Salvador Record

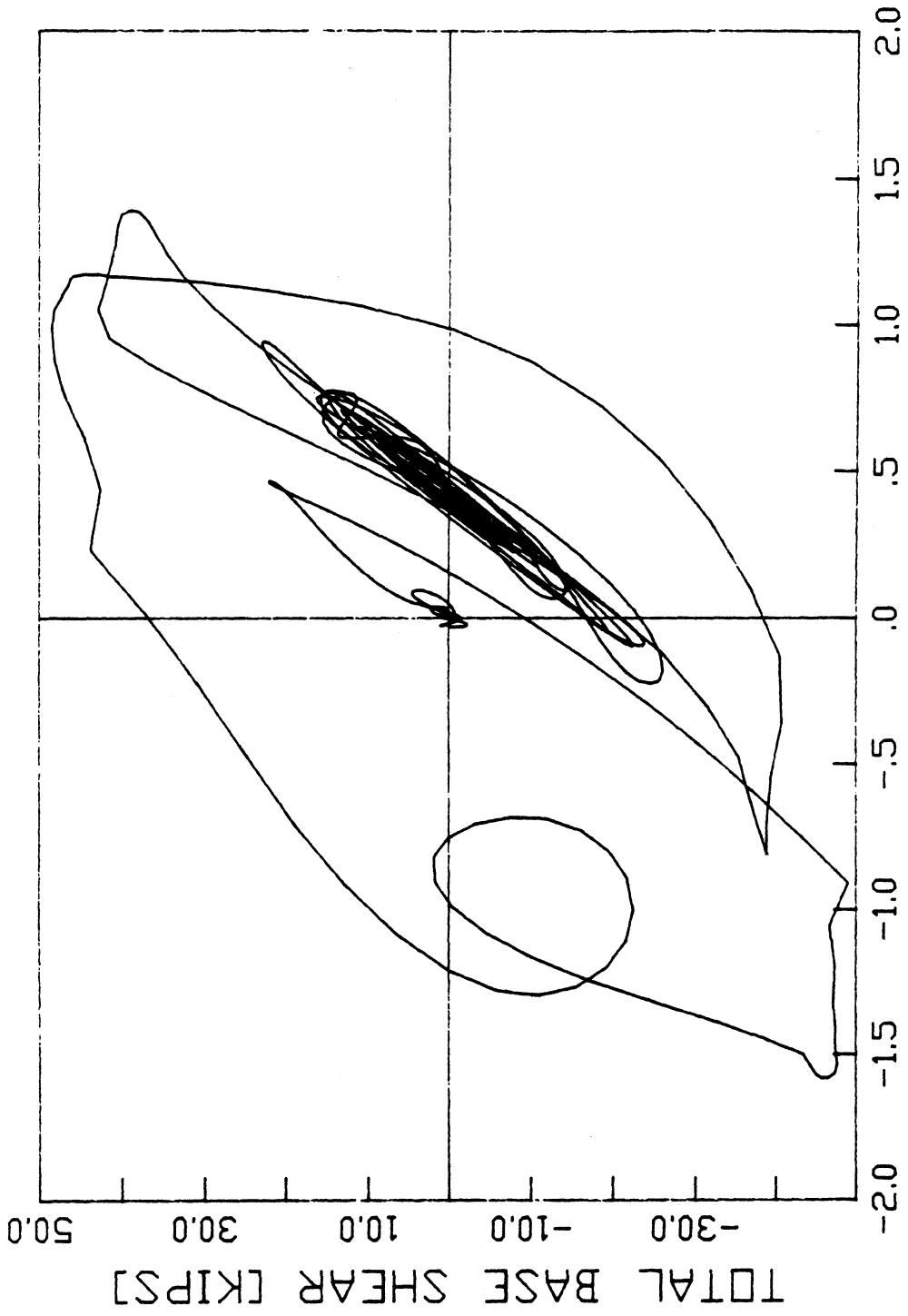

Fig. 7.19 Hysteresis Curves for The Original Frame Model, San Salvador Record

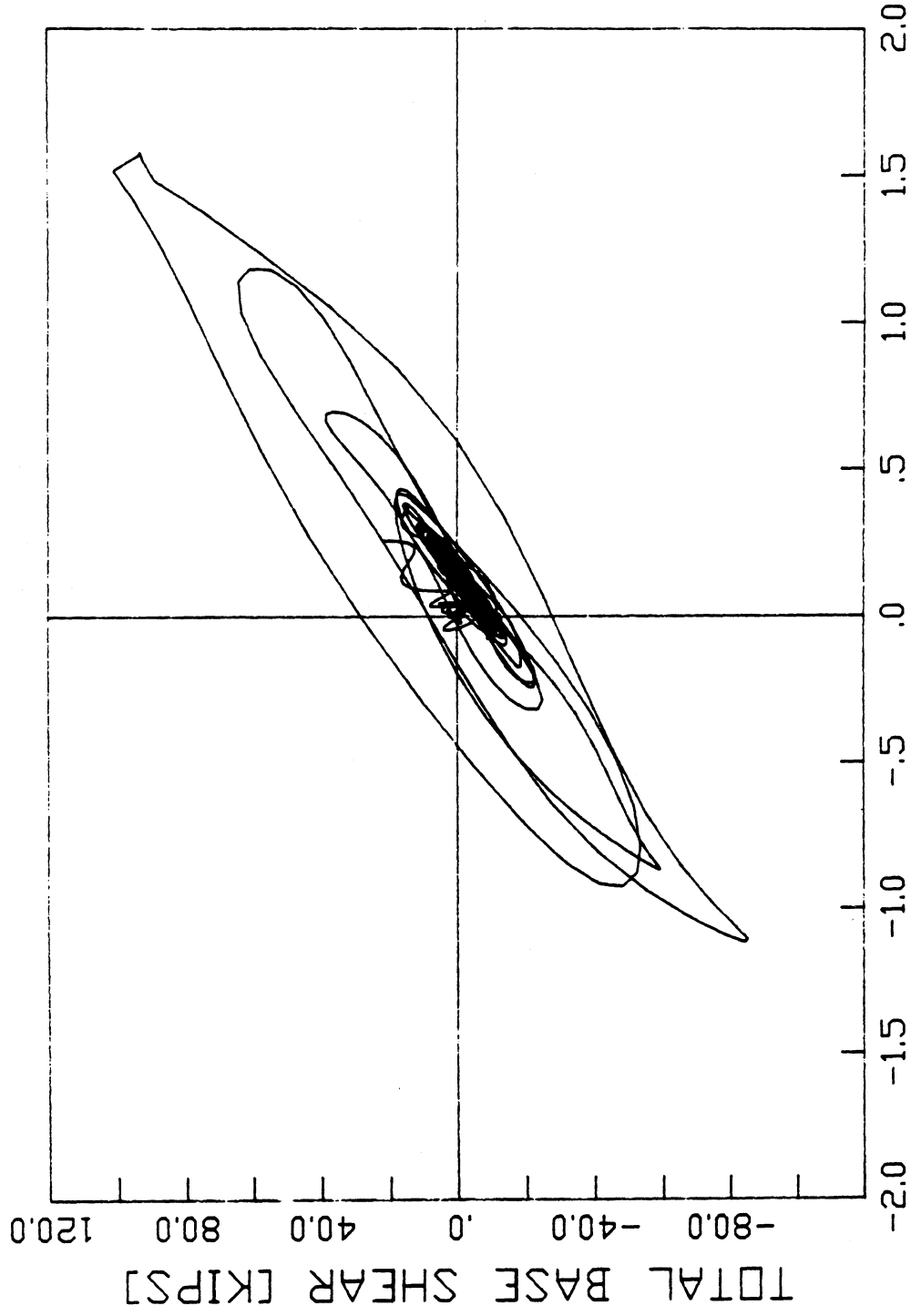

Fig. 7.20 Hysteresis Curves for The Strengthened Frame Model, San Salvador Record

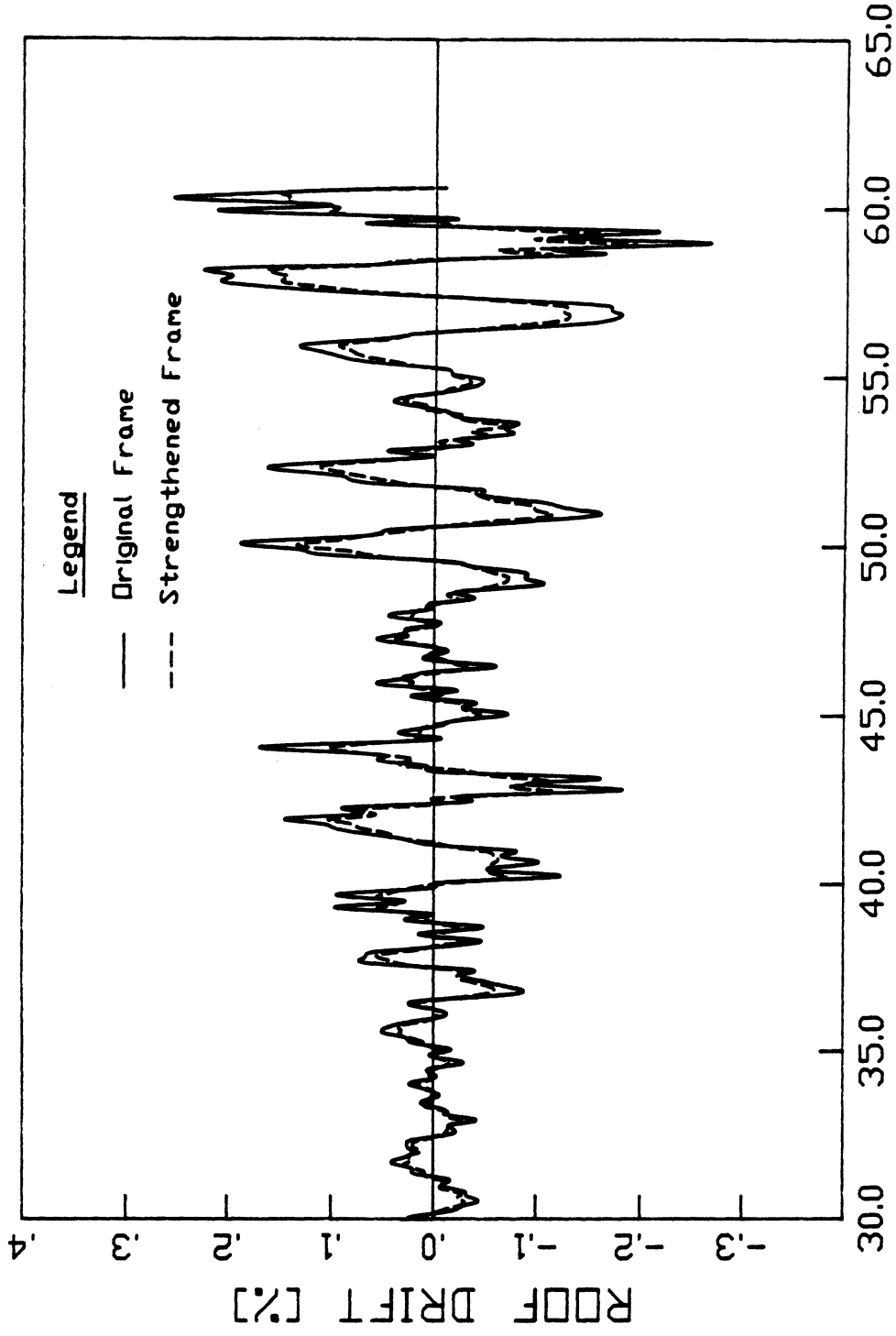

Fig. 7.21 Response of The Original and Strengthened Frame Models to The Mexico City SCT Record

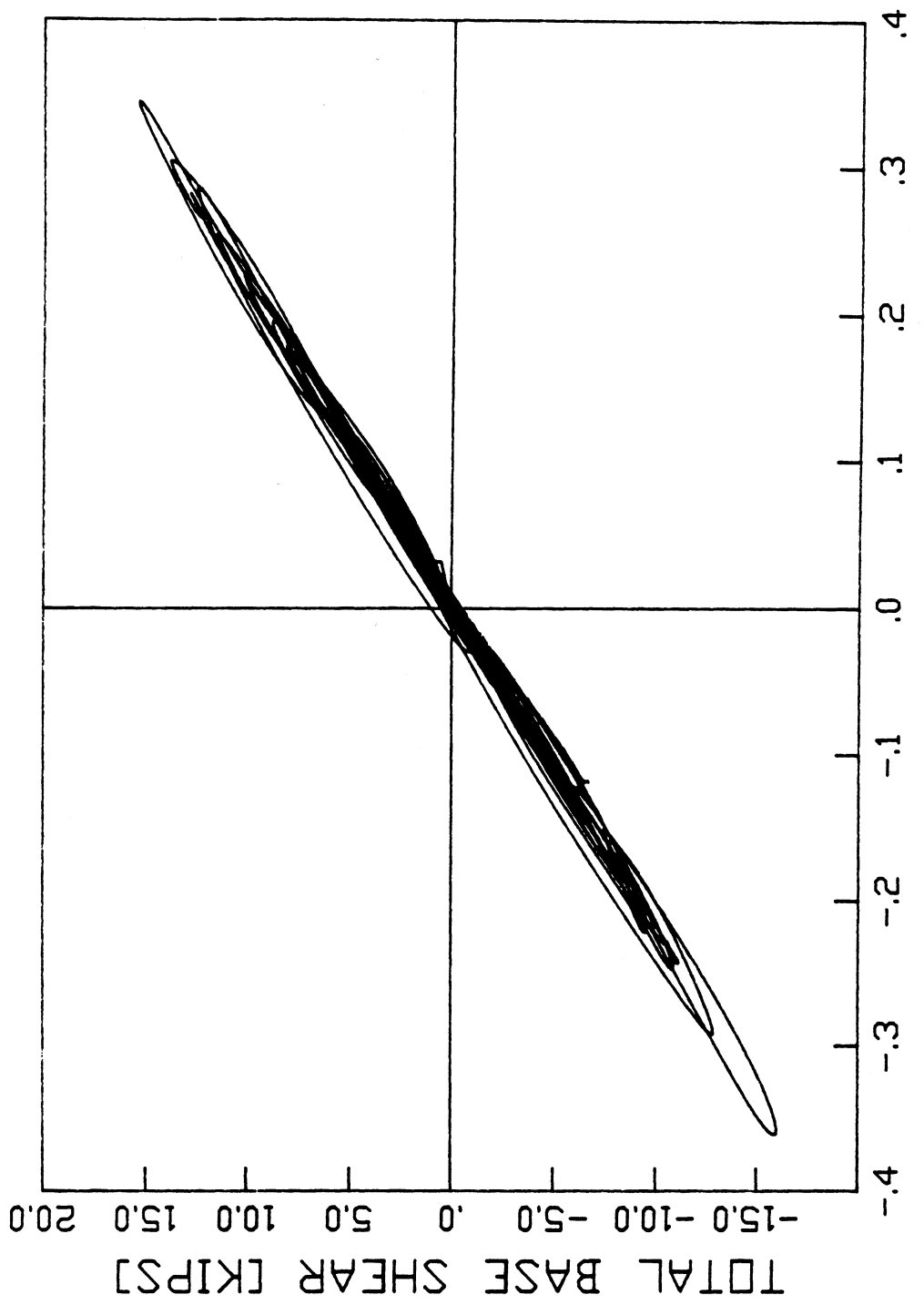

Fig. 7.22 Hysteresis Curves for The Original Frame Model, Mexico City SCT Record

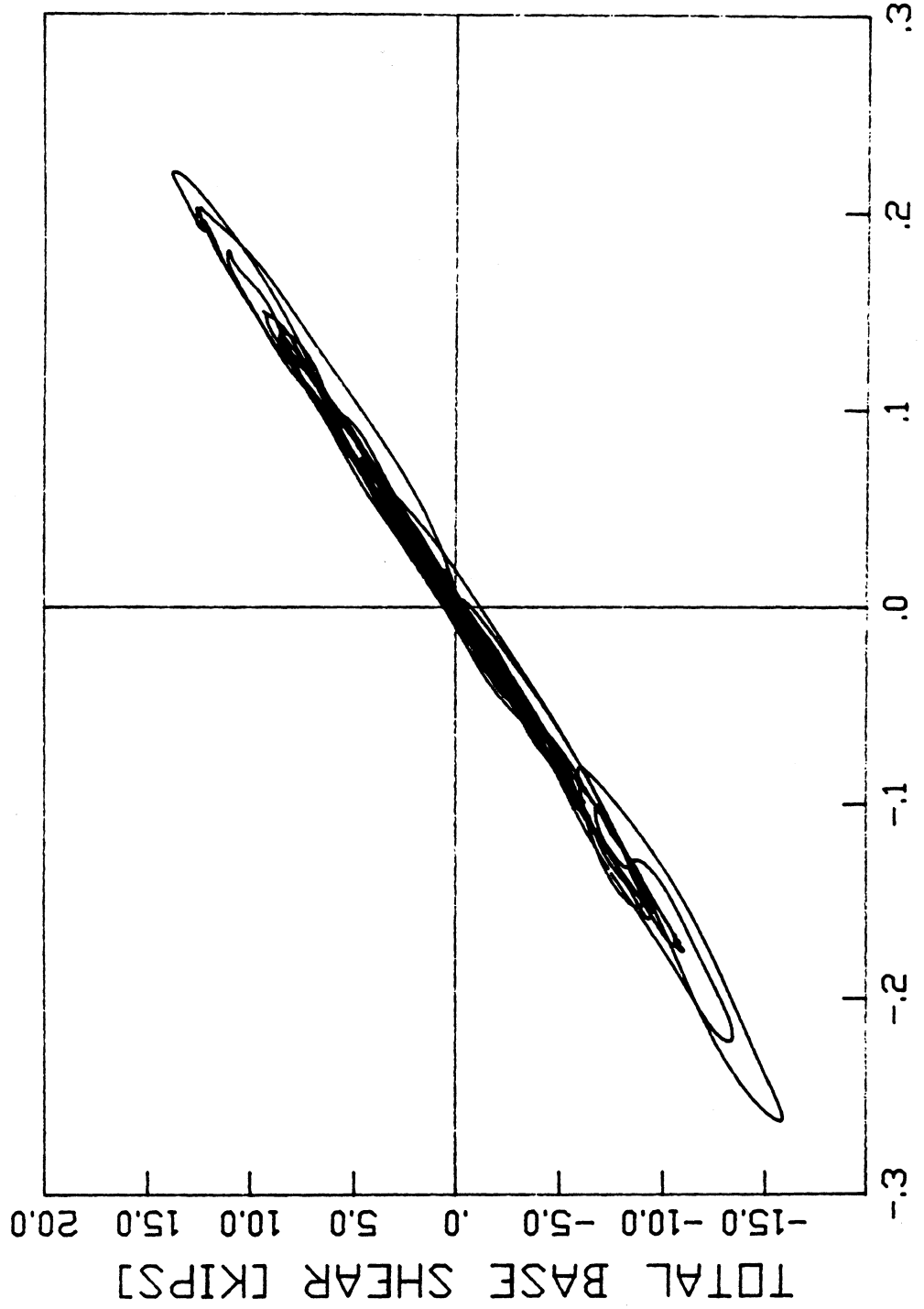

Fig. 7.23 Hysteresis Curves for The Strengthened Frame Model, Mexico City SCT Record

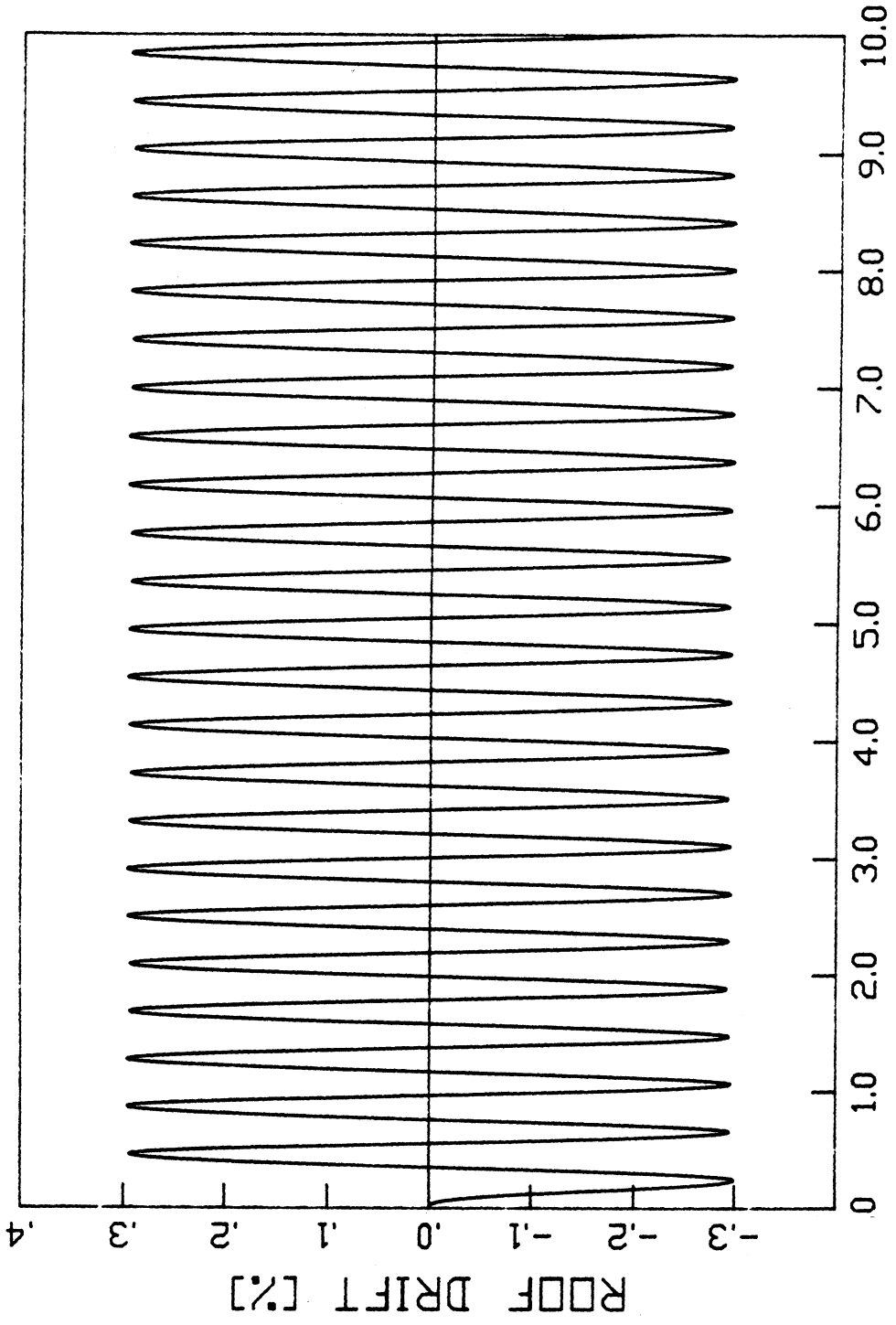

Fig. 7.24 Response of The Double Mass Model to a Pulse Load

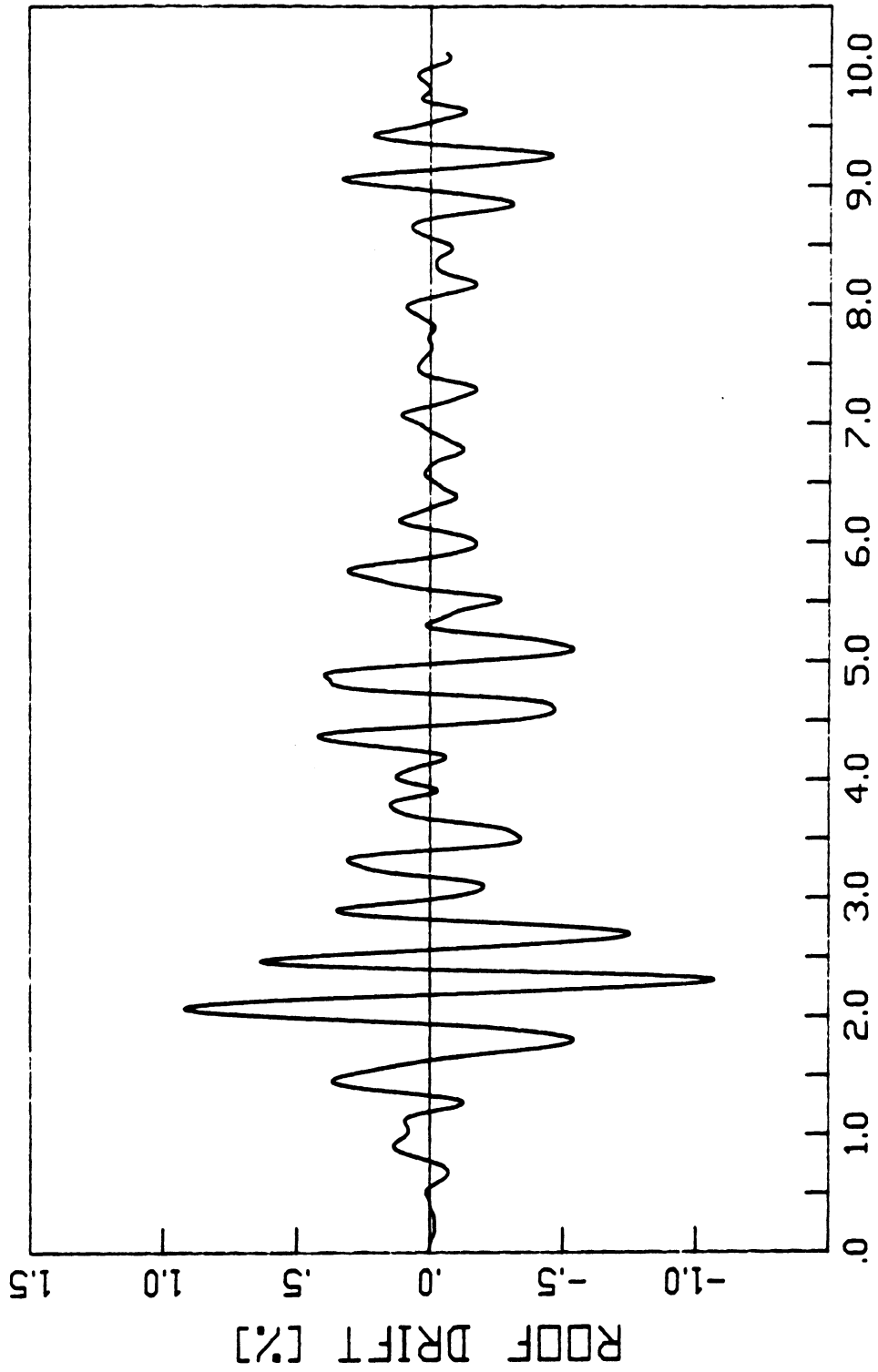

Fig. 7.25 Response of The Double Mass Model to The El Centro Record

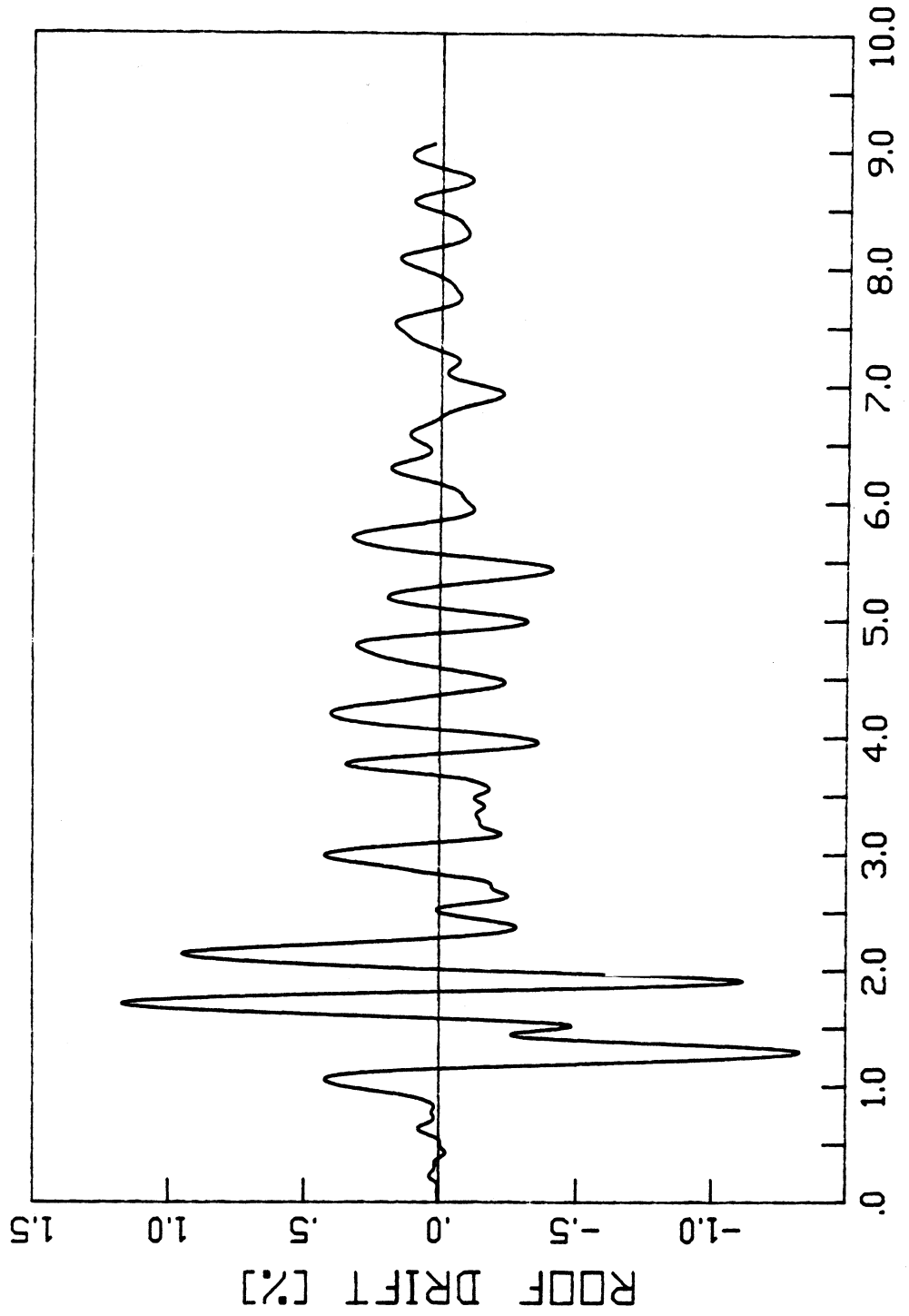

Fig. 7.26 Response of The Double Mass Model to The San Salvador Record

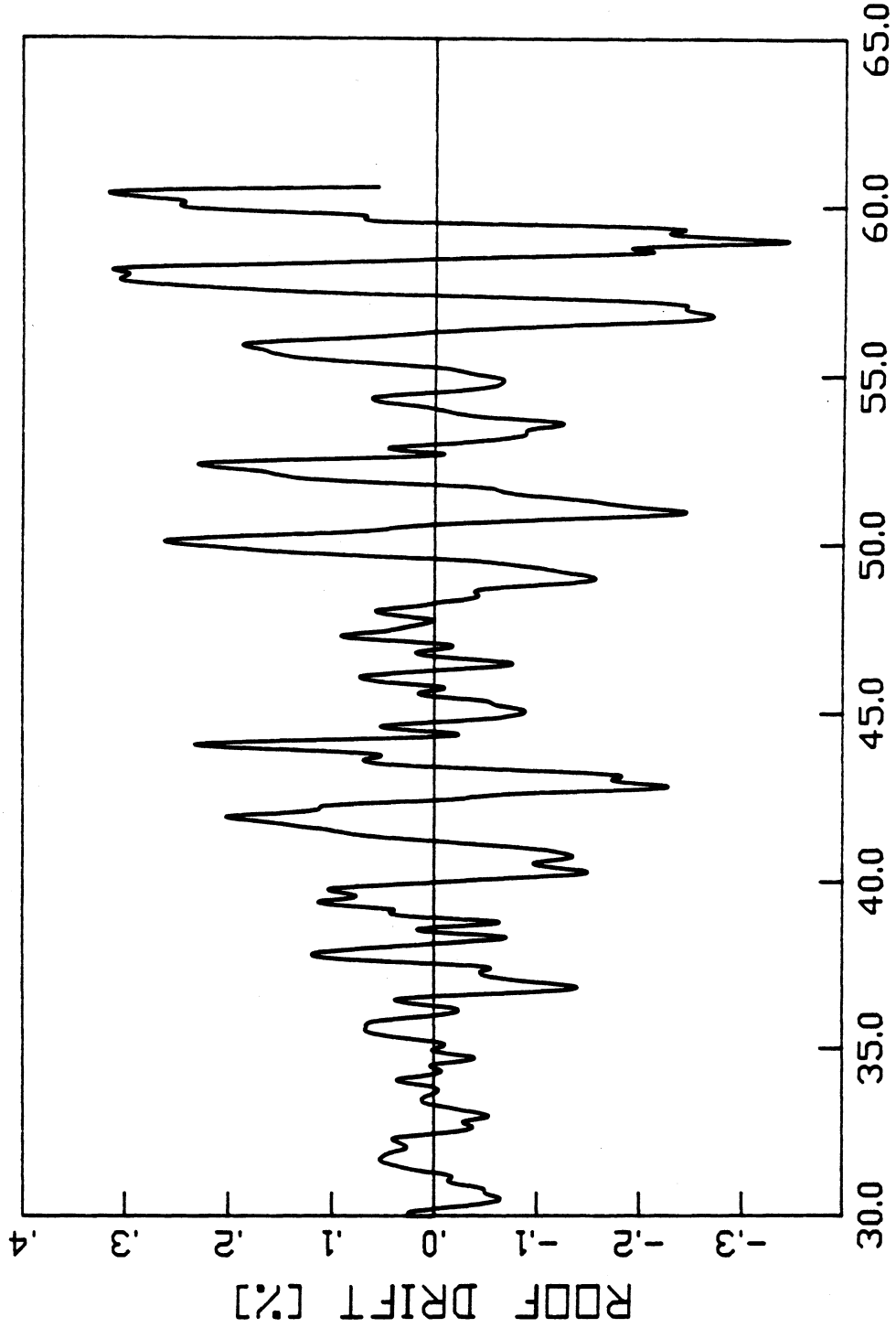

Fig. 7.27 Response of The Double Mass Model to The Mexico City SCT Record

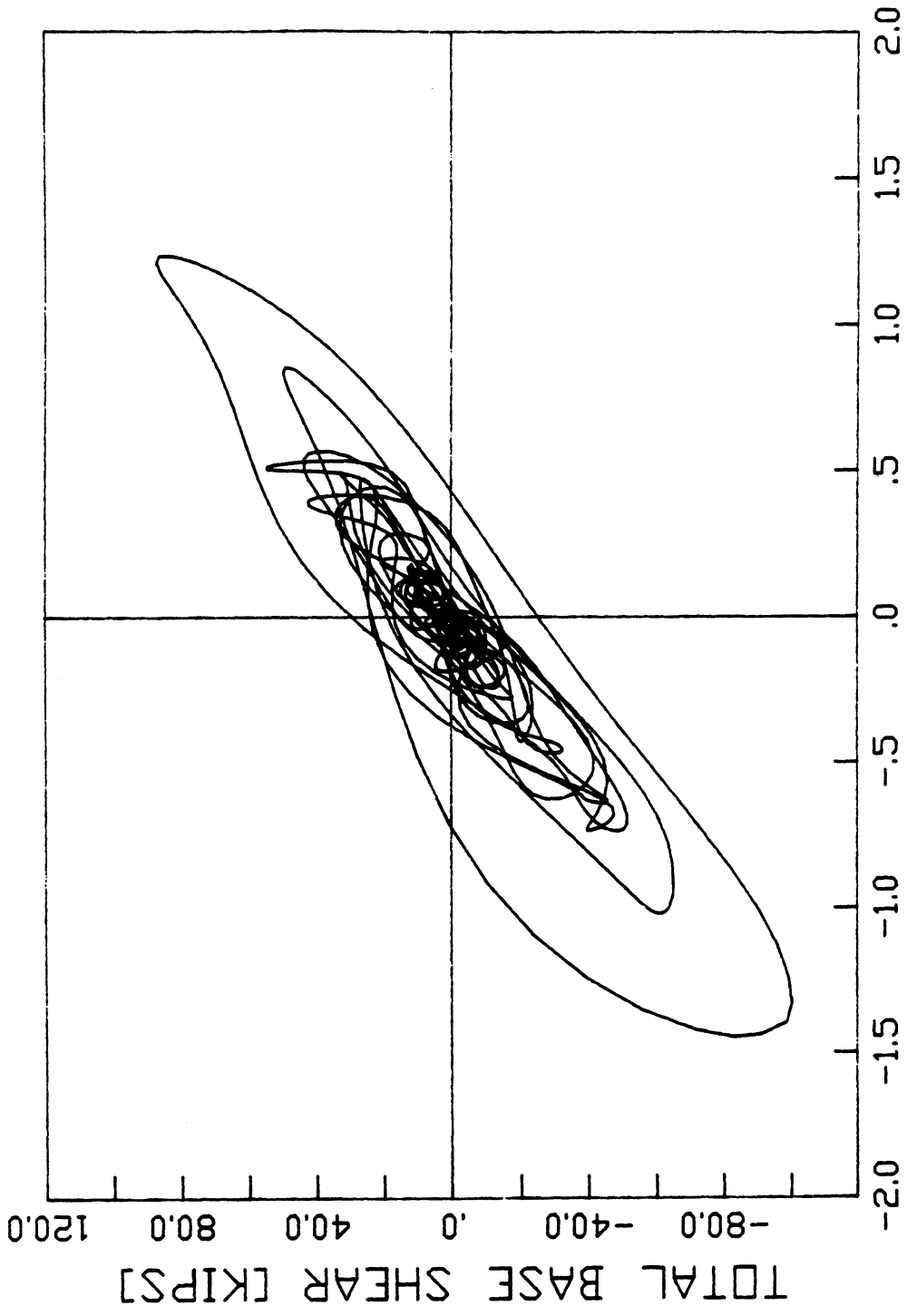

Fig. 7.28 Hysteresis Curves for The Double Mass Model, El Centro Record

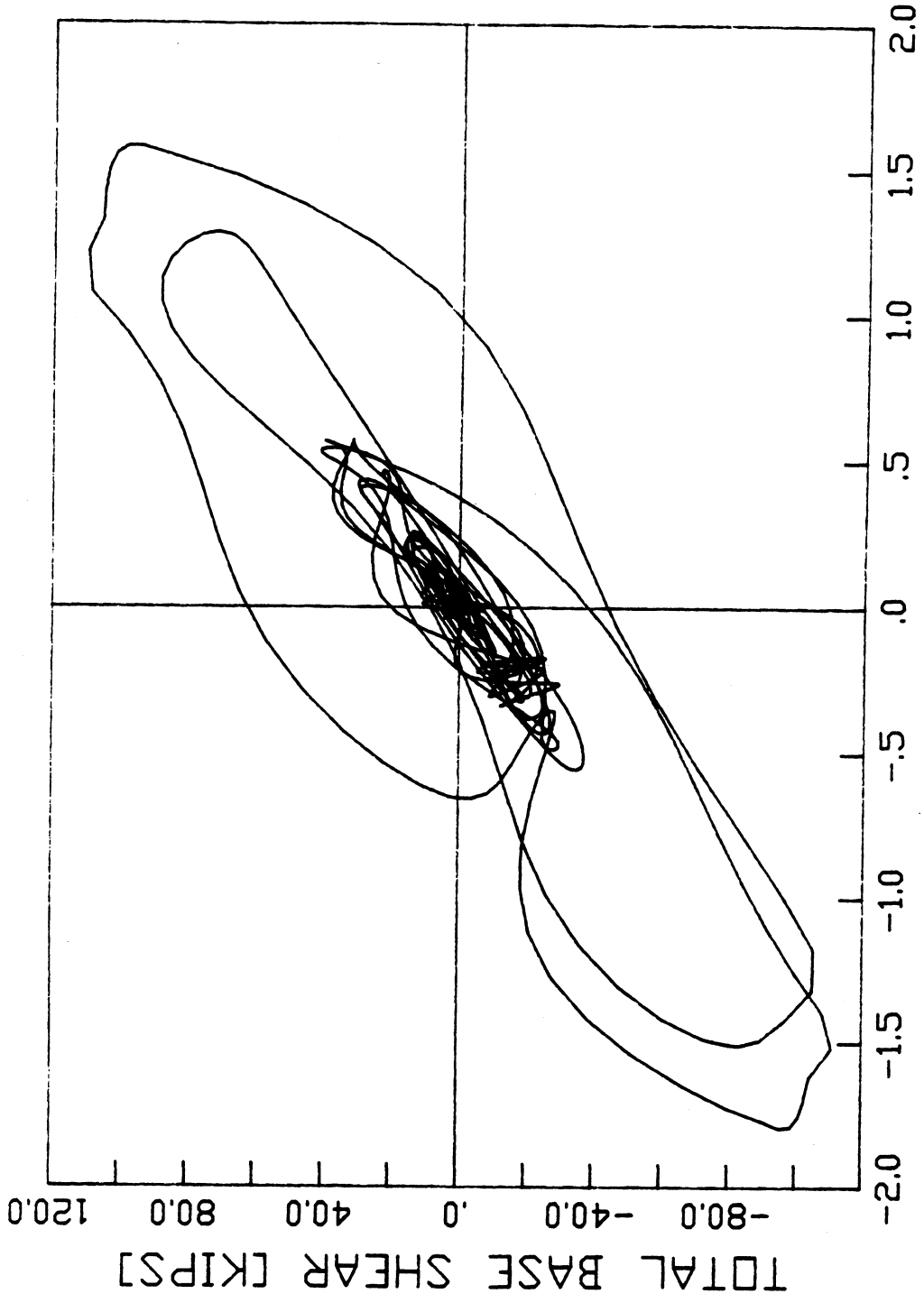

Fig. 7.29 Hysteresis Curves for The Double Mass Model, San Salvador Record

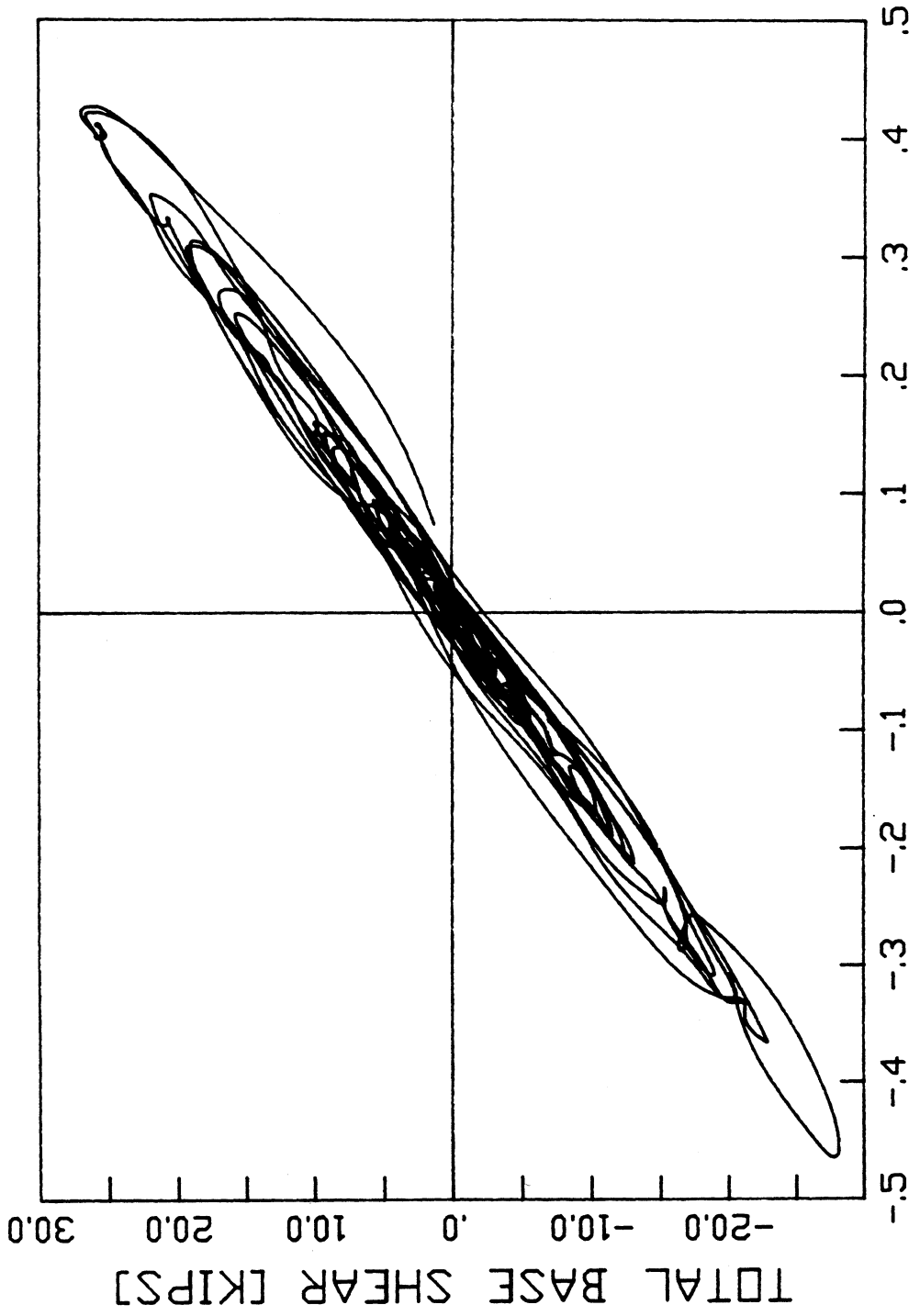

Fig. 7.30 Hysteresis Curves for The Double Mass Model, Mexico City SCT Record

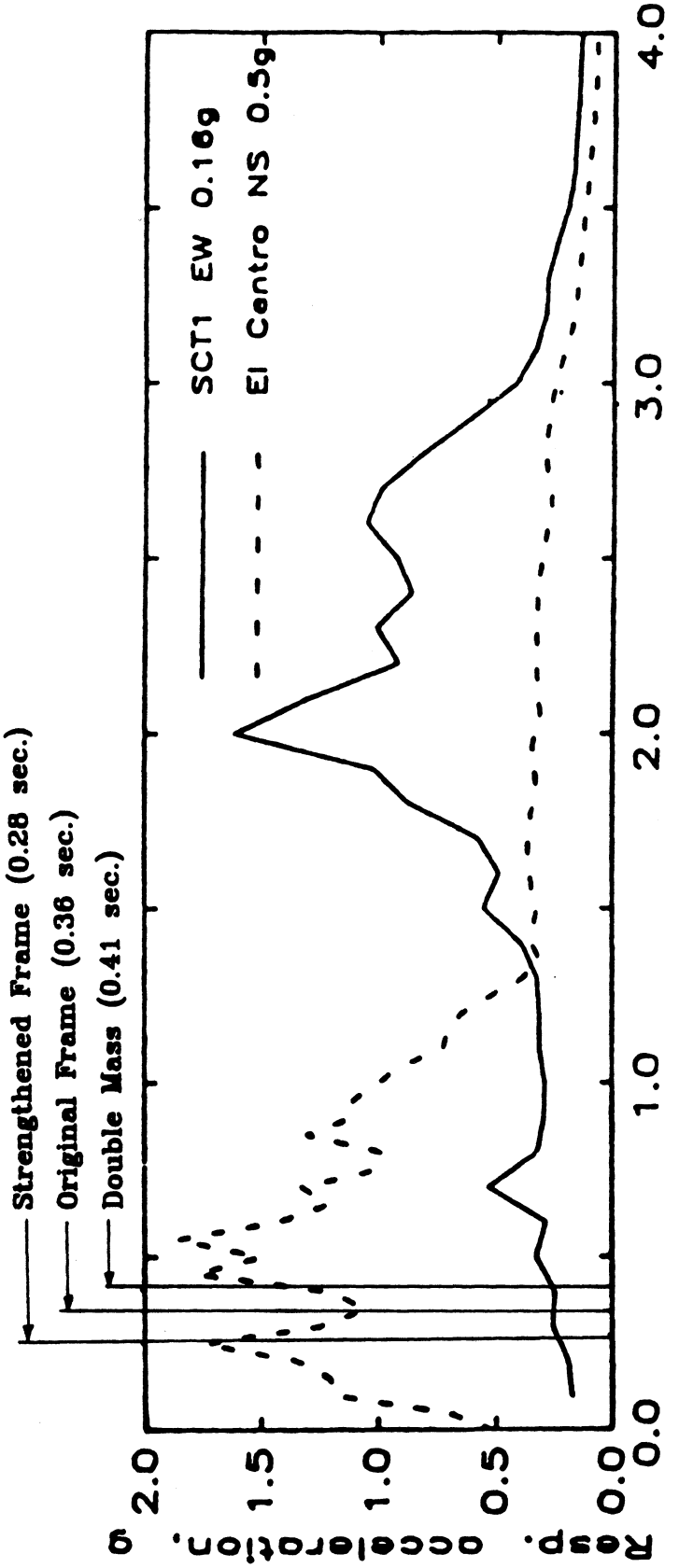

Fig. 7.31 Response Spectra for The Mexico City SCT and El Centro Records (Sozen and Lopez 1987)

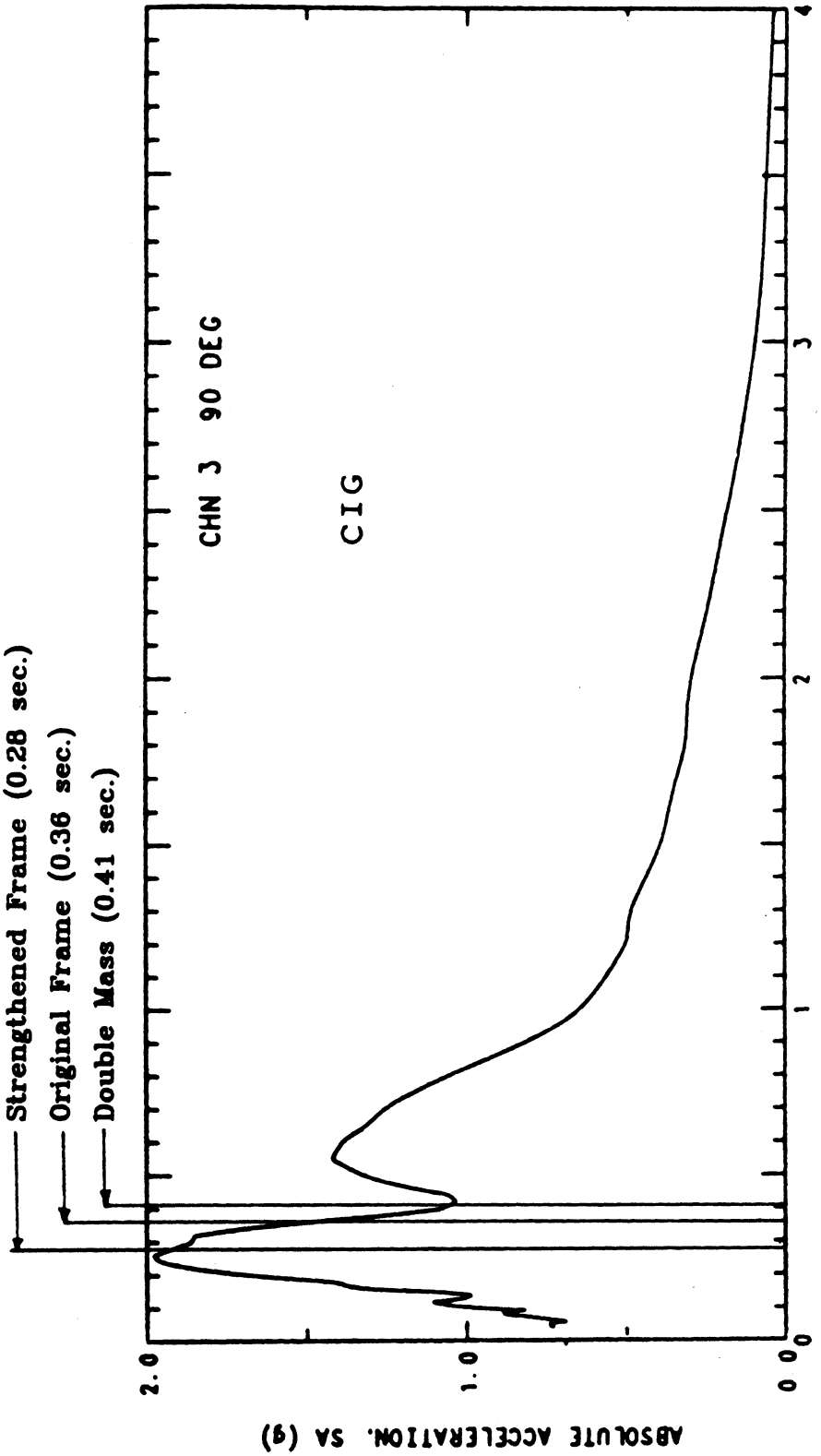

Fig. 7.32 Response Spectra for The San Salvador CIG Record (Shakal, Huang, and Linares 1987)

BIBLIOGRAPHY

BIBLIOGRAPHY

ACI Committee 318 (1989). "Building Code Requirements For Reinforced Concrete (ACI 318-89)," ACI, Detroit, 1989.

ACI-ASCE Committee 352 (1985). "Recommendations For Design Of Beam-Column Joints In Monolithic Reinforced Concrete Structures," Proceedings, Journal Of The American Concrete Institute, ACI, V. 82, No. 3, May-June, 1985, pp. 266-283.

Al-Haddad, M., and Wight, J. K. (1988). "Relocating Beam Plastic Hinging Zones For Earthquake Resistant Design Of Reinforced Concrete Buildings," Structural Journal, ACI, Vol. 85, No. 2, March-April, 1988.

Alcocer, S., and Jirsa, J. (1990). "Assessment Of The Response Of Reinforced Concrete Frame Connections Redesigned By Jacketing," Proceedings, Fourth U.S. National Conference On Earthquake Engineering, EERI, V. 3, May, 1990, pp. 295-304.

Anderson, R. (1987). "The San Salvador Earthquake Of October 10, 1986: Review Of Building Damage," Earthquake Spectra, EERI, V. 3, No. 3, August, 1987, pp. 497-541.

Benjamin, J., and Williams, H. (1958). "The Behavior Of One-Story Brick Shear Walls," Proceedings, American Society Of Civil Engineers (ASCE), V. 84, ST4, July, 1958, pp. 1723-1 -1723-30.

Bertero, V., and Brokken, S. (1983). "Infills In Seismic Resistant Buildings," Proceedings, Journal Of Structural Engineering, ASCE, V. 109, No. ST6, June, 1983, pp. 1337-1361.

Bertero, V.V., and Popov, E.P. (1977). "Seismic Behavior of Ductile Moment Resisting Reinforced Concrete Frames," Reinforced Concrete Structures In Seismic Zones, ACI SP 53, 1977, pp. 247-291.

Bett, B.J., Klingner, R.E., and Jirsa, J.O. (1985). "Behavior Of Strengthened And Repaired Reinforced Concrete Columns Under Cyclic Deformations," PMFSEL Report No. 85-3, The University Of Texas At Austin, December, 1985.

Bush, T., Roach, C., Jones, E., and Jirsa, J. (1987). "Behavior Of A Strengthened Reinforced Concrete Frame," Proceedings, Workshop On Repair and Retrofit Of Existing Structures, U.S.-Japan Panel on Wind and Seismic Effects, UJNR, Tsukuba, Ibaraki, Japan, May, 1987.

Clough, R.W. (1966). "Effect Of Stiffness Degradation On Earthquake Ductility Requirements," Structures And Materials Research Report No. 66-16, University Of California, Berkeley, October, 1966.

Corley, W., Kluver, M., Ghosh, S., Fratessa, P., Moreno, J., and Hogan, M. (1986). "In The Wake Of The Quake," Concrete International, ACI, V. 8, No. 1, January, 1986, pp. 9-12.

EERI (1989). Proceedings, Third U.S.-Mexico Workshop On 1985 Mexico Earthquake Research, EERI, March, 1989.

Esteva, L.(1966). "Behavior Under Alternating Loads Of Masonry Diaphrams Framed by Reinforced Concrete Members," Proceedings, The International Symposium On the Effects Of Repeated Loading On Materials and Structural Systems (RILEM), V. 5, Mexico, 1966.

Esteva, L. (1988). "The Mexico Earthquake Of September 19, 1985: Consequences, Lessons, and Impact On Research and Practice," Earthquake Spectra, EERI, V. 4, No. 3, August, 1988, pp. 413-426.

Filippou, F., and Issa, A. (1988). "Nonlinear Analysis Of Reinforced Concrete Frames Under Cyclic Load Reversals," Report No. UCB/EERC-88/12, University Of California, Berkeley, California, September, 1988.

Fintel, M. (1986). "Performance Of Precast and Prestressed Concrete In Mexico Earthquake," PCI Journal, PCI, V. 31, No. 1, January/February, 1986, pp. 18-42.

Fiorato, A., Sozen, M., and Gamble, W. (1970). "An Investigation Of The Interaction Of Reinforced Concrete Frames With Masonry Filler Walls," Report No. UILU-ENG-70-100, University Of Illinois, November, 1970.

Gergely, P. (1977). "Experimental And Analytical Investigations Of Reinforced Concrete Frames Subjected To Earthquake Loading," Proceedings, Workshop On Earthquake-Resistant Reinforced Concrete Building Construction, University of California, Berkeley, V.3, July, 1977, pp. 1175-1195.

Hutchinson, D.L., Yong, P.M.F., and McKenzie, G.H.F. (1984). "Laboratory Testing Of A Variety Of Strengthening Solutions For Brick Masonry Wall Panels," Proceedings, Eighth WCEE, V. 1, San Francisco, California, 1984.

Iglesias, J. (1986). "Repairing And Strengthening Of Reinforced Concrete Buildings Damaged In 1985 Mexico City Earthquakes," Proceedings, The Mexico Earthquakes 1985: Factors Involved And Lessons Learned, ASCE, September, 1986.

Jirsa, J. (1977). "Behavior Of Elements And Subassemblages--R.C. Frames," Proceedings, Workshop On Earthquake-Resistant Reinforced Concrete Building Construction, University Of California, Berkeley, V. 3, July, 1977, pp. 1196-1214.

Jirsa, J. O. (1987). "Repair Of Damaged Buildings: Mexico City," Proceedings, Pacific Conference On Earthquake Engineering, Wairakei, New Zealand, V. 1, August 5-8, 1987.

Jordan, R., and Kreger, M. (1990). "Evaluation Of Strengthening Schemes And Effects On Dynamic Characteristics Of Reinforced Concrete Frames," Proceedings, Fourth U.S. National Conference On Earthquake Engineering, EERI, V. 3, May, 1990, pp. 363-372.

Kahn, L.F. (1984). "Shotcrete Retrofit For Unreinforced Brick Masonry," Proceedings, Eighth WCEE, V. 1, San Francisco, California, 1984.

Kahn, L., and Hanson, R. (1976). "Reinforced Concrete Infilled Shear Walls For Aseismic Strengthening," Report No. UMEE 76S1, University Of Michigan, Ann Arbor, Michigan, January, 1976.

Kanaan, A., and Powell, G. (1973). "General Purpose Computer Program For Inelastic Dynamic Response Of Plane Structures," Report No. EERC 73-6, University Of California, Berkeley, April, 1973.

Klingner, R.E., and Bertero, V.V. (1976). "Infilled Frames In Earthquake Resistant Construction," Report No. EERC 76-32, University Of California, Berkeley, California, December, 1976.

Krause, G. L., Lopez, C. J., and Wight, J. K. (1988). "The Mexico City Research Program: Testing Of A Two-Story Reinforced Concrete Frame," UMCE 88-10, The University Of Michigan, Ann Arbor, Michigan, November, 1988.

Lara, M. (1987). "The San Salvador Earthquake Of October 10, 1986: Detailed Evaluation Of The Performance Of Eight Engineered Structures," Earthquake Spectra, EERI, V. 3, No. 3, August, 1987, pp. 543-562.

Lee, H., and Goel, S. (1990). "Seismic Behavior of Steel Built-Up Box-Shaped Bracing Members And Their Use In Strengthening Reinforced Concrete Frames," UMCE 90-7, The University Of Michigan, Ann Arbor, Michigan, May, 1990.

Luke, P.C., Chon, C.,and Jirsa, J.O. (1985). "Use Of Epoxies For Grouting Reinforcing Bar Dowels In Concrete," PMFSEL Report No. 85-2, The University Of Texas At Austin, September, 1985.

Mayes, R., Omote, Y., and Clough, R. (1976). "Cyclic Shear Tests Of Masonry Piers," Report No. EERC 76-8, University Of California, Berkeley, May, 1976.

Miranda, E., and Bertero, V. (1990). "Upgrading Of A School Building In Mexico City," Proceedings, Fourth U.S. National Conference On Earthquake Engineering, EERI, V. 3, May, 1990.

Otani, S. (1974). "Inelastic Analysis Of Reinforced Concrete Frame Structures," Journal Of The Structural Division, ASCE, Vol. 100, No ST-7, July, 1974.

Parducci, A., and Mezzi, M. (1980). "Repeated Horizontal Displacements Of Infilled Frames Having Different Stiffnesses and Connection Systems: Experimental Analysis," Proceedings, Seventh WCEE, V. 7, pp. 193-198, Istanbul, Turkey, 1980.

Prawel, S.P., Reinhorn, A.M., and Kunnath, S.K. (1986). "Seismic Strengthening Of Structural Masonry Walls With External Coatings," Proceedings, Third United States National Conference On Earthquake Engineering, EERI, V. II, Charleston, South Carolina, 1986.

Priestly, M. (1980). "Masonry Structural Systems For Regions Of High Seismicity," Proceedings, Seventh WCEE, V. 4, pp. 441-448, Istanbul, Turkey, 1980.

Rosenblueth, E. (1986). "The Mexican Earthquake: A Firsthand Report," Civil Engineering, ASCE, V. 56, No. 1, January, 1986, pp. 38-43.

Roufaiel, M., and Meyer, C. (1987). "Analytical Modeling Of Hysteretic Behavior Of R/C Frames," Journal Of Structural Engineering, ASCE, Vol. 113, No. 3, March, 1987.

Saiidi, M., and Sozen, M. (1979). "Simple And Complex Models For Nonlinear Seismic Response Of Reinforced Concrete Structures," Structural Research Report No. 465, Department Of Civil Engineering, University Of Illinois, Urbana, 1979.

Sauter, F. (1987). "The San Salvador Earthquake Of October 10,1986: Structural Aspects Of Damage," Earthquake Spectra, EERI, V. 3, No. 3, August, 1987, pp. 563-584.

Scribner, C., and Wight, J. (1977). "A Method For Delaying Shear Strength Decay Of RC Beams," Proceedings, Workshop On Earthquake-Resistant Reinforced Concrete Building Construction, University Of California, Berkeley, V. 3, July, 1977, pp. 1215-1241.

Shakal, A., Huang, M., and Linares, R. (1987). "The San Salvador Earthquake of October 10, 1986: Processed Strong Motion Data," Earthquake Spectra, EERI, Vol. 3, No. 3, August 1987, pp. 465-481.

Sozen, M., and Lopez, R. (1987). "R/C Frame Drift For 1985 Mexico Earthquake," Proceedings, The Mexico Earthquake-1985: Factors Involved and Lessons Learned, ASCE, 1987, pp. 279-307.

Stafford Smith, B., and Carter, C. (1969). "A Method Of Analysis For Infilled Frames," Proceedings, Institution Of Civil Engineers (London), V. 44, September, 1969, pp. 31-48.

Stoppenhagen, D.R., and Jirsa, J.O. (1987). "Seismic Repair Of A Reinforced Concrete Frame Using Encased Columns," PMFSEL Report No. 87-2, The University Of Texas At Austin, May, 1987.

Su, Y., and Hanson, R. (1990). "Comparison Of Effective Supplemental Damping Equivalent Viscous And Hysteretic," Proceedings, Fourth U.S. National Conference On Earthquake Engineering, EERI, V. 3, May, 1990, pp. 507-516.

Sugano, S., and Endo, T. (1987). "Seismic Strengthening Of Reinforced Concrete Buildings In Japan," Proceedings, Seminar On Repair And Retrofit Of Structures, US-Japan Panel On Wind And Seismic Effects, UJNR, Tsukuba, Iboraki, Japan, May 8-9, 1987.

Takeda, T., Sozen, M., and Nielsen, N. (1970). "Reinforced Concrete Response To Simulated Earthquakes," Journal Of The Structural Division, ASCE, Vol. 96, No. ST-12, December, 1970.

Tang, X., and Goel, S. (1988). "DRAIN-2DM: Technical Notes And User's Guide," UMCE 88-1, The University Of Michigan, Ann Arbor, Michigan, January, 1988.

Warner, J. (1982). "Reinforcing Steel Considerations Unique To Repair And Retrofit," Proceedings, The Third Seminar On Repair And Retrofit Of Structures, Ann Arbor, Michigan, Vol. 3, 1982.